Author's response to the reviewer comments for the revised manuscript

Dear Editor,

we have now completed major revisions of our initial submitted manuscript. We modified the structure and writing, and the presentation of the material in the manuscript substantially, taking into account the reviewer's concerns and comments. We feel that the revised manuscript has thereby improved substantially. Below we detail the substantial changes, and provide a point-by-point reply to the reviewers' comments.

On behalf of the Authors, Yongbiao Weng

Major changes

Summarizing the revisions to the content following the major comments from the three anonymous referees:

1. We have repeated two experiments (MIX2 and MIX3) regarding to the slight contrast dependency behaviour of $\Delta\delta^{18}$O for standard water MIX in Fig. 9a. In the repeated experiments, we have added measurements at lower humidity levels (down to 200 ppm) to reduce the fitting uncertainty due to the lack of constraining data points at those humidity levels. Each experiment consists one ascending and one descending sequence of the same standard water MIX. The results are shown in the figure below (the two repeated experiments are represented by MIX2 (green) and MIX3 (red) respectively). Though MIX3 somehow shows a stronger humidity dependency, no indication of a contrasting dependency behaviour is observed due to the measuring sequence in the two experiments. On contrary, both experiments show good consistency despite of the ascending and descending sequences. For simplicity, we have only presented the result from MIX2 and discussed the results from other two experiments in Appendix A3 in the revised manuscript.

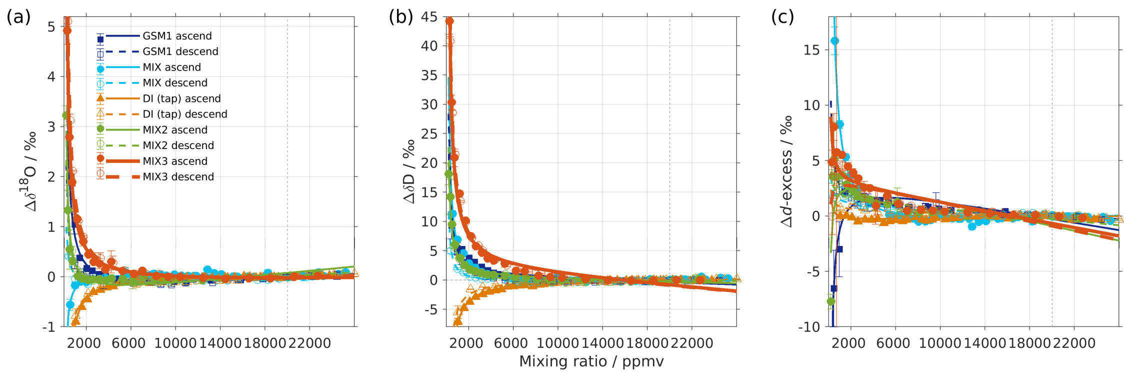

Figure 1. Mixing ratio dependency of GSM1 (dark blue symbol), MIX (light blue symbol), DI tap water (orange symbol), MIX2 (green symbol), MIX3 (red symbol) for **(a)** δ^{18}O, **(b)** δD and **(c)** *d*-excess, with ascending (closed symbol) and descending (open symbol) humidity sequences. Solid curves represent the fits for ascending humidity sequences and dashed curves the fits for descending humidity sequences. All the measurements are uncalibrated and carried out with discrete injections using an autosampler with N_2 being the carrier gas. The measurements for DI tap water, MIX, MIX2 and MIX3 are carried out on instrument HKDS2038 (Picarro L2140-i) (experiment 9 and 11). The measurements for GSM1 are carried out on instrument HKDS2039 (Picarro L2140-i) and one outlier around 500 ppmv has been excluded (experiment 15).

2. We have extended the discussion section with a detailed discussion on the spectroscopic origin of humidity dependency behaviour and have added a figure to demonstrate the absorption spectrum of the targeted water molecules.

3. We have updated the aircraft dataset with a more meaningful *d*-excess profile. First, we have replaced the every 10th data points to a one minute average dataset. Second, we have shifted the δD profile to account for a dephasing effect that contributes to artificially enhanced values of the *d*-excess profile. The delay in the response time for the δD profile is

probably due to the "wall effect" where water molecules stick to the inner wall surface of the system. Besides, uncertainties are indicated for all profiles in Fig. 4 to help clearly address the impact of different correction schemes. The aircraft data shown in Fig. 3 and presented in Sect. 6.1 are updated accordingly.

4. We have indicated the uncertainty (one standard deviation) of typical single injection in Fig. 1. Though, the uncertainty shown in the main figure is kept the same, which is accessed as the standard deviation of the means obtained from the 3 injections at each mixing ratio. This uncertainty is meant to be smaller, because it represents the dispersion of the means, or the uncertainty of the repetitions. For the present study, we consider the standard deviation of the mean, provided by multiple, repeated measurements, to be the most relevant information with regard to fitting the correction surfaces.

5. We have updated the dataset for "autosampler inject" in Fig. A1 (a-c). The dataset was mistaken from experiment 1 in the previous manuscript. Now it is changed to that of experiment 2. It has not affected our conclusions.

6. Have shortened certain repetitive parts and correct other small wording issues and typos. Details of these minor changes are found in the point-by-point response to the reviews of the three anonymous referees and the marked-up manuscript version below.

In addition, regarding the structure of the manuscript, we have changed the following aspects to improve overall readability and clarity:

- We have revised/rephrased the Introduction section.
- We have rearranged the Methods section and included a paragraph describing the instrument principle, L2130-i/L2140-i differences, and error budget.
- We have moved the detailed description of robustness/stability to an appendix and added a summary section on the stability/robustness based on a paragraph in the conclusions
- We have rephrased the results section.
- We have shortened and split the description of the surface function, and the example for HIDS2254
- We have added a thorough discussion on the spectroscopic effects in the discussion section, with a new figure of the spectral region targeted by the instrument
- We have shortened and rephrased the Conclusions.
- We have combined 3 figures regarding the robustness/stability analysis into one, and moved all related figures to the appendix.

Point-by-point response to the reviews of three anonymous referees

Replies to Anonymous Referee #1
Received and published: 17 November 2019

This paper shows detailed tests for the calibration of water isotopic composition vs humidity using Picarro CRDS instrument. Such calibration exercises are important and compulsory efforts to do when working with such instrument to provide records of d18O and dD of the atmospheric water vapor since water mixing ratio strongly varies on the different places (first because of temperature). Several groups are thus performing such exercises and it is interesting to see such results as a basis for discussion.

For each publication of new d18O and dD records in the water vapor, a methodology section is devoted to the so-called isotopes vs humidity calibration but the present paper is only focused on the method and does not show new records. The question is thus to know if the results displayed here are enough to make a publication by itself, especially since the applicability of the resuts obtained here are not easily transferable to another study and some results are questionable (see below).

AUTHOR'S REPLY:
The main novel aspect of the manuscript is that we systematically investigated the impact of the isotope composition on the mixing ratio dependency correction in the water vapour isotope measurements. Previous studies only investigated the mixing ratio dependency for one or more standard waters separately, and not the systematic dependency on isotope ratio. In the revised manuscript, we have brought this important new aspect of our study forward more clearly. We chose AMT as journal for publication because our results are mainly focused on method development. Presenting a new isotope record is not within the objectives of our manuscript.

Despite my mixed feeling on the outputs of the paper, I really appreciate the care given to the description of the measurements and the results. Even if some results seem strange (contrasted dependence to mixing ratio in ascending and descending mode for one standard, figure 9, cf later), they are not hidden or discarded from the study and I really appreciate this honesty in the treatment of the results. As a consequence, I would recommend not to accept the paper in its present form and incite the authors to make more links with previous studies and previous calibration. As an example, they only compare their correction with Bonne et al's correction (concluding that their approach was appropriate) while all studies publishing new d18O and dD records in the water vapor have a section on isotopes vs mixing ratio calibration. I therefore strongly urge the authors to discuss other paper dealing with such correction, discuss if it was appropriate given their new results and, if not, discuss the implications in term of uncertainties, signal detection, etc. . .

AUTHOR'S REPLY:
While we agree that application to previously published datasets could further demonstrate the relevance of our correction scheme, it is not possible or objective to directly do so within the present study. This would require subjecting those previously used analyzers to a similar kind of multi-standard characterization at first, as the isotope composition-mixing ratio dependency is an instrument-specific characteristic. Within the study we compare to the one previously published calibration scheme that approximates our correction scheme (Bonne et al., 2014). As highlighted by the other referees, in the revised manuscript, we have amended the discussion by relating the uncertainty of the correction scheme to the instrument precision at low mixing ratios.

My detailed comments along the text are given below.

- I am quite surprised by the performance obtained at low mixing ratios (below 2000 ppmv). In some cases, the error bars are even not visible on figure 1. By comparison, uncertainties displayed by other studies (e.g. Guilpart et al., JGR, 2017) are at least one order of magnitude larger. I would appreciate that the authors comment and explain such differences. This also has an impact on the outputs of the study. I had the feeling from previous studies that it was impossible / very difficult to perform accurate measurements below 2000 ppmv with a Picarro analyser because of the strong noise in the measurements. The very small error bars displayed on figure 1 do not go along previous studies in this sense.

AUTHOR'S REPLY:
In Figure 1, we now have also indicated the standard deviation of the single injections. It is correct that at lower mixing ratios, the standard deviation of each injection increases substantially. However, this uncertainty can be reduced by repetitions of the same measurement. For the present study, we consider the standard deviation of the mean, provided by multiple, repeated measurements, to be the most relevant information with regard to fitting the correction surfaces.

- P. 5, l. 28: can you precise what you mean by "the lower precision with SDM measurements"? Be more accurate, give number. . .

AUTHOR'S REPLY:
The lower precision is due to the less stable water vapour generation with the SDM unit. The precision is illustrated in the

figures such as Fig. A1 a-c.

- P. 6, l. 4: what does it mean "certified down to 200 ppmv" ?

AUTHOR'S REPLY:

According to manufacturer specification of Option S0508 (optimised performance during low mixing ratios, calibration to 200 ppm H2O), the instrument has an optimized performance during low mixing ratios compared to regular instruments (down to 200 ppmv instead of 1000 ppmv). This is a feature that the manufacturer has customized according to our order. The exact details of the calibration procedure have not been made available. We have provided some additional information in the revised manuscript.

- On figure 1, it would help the reader to have the isotopic value (at least d18O or dD) for each standard to see directly the influence of isotopic composition on the isotopes vs humidity relationship.

AUTHOR'S REPLY:

We have added d18O values to the legend of Figure 1.

- Everywhere in the paper, I do find that the term "bias" (e.g. on p. 8) is not used properly. Bias with respect to what ? Indeed, in all studies dealing with d18O and dD in the water vapor, there is a correction for isotopes vs humidity. This effect is well known and taken into account so I would not call it a bias. This is a classical procedure to correct for this influence especially for studies dealing with low humidity. If there is a bias, then, it is perhaps linked to the method used by others to correct for this effect if they considered only one standard and did not adjust the uncertainty bars properly. However, this is not discussed in the present manuscript. I encourage the authors to avoid using bias (which is misleading in my opinion) but better use the term "isotope (humidity relationship" or "isotope-humidity correction")

AUTHOR'S REPLY:

We agree with the reviewer and have replaced the word 'bias' by a more neutral expression 'deviation' throughout the revised manuscript.

- The section "correction framework" is a bit problematic. First, it implies that the readers should use such a frame but we can wonder if it is correct and if it is useful. The reason why we can wonder if it is correct is that in figure 9, the authors show huge difference (actually opposite) dependencies of isotopic composition to humidity for descending and ascending humidity during the calibration method. This strongly questions the validity of the conclusions presented here. Also, the fact that the error bars for low humidity are so small are questionable since previous studies have shown much different figures.

AUTHOR'S REPLY:

It is correct that the fits to standard MIX appear with an opposite sign for upward/downward calibrations. However, this opposite sign is only observed for standard MIX, which has a very limited number of data points. We have therefore repeated the experiments (MIX2 and MIX3) with more data points for this standard. In the repeated experiments, we have added measurements at lower mixing ratios (down to 200 ppm) to reduce the fitting uncertainty due to the lack of constraining data points at those mixing ratios. Each experiment consists one ascending and one descending sequence of the same standard water MIX. The results are shown in the figure below (the two repeated experiments are represented by MIX2 (green) and MIX3 (red) respectively). Though MIX3 somehow shows a stronger mixing ratio dependency, no indication of a contrasting dependency behaviour is observed due to the measuring sequence in the two experiments. On contrary, both experiments show good consistency despite of the ascending and descending sequences. For simplicity, we have only presented the result from MIX2 in the revised version of Fig. 9 (now Fig. A1(g-i)), and discussed the results from other two experiments in Appendix A3.

The reason why we can wonder if it is useful is that the author show that the correction performed by Bonne et al's using only the two standards bracketing the isotopic composition of the water vapor isotopic measured in their site is appropriate.

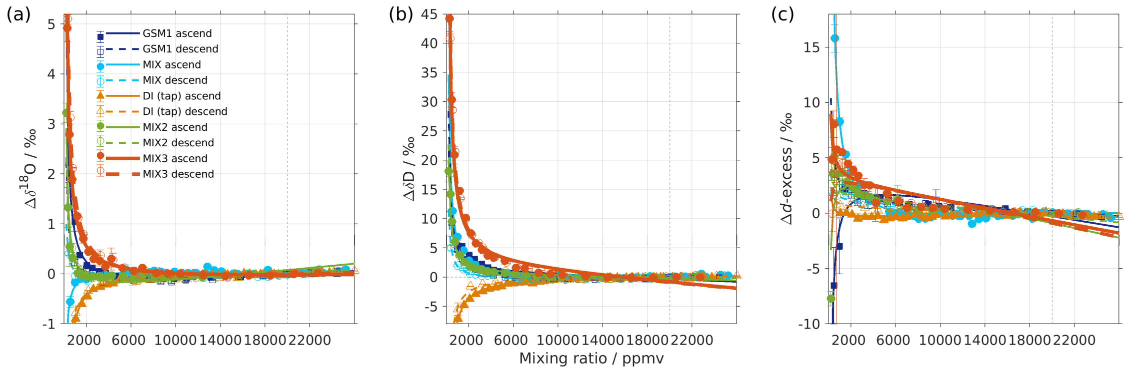

Figure 2. Mixing ratio dependency of GSM1 (dark blue symbol), MIX (light blue symbol), DI tap water (orange symbol), MIX2 (green symbol), MIX3 (red symbol) for **(a)** δ^{18}O, **(b)** δD and **(c)** *d*-excess, with ascending (closed symbol) and descending (open symbol) mixing ratio sequences. Solid curves represent the fits for ascending mixing ratio sequences and dashed curves the fits for descending mixing ratio sequences. All the measurements are uncalibrated and carried out with discrete injections using an autosampler with N_2 being the carrier gas. The measurements for DI tap water, MIX, MIX2 and MIX3 are carried out on instrument HKDS2038 (Picarro L2140-i) (experiment 9 and 11). The measurements for GSM1 are carried out on instrument HKDS2039 (Picarro L2140-i) and one outlier around 500 ppmv has been excluded (experiment 15).

Such approach (Bonne et al.) is actually a classical method used by many authors since SDM are equipped for performing calibration with two standards. I thus do not see the added value of such complicated procedure considering 5 standards, some of them being far from the range of values of interest.

AUTHOR'S REPLY:

If the instrument is deployed in ambient conditions with widely varying mixing ratio and isotope compositions, such as during aircraft measurements, characterisation across the entire range of measurement conditions is needed. Comparing with the approach in Bonne et al 2014, our approach provides new values in three perspectives. First of all, our approach provides a more accurate solution by actually being able to partly capture the non-linearity of the mixing ratio dependency on a large spread of isotope compositions since we use five laboratory standards. Using two standards, the approach by Bonne et al. 2014 (hereafter Bonne2014) assumes a linear dependency between the two response functions in order to correct the mixing ratio dependency for other isotope compositions. Secondly, our finding that the isotope composition-mixing ratio dependency is a robust instrument behaviour does not support Bonne2014's hypothesis that the contrasting mixing ratio responses of their two working standards is likely an artefact of residual water vapour in the dry air dried by Drierite. Finally, we show that using a dry gas cylinder (or a more advanced drying system) can preclude the possible influence of residual water vapour in the dry gas and thus lead to a more accurate mixing ratio dependency function. We have included these arguments in now Sec. 6.1 in the revised manuscript.

- It is also difficult to follow the authors when they propose equations 4 and 5 to fit the dependency to humidity and to isotopic composition. Since there is not any physical mechanism to explain the dependencies observed here, there is no reason why there should be a particular format for the fitting equations.

AUTHOR'S REPLY:

It is correct that the proposed fitting function is not chosen on physical basis; we choose it because it fits well with the observations we obtained for the tested instrument. While it is possible that physical processes/spectroscopy underly the determined fitting function (see discussion), the readers need to check and determine the best choice of fitting function according to the observations for their specific instrument. These points have been made clearer in the revised manuscript.

- Figure 4 is without error bars so that the comparison between the correction method can not be done. The authors should present a calculation of these error bars and use them for the comparison.

AUTHOR'S REPLY:
Error bars have been included in Fig. 4.

- P. 12, l.19 to 26: I am not really impressed by such discussion. In all studies dealing with such measurements, the authors chose a standard with an isotopic value close to the one of the measurements to be performed.

AUTHOR'S REPLY:
We have rephrased to clarify that, in the cases when the range of isotope compositions is known in advance, and proper standards can be chosen, there is no direct benefit from using our characterisation method. However, in the case of a previously unknown range of isotope ratios, or strongly varying conditions, a comprehensive characterisation provides advantages and should be preferred. Unknown ranges are particularly likely for atmospheric measurements of vertical profiles, or over a wide area from moving platforms.

- Similarly, I am moderately impressed by the fact that the correction is smaller for the measurements performed on the ship. It is obvious from figure 1 that the effect discussed here is not important for this humidity range. One sentence can easily replace section 5.2 (the results can also be omitted from this manuscript).

AUTHOR'S REPLY:
We have shortened the discussion at this point in the revised manuscript, but have kept the ship measurements as a contrasting example to emphasize the point made in the comment directly above.

- Section 6.3 can be summarized in 2 sentences (the tables already explained the methods and the results can be summarized in one sentence).

AUTHOR'S REPLY:
We have shortened the section and moved this section to appendix in the revised manuscript.

- Figure 8 shows that there is a significant effect of the carrier gas (considering the error bars). Also, I am surprised to see larger error bars here. So what is the conclusion? Could the authors end up with an estimate of the error bars after their corrections given the uncertainty on the determination of the isotopes vs humidity depending on the carrier gas and sequence of humidity variations (ascending or descending).

AUTHOR'S REPLY:
We confirm as found in previous studies that a change in the carrier gas induces a different isotope-mixing ratio dependency. Our results are most relevant for measurements in ambient air. We have also provided more information on the errors after correction with our proposed isotope-mixing ratio dependency correction scheme, as requested by Referee #3.

- Figure 9 is really rising many questions on the validity of the conclusion of this study and should be given extreme care if this manuscript is revised. It shows opposite evolution of isotopes vs humidity for different sequence of humidity variations. I am surprised that the authors did not try to understand deeper what happened here because it is central to their entire study. I would really urge the authors to repeat their measurements and see if they can repeat this opposing behaviour for different ways of varying the humidity. If this is a solid feature, then, there may be an explanation and it should be investigated. If this behaviour is indeed true, the correction proposed here is not be correct or at least error bars in the reconstruction should take it into account. In any case, the authors should comment more on this surprising result and on its implication. Actually, it is a very interesting result and it should definitively be investigated more to make progress on the isotopes vs humidity relationship in picaro instrument.

AUTHOR'S REPLY:
We agree with the referee that the contrasted dependence to mixing ratio in ascending and descending mode for the standard MIX needs corroboration. As mentioned above, we have repeated the experiment and confirmed our conclusions with more measurements at lower mixing ratios. This uncertainty in the dependency behaviour has been addressed in Appendix A3.

- I find that a background humidity of 60-80 ppmv (p. 17) is quite high when discussing measured values at 500 ppmv. It is quite surprising that you could not obtain lower values with dry air.

AUTHOR'S REPLY:
The background mixing ratio of 60-80 ppmv is not from the carrier gas, but from the remaining moisture in the system (including vaporizer chamber, analyzer chamber and the filter surface in between). The background mixing ratio in the analyzer when measuring the dry carrier gas is <10 ppmv. The discussion has been made clearer in this respect in the revised manuscript.

- Section 7 started well. We really would like to understand this dependence to isotopic composition. Unfortunately, the discussion is really short and disappointing.

AUTHOR'S REPLY:
The discussion has been thoroughly extended based on the input of all referees, and includes now a new section and figure based on the published literature.

Replies to Anonymous Referee #2
Received and published: 19 November 2019

This manuscript is a systematic laboratory study of the humidity dependency of water isotopologue measurements by commercial Picarro cavity ring-down spectrometers (CRDS). The authors characterized how water isotopologue ratios and d-excess are biased by water content ('humidity dependency'), in particular at low water mixing ratios below 1600 ppmv. Furthermore, this humidity dependency varies with isotopic composition, called 'isotope composition-humidity dependency' here. The dependency is seen in all three CRDS as an instrument characteristic that is, to first order, constant over 1 to 2 years of measurements. At higher humidities (>4000 ppmv), Picarro CRDS show negligible bias with water vapor mixing ratio or with the isotopic composition. The authors develop a procedure for correcting the isotope-composition-humidity dependency of Picarro CRDS.

My comments: I recommend that this paper be published only after major changes. My detailed comments are listed below: 1. I do not like the mixed terminology of 'humidity' and 'ppmv'. First of all, 'ppmv' or 'parts per million by volume' is not defined in the text. The unit ppmv is used only with mixing ratio. Instead, specific humidity is typically in units of mg/kg or 'parts per million by mass'. These are standard terms but unfortunately the literature uses 'Humidity dependency'. As a path forward, I suggest that the authors consider the following: 1.1 Define the water mixing ratio measured by the Picarro as units of 'ppmv' or 'parts per million by volume' where it first appears, page 2, line 2.

AUTHOR'S REPLY:
Done in the revised manuscript.

1.2 Every time the water mixing ratio is used, change 'humidity' to 'water mixing ratio', e.g., page 2, line 2, ". . .within a water mixing ratio range of 19,000∼21,000 ppmv (parts per million by volume)"

AUTHOR'S REPLY:
Mixtures of water vapour and dry air can be quantified by various measures of absolute humidity, such as specific humidity in

units of g/kg or water vapour mixing ratio in units of parts per million by volume or by mass, or as g/kg. Conversion from one definition to the other is straightforward. Importantly, the choice of the unit does not change the isotope-humidity dependency. However, we acknowledge that the term "humidity" does not clearly enough seperate between absolute and relative humidity. In the revised manuscript, we have now clearly stated our choice of the unit to be ppmv and use the term ’mixing ratio’ instead of ’humidity’ throughout the manuscript.

1.3 Every time you refer to humidity dependency, use ’humidity dependency’ (because this term is now accepted in the water isotope community).

AUTHOR’S REPLY:
Have changed to the term ’mixing ratio dependency’ in the revised manuscript.

2. Given that many papers have noted the concentration dependency (Wen et al., 2012, Bailey et al., 2015) or mixing ratio dependency (Aemisegger et al., 2012), then what specifically is new in this paper? The authors should emphasize that characterization of ’isotope composition-humidity dependency’ is new here (if that is the case?).

AUTHOR’S REPLY:
The new aspect of this study is indeed that the mixing ratio dependency is found to be systematically dependent on the isotope composition, which opens up the opportunity to correct for this influence, and leads us to coin the term *isotope composition–mixing ratio dependency*. We have further emphasized this point in the revised manuscript (also see reply to Referee #1).

3. It seems that the ’isotope composition-humidity dependency’ is instrument-specific. Can instrument issues like pump speed or plumbing details play a role? These are not discussed.

AUTHOR’S REPLY:
We do not think pump speed is likely to play a role here. The measurement system includes up to three pumps: an SDM air pump, and external vacuum pumps supplied by Picarro Inc (S2003). The flow through the Picarro analyzer depends on the measurement mode and analyzer type, and is regulated by the analyzer through different measures (critical orifice/flow regulator). The adjustment of the pump speed of the SDM air pump would affect the amount of dry gas and thus the mixing ratio of the humid air supplied to the analyzer. In liquid injection mode, a stronger vacuum pump connected to the vapourizer could potentially increase the efficiency of removing the remaining vapour in the vaporizer between injections, reducing the so-called memory effect from the previous measurement. However, as we have discussed in Sect. 7, due to the non-monotonous behaviour of the isotope-mixing ratio dependency, we consider it unlikely to be a result from mixing with remnant water in the system. Therefore, we do not think the adjustment of pump speed of the external vacuum pump would affect the behaviour of mixing ratio dependency that we have observed. Plumbing details are unlikely to play a role either, since different methods to generate the vapour provide very similar results. The exception may potentially be parts that are inside the analyzer and beyond the user’s control.

4. Section 7 aims to explore whether the isotope composition-humidity dependency is due to mixing with water remaining in the analyzer, or from spectroscopic or other instrument characteristics. The discussion of spectroscopic effects (page 18, lines 3-9) is too short, and I recommend more discussion here to provide basic instrument details. 4.1 What are the wavenumbers of the absorption lines? 4.2 What are typical absorption depths? 4.3 Demonstrate what is the uncertainty in fitting spectra. 4.4 What is the manufacturer’s recommended minimum humidity at which to take measurements?

AUTHOR’S REPLY:
Based on the input from all three referees, the discussion has now been thoroughly extended, also addressing the questions 4.1-4.4, see comment above.

5. Section 8 speculates, without supporting evidence, that 'the isotope composition-humidity dependency is to first order a constant instrument characteristics. It probably has a spectroscopic origin, resulting from a larger uncertainty in the fitting of absorption peak at low water molecular concentrations . . .'. Both in Section 8 and Section 7, this same language is used without supporting evidence. I strongly recommend the authors provide more detail on instrument error budget (in general) and the uncertainty in fitting spectra (as I said above).

AUTHOR'S REPLY:
In Section 7 we now discuss two possible causes of the observed isotope composition-mixing ratio dependency, i.e., whether it is a memory effect from mixing with water remaining within the analyser, or an instrument behaviour resulting from spectroscopic or other design characteristics. Our work does not support the hypothesis of mixing effect, to a large part because we would not expect mixing to produce a non-monotonic isotope composition-mixing ratio dependency. This therefore points to a spectroscopic origin, supported with previous studies including Rella et al., 2015 and others. In the revised manuscript, we now provide a general instrument error budget for water vapour measurements, and discussed the uncertainty from fitting spectra according to the available information, as suggested by all 3 referees.

Editing comments: 1. Page 6, line 25, change 'we have replaced the gas drying unit to dry gas cylinders' to 'we have replaced the gas drying unit with dry gas cylinders'. 2. Page 19, line 14: change 'revers' to 'reverse'. 3. Page 19, line 30: change "humidify" to "humidity"

AUTHOR'S REPLY:
Editing comments 1-3 have been implemented in the revised manuscript.

Replies to Anonymous Referee #3
Received and published: 21 November 2019

This paper presents an interesting study on the impact of the isotope composition on the specific humidity dependent correction of water vapour isotope measurements with different recent versions (L2130-2140) of commercial cavity ring-down spectrometers from Picarro. It presents results of an elaborate laboratory study on the topic, which is important for measurements conducted in very dry environments such as in polar regions or the lower to mid free troposphere. This study fits well into the scope of AMT and I recommend publication of this interesting and relevant manuscript after the following major comments have been convincingly addressed:

1) To me it is unclear, how the surface correction functions presented here relate to the total uncertainty of the measurements at low absolute humidity (1a) Specifically, the dependence of the measurement precision on the absolute humidity is normally considerable with these instruments, a fact that is only mentioned indirectly in one sentence in the manuscript (p.3, l.6). This aspect should be addressed explicitly. Clearly, the amplitude of the correction should be placed into the context of the uncertainty associated with the entire postprocessing framework to be able to judge its significance (including the normalisation to the VSMOW-SLAP scale, where the instrument precision is an important component).

AUTHOR'S REPLY: We agree that this aspect needed to be highlighted more clearly, now mention the typical uncertainties for different averaging time intervals when doing ambient water vapour measurements.

1b) The much smaller precision of CRDS measurements at low humidity is also the reason, why previous studies have found that the impact of the isotope composition on the humidity dependence is not significant for older instruments. The latter were characterised by very low signal to noise ratios at low humidity. This point deserves to be mentioned on p. 2, l. 18.

AUTHOR'S REPLY:
This point has been mentioned in the revised manuscript.

1c) The errorbars in the Figs with autosampler injections seem unrealistically small to me. Are these small errorbars due to the fact that the authors use the standard deviation of isotope variables averaged over 3-4 injections only, yielding an overconfident measure of uncertainty? A more adequate estimate should be used for the autosampler injections.

AUTHOR'S REPLY:
In Figure 1, we now have also indicated the standard deviation of the single injections. It is correct that at lower mixing ratios, the standard deviation of each injection increases substantially. However, the uncertainty of the mean can be constrained by repetitions of the same measurement. For the present study, we consider the standard deviation of the mean, provided by multiple, repeated measurements, to be the most relevant information with regard to fitting the correction surfaces.

2) Unfortunately, the reader is a bit disappointed at the end of the paper to have read this detailed analysis of the isotope humidity dependency with no answer at all to the question to why it exists. The reader thus remains not entirely convinced that the effect is really a spectroscopic one. It could also be related to how the calibration vapour is produced (see Kurita et al. 2012, their Fig. 7).

AUTHOR'S REPLY:
We have discussed with respect to two possible causes of the observed isotope composition-mixing ratio dependency, i.e., whether it is an artefact from mixing with water remaining within the analyser, or an instrument behaviour resulting from spectroscopic or other design characteristics. Our work does not support the hypothesis of mixing effect, but points to a likely spectroscopic origin. The spectroscopic effects has been discussed in more detail in the revised manuscript.

We have tested two vapour generating approaches and found the isotope composition-mixing ratio dependency is a robust feature for both approaches. Kurita et al. 2012 actually stated that they could not conclude from their experiment that the water vapor concentration dependency is related to their vapour production approach; they have rather suggested the concentration effect results are likely from the spectral fitting procedures used, including the removal of interferences in their analyzer (last paragraph of Sec. 3.2.3 in Kurita et al. 2012).

2a) I thus urge the authors to give the reader a bit more insight into what they would argue the spectroscopic effects are (in particular with respect to pressure broadening effects and baseline shifts, see also Chen et al. 2010, Johnson and Really, 2017).

AUTHOR'S REPLY:
We thank the referee for these references. As requested by all three referees we have formulated a more detailed discussion of the potential spectroscopic effects in the revised manuscript.

2b) For every setup a mean and standard deviation of the isotope variables obtained during dry runs should be provided (ideally in the respective Figures).

AUTHOR'S REPLY:
Unfortunately we are not entirely sure what information the referee asks for. We understand it as the isotope composition reported during dry air/N2 measurement only, but do not see directly how it is connected to our results.

3) As mentioned in my pre-review, I appreciate the level of detail that is provided to the reader and the careful analysis that is carried out. However, the paper is currently very long for the simple message it actually conveys and tends to loose the reader, who is interested in transferring the method to his own instrument. It is not clear to me, why the 2D fitting procedure in Section 4 is discussed in such a detail, this part should be put into the Appendix and the procedure summarised in one paragraph of the main text. It is anyway not clear at this stage if the proposed fitting procedure is necessarily the best for all instruments, since it has no physical foundation.

AUTHOR'S REPLY:
The proposed fitting function is not chosen based on physical processes; it has been chosen because it fits well with the observations we obtained for the tested instruments. While it it possible that the fitting function could represent underlying physical

processes/spectroscopy, readers should carefully check and determine the best choice of fitting function for their specific instrument. This point has been made clearer in the revised manuscript. We have furthermore shortened the section.

4) I am very critical of the results shown in Fig. 4, because I think that the data suffers from a measurement artefact: 4a) Could the author provide more information about the temporal resolution of the data points shown in the profiles (1.25Hz?, 0.1Hz?)?

AUTHOR'S REPLY:
The raw measurement was taken with a temporal resolution of 1.25Hz. But the temporal resolution of the data points shown in Fig. 4 is 0.125 Hz. We have previously plotted every 10th data point for the sake of clarity. We have now updated the figure with one min averaged data which has alleviated potential measurement artefacts.

4b) In my opinion, a flow rate of 35 sccm is very low (if not too low) for performing precise and high resolution aircraft measurements given the Picarro cavity size. With this flow rate and a cavity size of 35 ccm, the air sample in the cavity volume is exchanged only once per minute. The response times of d18O and d2H have been shown in earlier studies to be different with an up to 10s slower response of d2H than d18O at such low flow rates. This difference in response time can lead to an artificial lowering of d-excess in a downward profile with the d2H lagging behind the d18O signal. Before publishing such very low values of d-excess (-40 ‰) at the upper edge of a cloud layer as naturally occurring, the data quality also in terms of other instrument setup characteristics (response time, precision) should be carefully checked.

AUTHOR'S REPLY:
The flow rate of the instrument was about 35 sccm, and it was connected with short tubing to an inlet tube providing ambient air with a much higher flow rate of about 8 slpm. We are aware of the very low values of d-excess in the profile shown here. This is potentially an artefact due to the dephasing of d18O and dD profiles. In the revised manuscript, this aspect has been addressed by shifting the dD profile by 30 seconds forward in time, and using a one-min averaged profile. At the same time, we also emphasize that we do not attempt an interpretation of the isotope data in terms of atmospheric processes in this manuscript. The low values of d-excess will not affect our discussion of the impact of the different correction schemes.

4c) Errorbars (2D) are indispensable for being able to show that the differences between the correction scenarios are actually larger than the measurement uncertainty (total uncertainty). The precision of L2130 instruments at 1000 ppmv is usually around 10‰ (d2H), 1-2 permil (d18O) and 10-15‰ (dexcess).

AUTHOR'S REPLY:
We had excluded the error bars for clarity of the figure, but have now included error bars in the revised figure to allow for a comparison of the correction to measurement uncertainty.

Minor comments and typos: 1) Title: "Impact of the isotope composition. . ."

AUTHOR'S REPLY:
Done in the revised manuscript.

2) P.1, l.1: isn't the main point here that measurements can be performed in remote areas in general and specifically on mobile platforms?

AUTHOR'S REPLY:
Have changed to "in remote areas, on platforms such as ship and aircraft"

3) P.1, l.4 and other locations: I think the wording "humidity" or "humidity dependency" is a bit unprecise. The authors should choose what they like best, but they should avoid any confusion with an effect that would be relative humidity depen-

dent. A clear definition at the beginning of the manuscript would be helpful and I would suggest always adding "absolute" or "specific "humidity" everywhere in the abstract.

AUTHOR'S REPLY:
We have consistently changed "humidity" to "mixing ratio" in the revised manuscript.

4) P.1, l. 7: of the measured water vapour

AUTHOR'S REPLY:
Done in the revised manuscript.

5) P.1, l. 8: humidity correction at low absolute humidity

AUTHOR'S REPLY:
We have changed "humidity" to "mixing ratio" in the revised manuscript.

6) P. 1, l12 and L17 replace "cold" by "dry". The temperature of the environment is not the relevant factor in this technical study.

AUTHOR'S REPLY:
Done in the revised manuscript.

7) P. 2, l. 19: likely an artefact

AUTHOR'S REPLY:
Done in the revised manuscript.

8) P.2, l. 29: the masking came mainly from the lower precision of the older versions of the CRDS instruments

AUTHOR'S REPLY:
We have emphasized the lower precision from the older versions of the CRDS instruments. However, we also think that the characterisation method (number of standards used, dry gas supply, etc) is another important factor. Therefore we have stated both factors in the revised manuscript.

9) P. 3, l. 19: Eq. 1: missing factor 2 for the H216O concentration in the denominator. Or alternatively write the equation for the atomic ratio.

AUTHOR'S REPLY:
Because laser spectrometry measures the absorption intensity of the isotopic water molecules, we use the definition of molecular isotope ratio here. Therefore the factor 2 is not needed. We have made it clear that we are using the definition of molecular isotope ratio in the revised manuscript.

10) P. 5, l. 3: here the "measurement uncertainty" is mentioned but it is unclear what the authors mean. The uncertainty of the estimated drift?

AUTHOR'S REPLY:
Have replaced the "measurement uncertainty" with "the uncertainty associated with the estimated drift".

11) P. 5, l. 22: a humidity step

AUTHOR'S REPLY:
Done in the revised manuscript.

12) P.5, l. 27: with the SDM

AUTHOR'S REPLY:
Done throughout the revised manuscript.

13) P. 5, l. 29: again not clear what "measurement uncertainty" is, I would rather say that this is the uncertainty associated with the estimated drift.

AUTHOR'S REPLY:
Have replaced the "measurement uncertainty" with "the uncertainty associated with the estimated drift".

14) P.6, l. 21: replace "may have" by "have": the type of dry gas supply has an influence that's a fact, there are several studies showing this: Aemisegger et al. 2012 is one but several others show this as well: Casado et al. 2016, Johnson and Rella 2017 including other greenhouse gas CRDS studies (Chen et al. 2010, Nara et al. 2012, Long et al. 2013). These studies recommend to perform CRDS calibrations for atmospheric observations in natural air backgrounds or to develop transfer functions that translate between the calibration and observation backgrounds (Johnson and Rella 2017).

AUTHOR'S REPLY:
Done in the revised manuscript. Have also included a reference to some of the cited studies.

15) P.6, l. 24: The use of several drying units in a row, vertical arrangement of drying units to prevent preferential gas flow and careful handling of tubing tightness usually provides the same background humidity as with a gas cylinder.

AUTHOR'S REPLY:
We have added this point in the revised manuscript. Kurita et al. 2012 obtained dry air with mixing ratios < 10 ppmv using two drying units in a row.

16) P. 7, l.10: what is the residence time of the sample within the system?

AUTHOR'S REPLY:
Referring to the reply to issue 4b) above, the residence time/response time of the system is estimated to be in the order of 1 min (i.e., 35 cm³ / 35 sccm) within the Picarro analyzer at standard pressure. We have included the flow rate number in this context.

17) P.7, l.25-30: this sounds like a lot of repetition from the methods section.

AUTHOR'S REPLY:
This paragraph has been shortened by removing repetitions.

18) P.11, l.14: as mentioned in the major comments, I don't think -40‰ is a physically sensible value. Even with extremely high ice supersaturation, I would not expect such low dexcess values in vapour to occur. Particularly in the context of the conclusion drawn on p. 20, l. 17 a careful check of the data would be appreciated here.

AUTHOR'S REPLY:
We are also aware of these low d-excess values. As mentioned in the reply to major comment 4a) and 4b) above, this is most

likely an artefact caused by the dephasing of d18O and dD profile. In the revised manuscript, this aspect has been addressed by shifting the dD profile by 30 seconds forward and using a one-min averaged profile. Ultimately, however, this artefact will not affect the conclusion of this study, since we do not attempt to interpret the isotope profile in terms of processes, but rather focus on the impact of the different correction schemes across a range of isotope composition and mixing ratios, especially at the level above 2000 m (where the d-excess profile depicts normal values).

19) P.13, l. 3: consequently, the measurements after calibration are. . ."

AUTHOR’S REPLY:
Done in the revised manuscript.

20) P.13, l.19: remove "relatively" (see my minor comment 3 above)

AUTHOR’S REPLY:
Done in the revised manuscript.

21) P. 14, l. 24: replace "substantially" by "substantial"

AUTHOR’S REPLY:
Done in the revised manuscript.

22) P. 15, l. 1 (& at other instances): I don’t particularly like the "heavy-enriched" and "heavy-depleted" formulation and have not seen it elsewhere. I actually find it slightly confusing. But this is a matter of taste.

AUTHOR’S REPLY:
We have replaced these terms by "enriched" and "depleted" respectively.

23) P. 16, l. 17 around the 1H218O and H216O absorption peaks, d18O is a derived Variable.

AUTHOR’S REPLY:
Done in the revised manuscript.

24) P. 16, l. 28: replace "by" by for

AUTHOR’S REPLY:
Done in the revised manuscript.

25) P. 17, l. 8: that does not

AUTHOR’S REPLY:
Done in the revised manuscript.

26) P. 17, l. 27 of the same

AUTHOR’S REPLY:
Done in the revised manuscript.

27) P. 19, l.13: this is inconsistent with what is described on p. 6, l. 21 (see also my minor comments 14 & 15).

AUTHOR'S REPLY:
We have revised the section with respect to dry gas supply and address the discrepancy in the characterisation results between dry air and N2, especially for d18O.

28) P. 19, l. 30 replace "humidify" by "humidity"

AUTHOR'S REPLY:
Done in the revised manuscript.

29) P. 20, l. 4: I find this recommendation a bit random because the number of standards to be used certainly depends on the application and the correction function of each individual instrument.

AUTHOR'S REPLY:
We have revised the recommendation such that the standard waters that span the full range of ambient vapour isotope compositions are recommended to determine the isotope composition-mixing ratio dependency surface.

30) Figures: 30a) Fig. 3: would a log scale for the x-axis help to make this Figure more effective? Furthermore, could the authors add an uncertainty estimate (contours) of the fit. I assume the uncertainty is also much larger at low humidities (due to a combined effect of less data points and lower precision of the measurements).

AUTHOR'S REPLY:
The log scale has not made the figure more effective, since there are only two data points below 1000 ppmv. A plot with normal scale is also more consistent with the previous figures. The uncertainty estimate has been added.

30b) Are the GSM1 ascent fit in Fig. 9b,c really correct? The fit seems not particularly good from eye.

AUTHOR'S REPLY:
We have checked and made sure the fit is correct in the revised manuscript.

~~Impact~~ Correcting the impact of isotope composition on the ~~humidity~~ mixing ratio dependency ~~correction~~ of water vapour isotope measurements with ~~infra-red~~ cavity ~~ring-down~~ ring–down spectrometers

Yongbiao Weng[1,2], Alexandra Touzeau[1,2], and Harald Sodemann[1,2]

[1]Geophysical Institute, University of Bergen, Bergen, Norway

[2]Bjerknes Centre for Climate Research, Bergen, Norway

Correspondence to: Yongbiao Weng (yongbiao.weng@uib.no)

Abstract.

~~Advances in laser spectroscopic techniques now enable high-frequency~~ Recent advances in laser spectroscopy enable high frequency in situ measurements of the water vapour isotope composition~~on platforms such as ship and aircraft. However, the isotope compositions and the *d*-excess measured by this technique~~ . At low water vapour mixing ratios, however, the measured stable water isotope composition can be substantially affected by ~~water concentrations, especially at low humidity. This measurement artefact is~~ a measurement artefact known as the ~~"humidity dependency", and is commonly corrected for uniformly across all isotope compositions~~mixing ratio dependency, which is commonly considered independent of isotope composition. Here we systematically investigate ~~the behaviour of the humidity dependency on~~ how the mixing ratio dependency of three commercial cavity ~~ring-down spectrometers for different water standards within a humidity range of 500 to 23'000~~ring–down spectrometers is affected by isotope composition in a range from 500 to 23′000 ppmv. We find that the ~~isotope compositions of measured water do have a substantial~~ water vapour isotope composition has a substantial and systematic impact on the ~~shape of the humidity dependency at low humidity (below 4'000 ppmv)~~mixing ratio dependency for all three analysers, in particular at mixing ratios below 4′000 ppmv. This isotope composition dependency can ~~, for example, create an offset of $\pm$0.5 and $\pm$6~~ create a deviation of $\pm$0.5 and $\pm$6.0 ‰ for δ^{18}O and δD ~~at $\sim$2'000 ppmvin the case of a Picarro L2130-i~~respectively at $\sim$ 2′000 ppmv, resulting in ~~an offset of 2–3~~ about 2–3 ‰ deviation for the *d*-excess. ~~We show that the combined isotope composition–humidity dependency can be expressed by a surface function, which allows to build a correction framework. The impact of this correction is illustrated for a case of aircraft measurements and ship-based measurements in cold environments. A systematic~~ An assessment of the robustness of our findings ~~for three laser spectrometers shows overall constant behaviour with time (for periods ranging from one month~~ shows overall reproducible behaviour over up to two years ~~),~~ for different dry gas supplies, while being independent of the method ~~of characterisation (discrete liquid injection and continuous vapourstreaming), dry gas supply (N_2 and synthetic air), or the sequence of humidity levels~~for generating the water vapour, and to first order of the evaluation sequence. We propose to replace univariate mixing ratio dependency corrections by a new combined isotope composition–mixing ratio dependency correction. Using aircraft and ship-based measurements in an Arctic environment,

we illustrate the most relevant application of the correction. Based on our ~~analysis, we recommend a procedure for the characterisation and subsequent correction of~~ findings, we suggest that the dependency on isotope composition may be primarily related to spectroscopy. Repeatedly characterising the combined isotope ~~composition–humidity dependency for this type~~ composition–mixing ratio dependency of laser spectrometers when performing water vapour measurements in ~~cold and dry conditions~~the Arctic, at high elevation, or on aircraft, appears critical for enabling reliable data interpretation in dry environments.

1 Introduction

Stable water isotopes (hydrogen and oxygen) are natural tracers in the atmosphere and hydrosphere, and have long been used to improve our understanding of the hydrological cycle and climate processes (Dansgaard, 1953, 1954; Gat, 1996). Advances in laser ~~spectroscopic techniques now allow high-frequency~~ spectroscopy now allow high frequency in situ measurements of ~~isotope compositions~~ the isotope composition of water vapour in the atmosphere (Kerstel, 2004; Kerstel and Gianfrani, 2008). One commercially available ~~instrument of this type~~ type of instrument is the Cavity ~~Ring-Down~~ Ring–Down Spectrometer (CRDS) manufactured by Picarro Inc., USA. The measurement principle of CRDS is based upon the absorption of a laser pulse at a wavelength specific to a given isotopologue (Crosson, 2008). The ~~CRDS has~~ L2130-i and L2140-i CRDS analysers have an optimal performance within a ~~humidity range of 19'000~21'000 ppmv , where~~ water vapour mixing ratio of $19'000 \sim 21'000$ ppmv (parts per million by volume), where high signal-to-noise ratios enable precise measurements. ~~Beyond this optimal humidity range~~ This range is typically maintained during liquid sample analysis. In situ measurements of the atmospheric water vapour isotopes are not constrained to this optimal mixing ratio range (Gupta et al., 2009). At lower water vapour mixing ratios, the measurement uncertainty increases due to weaker absorption, and thus lower signal-to-noise ratios. Additionally, outside of this range, the measurement suffers from a ~~bias depending on the humidity level. While liquid measurements are performed within the optimal humidity range, in situ water vapour measurements in the atmosphere are commonly not constrained to this optimal humidity range. The fact that the humidity in the atmosphere~~ mixing ratio-dependent deviation of the isotope composition. Since atmospheric mixing ratios can vary from below 500 ppmv in ~~cold and~~ dry regions (e.g., polar regions or the middle and upper troposphere) to ~~about 30'000 ppmv in warm and~~ $30'000$ ppmv or more in humid regions (e.g., tropics)~~requires~~, an appropriate correction to this ~~*humidity*~~ *mixing ratio* *dependency* for high-quality in situ measurements of atmospheric water vapour is required (e.g., Aemisegger et al., 2012; Bonne et al., 2014).

~~Humidity dependency , sometimes named~~ The water vapour mixing ratio dependency (hereafter *mixing ratio dependency*), sometimes also named humidity–isotope response (Steen-Larsen et al., 2013, 2014) or concentration dependency (Wen et al., 2012; Bailey et al., 2015) ~~or water vapour mixing ratio dependency (Aemisegger et al., 2012) of infra-red~~ of infrared laser spectrometers for water isotopes ~~is a prominent source of measurement bias and~~ has been described in numerous studies ~~(e.g., Lis et al., 2008; Schmidt et al., 2010; Sturm and Knohl, 2010; Steen-Larsen et al., 2013, 2014; Bastrikov et al., 2014)~~(e.g., Lis et al.,
. Many studies found the ~~humidity~~ mixing ratio dependency to be nonlinear and to some extent specific to both the instrument used and the isotope composition measured. For example, reviewing the then available ~~characterisation systems~~ systems for vapour generation on a Picarro L1115-i and L1102-i, Wen et al. (2012) showed that the ~~humidity~~ mixing ratio dependency could

vary for each specific instrument. Aemisegger et al. (2012) demonstrated that the ~~humidity dependency is different~~ mixing ratio dependency varies for different instrument types and generations, and ~~found that a dry gas supply of dried ambient air using a dry unit (Drierite) or synthetic dry air from a gas cylinder can affect the humidity dependence behaviour~~is affected by the matrix gas used during calibration. However, ~~they~~ these authors did not find a substantial impact of the isotope composition ~~after~~ when testing four different standards. Bonne et al. (2014) ~~suspect the different humidity~~ speculated that the different mixing ratio dependency functions at low ~~humidity levels (below 2'000~~ mixing ratios (below 2′000 ppmv) for their two working standards ~~to be likely~~ are likely an artefact of residual ~~humidity in the dry air dried by Drierite. Bailey et al. (2015) shows that the humidity dependence is~~ water vapour after using a molecular sieve. Bailey et al. (2015) found mixing ratio dependency to be clearly different for ~~the tested three~~ three tested standard waters, while emphasizing the uncertainty from statistical fitting where the characterisation data are infrequent. Sodemann et al. (2017) found a substantial impact of ~~the humidity~~ a mixing ratio dependency correction when processing aircraft measurements of d-excess over the Mediterranean, but did not account in detail for different isotopic standards. Bonne et al. (2019) ~~has characterised the humidity~~ characterised the mixing ratio dependency of their ~~isotope measurements throughout the Atlantic and Arctic Oceans~~ ship-based water vapour isotope measurements using four water standards, noting a dependency of the mixing ratio dependency on isotope standard. They did not observe ~~any~~ a significant drift for the dependency for measurements separated by several months. ~~However, they found that the humidity dependency does depend on the isotopic standard used.~~

To summarize, ~~in these previous studies ,~~ only some previous studies have recognized the impact of the isotope composition of measured standards on ~~humidity dependence has not been recognized~~ the mixing ratio dependency as a significant ~~bias source, or has so far not been systematically investigated, in particular for very low humidities. We hypothesize that a potential isotope composition dependence could have been masked by the different versions of the laser spectrometers and the different characterisation methods (e.g., characterisation system, dry gas supply, etc.) used in these studies.~~ uncertainty source. More importantly, so far no systematic investigation of the influence of the isotope composition on the mixing ratio dependency has been conducted. Given the potentially large impact of such corrections at very low water vapour mixing ratios, this is an important piece required for enabling the reliable interpretation and comparison of measurements at dry conditions, such as the Arctic, high elevation regions, or from research aircraft.

Here we ~~carry out~~ present a systematic analysis ~~on the humidity dependence behaviour of three~~ of the impact of isotope composition on the mixing ratio dependency for three commercial CRDS analysers, one Picarro L2130-i and two Picarro L2140-i~~. Using~~ , using five standard waters with different isotope compositions~~, we characterise the impact of isotope composition of the standard water on the humidity dependence behaviour for each analyser. Based on the characterised isotope composition–humidity dependence, a correction scheme is developed.We then identify~~ . Methods and data are presented in Sec. 2. Using the measurements from one analyser, we demonstrate the characterisation of the isotope composition–mixing ratio dependency in Sec. 3. We then evaluate the robustness of the isotope ~~composition–humidity dependence across~~ composition–mixing ratio dependency across the three analysers, ~~two characterisation methods, two dry gas supplies, two~~ considering as well the different vapour generators, matrix gas compositions, measuring sequences, and ~~with respect to time at monthly to yearly time scales.Finally, we demonstrate the~~ temporal stability (Sec. 4). A new correction scheme is proposed in Sec. 5. Using water vapour isotope measurements from aircraft and ship acquired during the IGP measurement campaign in the Iceland-Greenland Seas (Renfrew et al., 2019) as a test case, we investigate in Sec. 6 the potential impact of the ~~humidity dependence correctionon the vapour measurement during a cold air outbreak event and an aircraft campaign, and~~ isotope composition–mixing ratio dependency correction. We then discuss the potential sources of the dependency of the mixing ratio dependency on isotope composition (Sec. 7). Finally, we provide recommendations on how to apply the correction scheme to other analysers ~~.~~ (Sec. 8).

2 Methods and data

~~Because of the large impact of the correction on a range of measurement at the low humidity where instrument noise is high, in this section we carefully test the validity across a range of possible influencing factors, thereby excluding possible artefacts. These influencing factors include the method to generate the vapour, the specific analyser that is used , the potential instrument drift over time, the possible artefacts introduced by the matrix gas and the measuring sequence of the humidity steps. We have therefore designed in total 14~~ This section introduces the terminology used throughout the manuscript, the measurement principle of the used instruments, and provides an overview of the total 15 experiments (Table 1) ~~to evaluate all these factors~~ that have been conducted to evaluate the potential influencing factors on the isotope composition–mixing ratio dependency separately and repeatedly. These ~~14~~ 15 experiments can be separated into five categories with respect to their aims (Table 3). With these five categories, we assess influencing factors including the dependence on vapour generating method, the dependence on the ~~tested~~ specific instrument, the long term stability of the dependence behaviour, the influence from dry gas ~~supply~~ matrix and the influence from the measuring sequence. In the end, we introduce the in situ measurement data that are used to illustrate the impact of correction.

2.1 ~~Quantification of the isotope composition and $\Delta\delta$ notation~~Terminology

The abundance of stable water isotopes in a reservoir is quantified ~~by isotope ratios, defined as the ratio of concentrations of the heavy, rare isotopologue~~ as the concentration ratio of the rare ($HD^{16}O$ or $H_2^{18}O$) to the abundant ~~, light~~ isotopologue ($H_2^{16}O$). ~~For example, the isotope ratio~~ Note that the definition here is referred as molecular isotope ratio, as measured by laser spectrometry. This definition can be shown to be equal in first-order to the atomic isotope ratio determined by mass spectrometry (Mook et al., 2001). The (molecular) isotope ratio of hydrogen in a water reservoir~~is~~, for example, is then:

$$^{2}R = \frac{[HD^{16}O]}{[H_2^{16}O]}. \tag{1}$$

~~The absolute value of R is very small (typically consisting of 5–6 digits). In addition, the absolute ratios are in principle less relevant than the changes in ratios occurring during phase transitions. Therefore, an isotope~~ Isotope abundance is generally reported as a deviation of the isotope ratio of a sample relative to that of a standard, known as δ ~~notation:~~

$$\cancel{\delta = \frac{R_{\text{sample}} - R_{\text{standard}}}{R_{\text{standard}}} \cdot 1000\,‰.}$$

~~A δ valuefor water isotopes is generally indicated in~~ value, and commonly expressed in units of per mil (‰) ~~relative to the internationally accepted~~ deviation from Vienna Standard Mean Ocean Water (~~VSMOW2) ,~~ V-SMOW) distributed by the International Atomic Energy Agency ~~(IAEA) at Vienna (IAEA, 2009); it is directly used to represent the isotope composition of the water sample.~~ (IAEA, 2009):

$$\delta = \frac{R_{\text{sample}} - R_{\text{standard}}}{R_{\text{standard}}} \cdot 1000\,‰. \qquad (2)$$

The magnitude of the ~~bias~~ deviation introduced by the ~~humidity dependence appears to be~~ mixing ratio dependency is typically at least one order ~~smaller~~ of magnitude less than the span of the isotope compositions of the measured standards. To focus on the ~~bias dependency on humidity, we introduce here the $\Delta\delta$ notation, defined as the~~ deviation of the measured isotope compositions at various ~~humidities~~ mixing ratios (δ_{meas}) from the isotope composition at a reference ~~humidity~~ mixing ratio (δ_{ref})~~:~~ , we use the $\Delta\delta$ notation, which is defined as:

$$\Delta\delta = \delta_{\text{meas}} - \delta_{\text{ref}}. \qquad (3)$$

~~The reference humidity is chosen to be 20'000 ppmv where the CRDS provides optimal performance~~

We choose 20′000 ppmv as reference level, within the nominal optimal performance range of the CDRS analyser. The isotope composition at ~~20'000 ppmv is~~ the exact value of 20′000 ppmv is thereby obtained by a linear interpolation between the closest measurements above and below ~~20'000~~ 20′000 ppmv (mostly between ~~19'000 and 21'000~~ 19′000 and 21′000 ppmv). Note that all ~~the presented humidities~~ mixing ratios reported in this study are ~~raw~~ direct (raw) measurements from the CRDS, ~~since the humidity~~ and that the isotope–mixing ratio dependency correction is applied to raw data before calibration.

While $\Delta\delta^{18}$O and $\Delta\delta$D are given directly by the definition above, ~~Δd-excess is a secondary parameter that~~ the deviation for the secondary parameter d-excess $= \delta\text{D} - 8 \cdot \delta^{18}\text{O}$ (Dansgaard, 1964) is obtained from calculation: ~~firstly we calculate d-excess at each data point from corresponding~~ Δd-excess $= \Delta\delta\text{D} - 8 \cdot \Delta\delta^{18}\text{O}$.

2.2 Instruments

The instruments investigated in this study include two Picarro L2140-i (serial numbers HKDS2038 and HKDS2039) and one Picarro L2130-i (serial number HIDS2254) (all from Picarro Inc, Sunnyvale, USA). Hereafter, we refer to each instrument with their serial number. The instruments report at a data rate of ∼1.25 Hz and with a air flow of ∼ 35 sccm through the cavity. To minimize instrument drift and errors from the spectral fitting, these CRDS systems precisely control the pressure and temperature of their cavities to be at 80 ± 0.02 °C and 50 ± 0.1 Torr. For the spectral fitting, the instruments target three absorption lines of water vapour in the region 7199–7200 cm^{-1} (Steig et al., 2014). In CRDS, a laser saturates the measurement cavity at one of the selected absorption wavelengths. After switching the laser off, a photodetector measures the decay (ring–down) of photons leaving the cavity through a semi-transparent mirror. The ring–down time is then proportional to the absorption at a specific part of the spectrum, and used to obtain the water vapour isotopologue concentration in the cavity from spectral fitting. A single data point consists of 300–400 ring downs. At lower water vapour concentrations, the signal-to-noise ratio decreases, and fitting algorithms are affected by various error sources (see Sec. 7). As a custom modification, the L2130-i with serial number HIDS2254 operates with two additional lasers, that allows for rapid switching between the three target wavelengths, enabling a higher (5 Hz) data acquisition rate, and larger cavity flow rates than a regular L2130-i. In the present study, we used the flow rates and measurement frequency as for regular L2130-i analysers. The L2130-i use peak absorption for the spectral fitting, whereas the L2140-i uses an areal integral of the absorption within the spectral features (Steig et al., 2014). The L2140-i is therefore substantially less sensitive to pressure broadening and narrowing of the absorption lines, for example due to changes in the matrix gas which can affect older-generation analysers, such as the L2120-i (Johnson and Rella, 2017). Manufacturer specifications commonly state a measurement range for vapour of $1'000$ to $50'000$ ppmv. As a custom modification, all instruments used here have been calibrated by the manufacturer down to 200 ppmv with a not further specified procedure.

Water vapour measurements with these instruments have a total error budget that involves the uncertainty from the calibration standards projecting onto the VSMOW2–SLAP2 scale, and from the time averaging employed on the native time resolution data. The Allan deviation quantifies the precision depending on averaging time interval. Previous studies found typical Allan deviations < 0.1 ‰ for δ^{18}O, and ~ 0.1 ‰ for δD at $15'700$ ppmv for averaging times of 1–2 min for the L2130-i (Aemisegger et al., 2012), and similar values for these averaging times for the L2140-i (Steig et al., 2014). Any corrections for the mixing ratio dependency are applied to the raw data at native time resolution. The uncertainty of any correction is thereby given by a combination of the averaging time of the vapour measurements at a given mixing ratio, and the uncertainty of the employed calibration standards.

2.3 Standard waters

To identify the influence of isotope composition on the mixing ratio dependency, we have used multiple internal standard waters calibrated on the international VSMOW2–SLAP2 scale to characterise the mixing ratio dependency. The standard waters include four laboratory standards in use at Facility for Advanced Isotopic Research and Monitoring of Weather, Climate and Biogeochemical Cycling (FARLAB), University of Bergen and three laboratory standards in use at the Isotope Laboratory of University of Iceland (UI) (Table 2). For the FARLAB standards, one is obtained from snow in Greenland (GSM1), one made of mountain snow from Norway (VATS), one that consists of deionized tap water at Bergen (DI) and one made of evaporated DI water (EVAP). Besides the four laboratory standards, we have also used an even mixing between GSM1 and VATS (named MIX) and the uncalibrated deionized tap water (TAP). For the UI standards, one is from snow at NEEM ice core drilling site in Greenland (NEEM), one consists of groundwater in Reykjavik (GV) and one made of Milli-Q purified water based on ocean water from Bermuda (BERM). The isotope compositions of all the used waters span from -33.52 to 5.03 ‰ for δ^{18}~~O and~~ O, and from -262.95 to 6.26 ‰ for δ~~D with the definition d-excess = δD − 8 · δ^{18}O (Dansgaard, 1964); then we obtain Δd-excess by calculating the deviation of the d-excess at each data point from the d-excess at the reference humidity (20'000 ppmv)~~ D (Table 2). ~~The obtained $\Delta\delta^{18}$O, $\Delta\delta$D and Δd-excess are used to determine isotope composition–humidity dependencyfunctions in Sect. 3 and Sect. 5.~~

2.4 ~~Characterisation~~ Vapour generation methods

We ~~have used~~ use two methods to ~~characterise humidity dependence behaviour~~ generate vapour for characterizing the isotope composition–mixing ratio dependency of the three instruments~~: ,~~ , namely discrete liquid injections and continuous vapour streaming. These are essentially two ways of generating a vapour sample to be analysed by the ~~spectrometer~~infrared spectrometers. Both methods ~~require~~ involve injection of a liquid standard water into a heated evaporation chamber where the injected water is completely evaporated and mixed with a dry ~~carrier gas. The former method generates a fixed amount of vapour sample by a single injection from a syringe, while the latter one continuously delivers liquid water from a syringe pump, and generates a continuous vapour stream lasting in practice 20–30 min~~matrix gas.

2.4.1 Dry gas supply

Previous studies for Picarro CRDS analysers preceding the L2140-i show that the matrix gas has an influence on the characterisation of mixing ratio dependence on the CRDS isotope measurement of water vapour (Aemisegger et al., 2012; Johnson and Rella, 2017) . It is therefore important to know the influence of the matrix gas on the isotope composition–mixing ratio dependency to determine a preferred method for obtaining the final correction relationship depending on measurement situation. The manufacturer recommends a customer-supplied gas drying unit (e.g. Drierite desiccants) to supply dry gas for the SDM unit. Here, we either used a single drying unit with ambient air, or dry gas cylinders that contain synthetic air (synthetic air 5.5, purity 99.9995 %, Praxair Norge AS) or N_2 (Nitrogen 5.0, purity $>$ 99.999 %, Praxair Norge AS). We have tested the three types of dry gas supply with the characterisation on instrument HIDS2254 for continuous vapour streaming and characterized the three analysers using synthetic air and/or N_2 for discrete liquid injections. Ambient air dried through Drierite can still contain some moisture (typically about 200 ppmv when the ambient water vapour is around 10′000 ppmv), which can contribute a non-negligible fraction to the measured isotope composition at low mixing ratios (e.g., 10 % below 2′000 ppmv). The use of several drying units in a row, vertical arrangement of drying units to prevent preferential gas flow and careful handling of tubing tightness may provide the same background mixing ratio as with a gas cylinder (Kurita et al., 2012), but has not been tested here.

2.4.2 Discrete liquid injections

~~Standard water is injected~~ The discrete liquid injections repeatedly generate vapour pulses by injecting between 0-2μl of standard water from 1.5 ml PTFE/rubber-septum sealed vials with a ~~10 μl~~ 10 μl syringe (VWR, Part No.: 002977). Injections are operated by an autosampler (A0325, Picarro Inc, USA) or by manual injection. Vaporization of liquid water is achieved within a Picarro vaporizer (A0211, Picarro Inc, USA) set to ~~110 °~~110 °C. The vaporizer ~~then obtains synthetic air (synthetic air 5.5, purity 99.9995%, Praxair Norge AS)~~ mixes the water vapour with synthetic air or N_2 ~~(Nitrogen 5.0, purity > 99.999%, Praxair Norge AS)~~ from a gas cylinder at a pressure set to ~~~2.5~~ $\sim$ 2.5 psi. The vaporizer chamber seals off for a few seconds to allow sufficient mixing between vapour and ~~dry air~~the matrix gas, before delivering the mixture to the analyser at a highly stable ~~humidity level~~mixing ratio.

Each time before switching to a new standard water, ~~8–12~~ 8–12 injections of the new standard water at a ~~humidity level of ~20’000~~ mixing ratio of $\sim 20'000$ ppmv were applied to account for memory effects from the previous injections. Then the sequence begins from the lowest (~~~500~~ ~ 500 ppmv) and ends to the highest (~~~ 23’000 ppm) humidity level. Various humidity levels~~ $\sim 23'000$ ppmv) mixing ratio. Various mixing ratios are obtained by adjusting the injection volume in the ~~10 μl~~ 10 μl syringe. Injection volume was modified to be between 0.05 and 2.5 μl with a step of ~~0.05 μl~~0.05 μl, resulting in ~~humidity levels between approximately 500 and 23’000~~ mixing ratios between approximately 500 and $23'000$ ppmv with a step of ~~~450~~ ~ 450 ppmv. Four injections in high precision mode (longer measurement period, approximate 10 min per injection) were applied at each ~~humidity level~~mixing ratio, and the last three injections were then averaged for further analysis. Injections with an injection volume of ~~2 μl (~19’000~~ 2 μl ($\sim 19'000$ ppmv) were carried out at the beginning and end of a sequence to account for potential instrument drift. A sequence for one standard water approximately lasts 35 hours. The instrument drift within a sequence has typically a magnitude of ~~0.05±0.02~~0.05 ± 0.02‰, ~~0.7±0.1~~ 0.7 ± 0.1 ‰ and ~~0.4±0.1~~ 0.4 ± 0.1 ‰ for δ^{18}O, δD and d-excess, respectively. The drift is ~~3–7~~ 4–7 times larger than the ~~measurement uncertainty~~ uncertainty associated with the estimated drift but one order smaller than the ~~bias~~ deviation introduced by the ~~humidity dependence~~mixing ratio dependency; it is corrected by assuming a temporal linearity during the sequence period.

Manual liquid injections were carried out during a field deployment where no autosampler was available. During manual injections, it is challenging to maintain a constant injection volume, and thus difficult to achieve precise ~~humidity levels~~control of water vapour mixing ratios. In this case, only injection volumes between ~~0.2 and 1.6 μl~~ 0.2 and 1.6 μl with a step of ~~~0.2 μl are employed(~~~ 0.2 μl are employed, roughly corresponding to ~~humidity levels between 2’400 and 24’000~~ mixing ratios between $2'400$ and $24'000$ ppmv with a step of ~~~3’000 ppmv). With fewer steps, a sequence for one standard water with manual injection only lasts about 6 hours.~~ $\sim 3'000$ ppmv. Despite the shorter measurement period (about 6 hours), the instrument drift within a sequence increased by a factor of ~~2–3~~ 2–3 for δ^{18}O (0.16 ± 0.03 ‰) and δD ~~, being 0.16±0.03~~ (1.65 ± 0.18 ‰~~ and 1.65±0.18‰ respectively~~), resulting in a drift of ~~0.37±0.22~~ 0.37 ± 0.22 ‰ for d-excess. The relatively high instrument drift compared to the autosampler injections in the laboratory is most likely due to the uncertainty introduced by the ~~inconstant injection volumeand the installation on a mobile platform (~~variable injection volume, and the operation on a container on the deck of a research vessel ~~in our case). The drift is again~~ (Renfrew et al., 2019). Instrument drift is corrected by assuming ~~a temporal linearity during the sequence period~~linear drift during each characterisation experiment. In all characterisation experiments, we applied three to five FARLAB standard waters when using an autosampler, or three UI standard waters in the case with manual injections.

2.4.3 Continuous vapour streaming

To test the influence of the vapour generation method, we used continuous water vapour streaming of two laboratory standard waters (DI and GSM1). A continuous vapour stream is generated via a so-called standard delivery module (SDM, A0101, Picarro Inc, USA). The SDM is a device with two syringe pumps, that provides automated delivery of two standard waters at up to three water concentrations per standard. The standard water is delivered to the Picarro vaporizer, where the standard water is instantly vaporized at ~~140 °C~~ 140 °C and simutaneously mixed with ~~dry gas. Various humidity levels between 600 ppmv~~

~~and 24'000~~ a dry matrix gas. The routines for vapour streaming at different mixing ratios applied here follow recommendations by the manufacturer to characterize each instrument's mixing ratio dependency (SDM user manual, Picarro Inc). Mixing ratios between 600 ppmv and 24′000 ppmv were obtained by adjusting liquid water injection speed of the syringe pumps from ~~0.002 $\mu l\,s^{-1}$ to 0.8 $\mu l\,s^{-1}$~~ $0.002\ \mu l\,s^{-1}$ to $0.8\ \mu l\,s^{-1}$. The generated standard vapour is continuously delivered to and measured by the spectrometer. During the characterisation, we measured a total of about ~~25 humidity levels with an humidity step of ~1'000 ppmv (0.003$\mu l\,s^{-1}$) have been measured~~ 25 mixing ratios at a step of $\sim 1'000$ ppmv ($0.003\ \mu l\,s^{-1}$) for each standard water. Each ~~humidity level~~ mixing ratio is measured for ~~20–40~~ 20–40 minutes and the averaged value of a ~~5~~ 5 minutes period close to the end of the measurement is used in the analysis. Due to unstable calibration performance, only ~~1–2~~ 1–2 min long sections were used for the characterisations done in July 2016 and Feb 2018 for the laboratory standard DI on instrument HIDS2254.

A measurement sequence of standard GSM1 with ambient air dried through Drierite shows that the magnitude of the instrument drift during a ~~22~~ 22 hour measurement with the SDM is similar to that of the liquid injection with an autosampler. However, due to the lower precision with the SDM measurement, the instrument drift is comparable (~~0.10±0.09~~ 0.10 ± 0.09 ‰ and ~~0.96±0.36~~ 0.96 ± 0.36 ‰ for δ^{18}O and δD respectively) or smaller (~~0.24±0.78~~ 0.24 ± 0.78 ‰ for d-excess) compared to the ~~measurement uncertainty~~ uncertainty associated with the estimated drift. Therefore, except for the measurement with standard GSM1 above, the measurements with the SDM are not corrected for instrument drift.

~~The instruments investigated in this study include two Picarro L2140-i (serial numbers HKDS2038 and HKDS2039) and one Picarro L2130-i (serial number HIDS2254), the latter being custom-modified with an option for higher data acquisition and flow rate. Hereafter, we refer to each instrument with the corresponding serial number. To convert observed absorption intensity to actual water concentration and to minimize instrument drift, these CRDS systems precisely control the pressure and temperature of their cavities to be at 80C and 50 Torr. The typical measurement range for vapour is 1'000 to 50'000 ppmv (certified down to 200 ppmv for the instrument HIDS2254). During the experiments, all instruments were running in low flow mode with a sample inlet flow rate of ~35 sccm and a measurement frequency of ~1.25 Hz.~~

2.5 ~~Standard waters~~

~~To identify the dependency on the isotope composition, we have applied multiple internal standard waters to characterise the humidity dependence. The standard waters include four laboratory standards in use at Facility for Advanced Isotopic Research and Monitoring of Weather, Climate and Biogeochemical Cycling (FARLAB), University of Bergen and three laboratory standards in use at the Isotope Laboratory of University of Iceland (UI) (Table 2). For the FARLAB standards, one is obtained from snow in Greenland (GSM1), one made of mountain snow from Norway (VATS), one that consists of deionized tap water at Bergen (DI), one made of evaporated DI water (EVAP). Besides the four laboratory standards, we have also used an even mixing between GSM1 and VATS (named MIX) and the uncalibrated deionized tap water (DI (tap)). For the UI standards, one is from snow at NEEM ice core drilling site in Greenland (NEEM), one consists of groundwater in Reykjavik (GV) and one made of Milli-Q purified water based on ocean water from Bermuda (BERM). The isotope compositions of all the used waters span from −33.52 to 5.03 and from −262.95 to 6.26~~ In situ measurement data for ~~δ^{18}O and δD respectively (Table 2).~~

~~For the measurement using discrete liquid injection, we applied 3–5 FARLAB standard waters with an autosampler and three UI standard waters with manual injections. As the continuous vapour streaming is primarily used for testing the robustness of humidity dependence, we only applied the standards GSM1 and DI with this vapour generation method.~~

2.5 ~~Dry gas supply~~

~~The type of dry gas supply may have an influence on the characterisation of humidity dependence (Aemisegger et al., 2012). The manufacturer recommends a customer-supplied gas drying unit (e.g. Drierite desiccants) to supply dry gas for the SDM unit. However, the ambient air dried through Drierite can still contain a certain amount of moisture (typically below 200 ppmv when the ambient humidity is around 10'000 ppmv), which can contribute to the measured isotope ratio at low humidity levels (e.g., 10% below 2'000 ppmv). In most of our experiments we have replaced the gas drying unit to dry gas cylinders that contain synthetic air (synthetic air 5.5, purity 99.9995%, Praxair Norge AS) or N_2 (Nitrogen 5.0, purity > 99.999%, Praxair Norge AS). We have tested all the three types of dry gas supply with the characterisation on instrument HIDS2254 for continuous vapour streaming. We also carried out the test of synthetic air and N_2 for discrete liquid injections.~~

2.5 ~~In situ measurement data for studying the impact of isotope composition–humidity dependency correction~~

studying the impact of isotope composition–mixing ratio dependency correction]~~Instruments~~

~~The instruments investigated in this study include two Picarro L2140-i (serial numbers HKDS2038 and HKDS2039) and one Picarro L2130-i (serial number HIDS2254), the latter being custom-modified with an option for higher data acquisition and flow rate. Hereafter, we refer to each instrument with the corresponding serial number. To convert observed absorption intensity to actual water concentration and to minimize instrument drift, these CRDS systems precisely control the pressure and temperature of their cavities to be at 80C and 50 Torr. The typical measurement range for vapour is 1'000 to 50'000 ppmv (certified down to 200 ppmv for the instrument HIDS2254). During the experiments, all instruments were running in low flow mode with a sample inlet flow rate of ~35 sccm and a measurement frequency of ~1.25 Hz.~~

2.5 ~~Standard waters~~

~~To identify the dependency on the isotope composition, we have applied multiple internal standard waters to characterise the humidity dependence. The standard waters include four laboratory standards in use at Facility for Advanced Isotopic Research and Monitoring of Weather, Climate and Biogeochemical Cycling (FARLAB), University of Bergen and three laboratory standards in use at the Isotope Laboratory of University of Iceland (UI) (Table 2). For the FARLAB standards, one is obtained from snow in Greenland (GSM1), one made of mountain snow from Norway (VATS), one that consists of deionized tap water at Bergen (DI), one made of evaporated DI water (EVAP). Besides the four laboratory standards, we have also used an even mixing between GSM1 and VATS (named MIX) and the uncalibrated deionized tap water (DI (tap)). For the UI standards, one is from snow at NEEM ice core drilling site in Greenland (NEEM), one consists of groundwater in Reykjavik (GV) and one~~

~~made of Milli-Q purified water based on ocean water from Bermuda (BERM). The isotope compositions of all the used waters span from −33.52 to 5.03 and from −262.95 to 6.26~~ In situ measurement data for ~~δ^{18}O and δD respectively (Table 2).~~

~~For the measurement using discrete liquid injection, we applied 3–5 FARLAB standard waters with an autosampler and three UI standard waters with manual injections. As the continuous vapour streaming is primarily used for testing the robustness of humidity dependence, we only applied the standards GSM1 and DI with this vapour generation method.~~

2.5 ~~Dry gas supply~~

~~The type of dry gas supply may have an influence on the characterisation of humidity dependence (Aemisegger et al., 2012). The manufacturer recommends a customer-supplied gas drying unit (e.g. Drierite desiccants) to supply dry gas for the SDM unit. However, the ambient air dried through Drierite can still contain a certain amount of moisture (typically below 200 ppmv when the ambient humidity is around 10'000 ppmv), which can contribute to the measured isotope ratio at low humidity levels (e.g., 10% below 2'000 ppmv). In most of our experiments we have replaced the gas drying unit to dry gas cylinders that contain synthetic air (synthetic air 5.5, purity 99.9995%, Praxair Norge AS) or N_2 (Nitrogen 5.0, purity > 99.999%, Praxair Norge AS). We have tested all the three types of dry gas supply with the characterisation on instrument HIDS2254 for continuous vapour streaming. We also carried out the test of synthetic air and N_2 for discrete liquid injections.~~

2.5 ~~In situ measurement data for studying the impact of isotope composition–humidity dependency correction~~

studying the impact of isotope composition–mixing ratio dependency correction

~~To demonstrate~~ In order to test the impact of the isotope ~~composition–humidity dependence correction on the measurement~~composition–m ratio dependency correction on actual measurements, we applied the proposed correction scheme to two datasets obtained from in situ vapour measurements during the Iceland Greenland Seas Project (Renfrew et al., 2019) in March 2018 onboard ~~an aircraft~~ a research aircraft (analyser HIDS2254) and a research vessel ~~respectively (Renfrew et al., 2019)~~(analyser HKDS2038) in the Iceland-Greenland Seas (∼ 68°N;12°W).

The analyser HIDS2254 was ~~employed for the measurement onboard the~~ installed onboard a Twin Otter research aircraft. The instrument was fixed on a rack on the ~~left~~ right side of the non-pressurized cabin~~of a Twin Otter aircraft. A metal tube with 3/8~~. A 3.5 m stainless steel tube with 3/8 inch diameter, insulated and heated to ~~50~~ 50 °C, was ~~running from the analyser to~~ leading from a backward facing inlet located ~~slightly~~ behind the right cockpit door ~~. A rear-facing~~ to the analyser. A rearward-facing inlet was selected to ensure that only vapour (and not particles or droplets) would be ~~collected. A flush~~ sampled. A manifold pump was used to draw the vapour ~~from outside the aircraft into the cabin~~ through the inlet at a flow rate of about ~~5 slpm, from which the~~ 8 slpm. The HIDS2254 was taking a sub-sample ~~in low flow mode~~ through a 0.2 m stainless steel tubing in low-flow mode at a flow rate of ∼ 35 sccm. The selected vapour measurements from the aircraft were taken in the lower troposphere above the Iceland sea during a Cold Air Outbreak (CAO) on March 4, 2018. The ~~vapour measurement lasts 9 min and~~ particular water vapour measurement segment utilized here was taken during ~~descent period~~ a 9 min long descent of the aircraft ~~. Due to a situation of~~ from 2′900 m a.s.l. to 180 m a.s.l. A Greenland blocking associated ~~to~~ with northerlies in the Greenland-Iceland Seas ~~, the temperature during the flight was low,~~ caused cold atmospheric temperatures, with an average ~~temperature~~

~~of -12~~ of -12 °C at altitudes ~~lower than 200 m. Coherent with the low temperatures encountered, the humidity~~ below 200 m. Accordingly, mixing ratios at low levels ~~was ranging from 2'000 to 2'700 ppmv. Even lower humidity (down to about 900 ppmv) was observed at higher levels. Concurrent radiosonde ascent indicated a relative humidity at surface of around 80 % and saturated conditions from 800 to 2'000 m.~~were ranging from 2′000 to 2′700 ppmv. At higher levels, mixing ratios were as low as about 900 ppmv. After applying any correction schemes (see below), the water vapour isotope data from the aircraft are calibrated to the VSMOW2-SLAP2 scale using the long-term average of calibrations with internal FARLAB laboratory standards GSM1 and DI using the SDM before and after the flight survey (details described in a forthcoming publication).

For the vapour measurements onboard the research vessel (R/V Alliance), the analyser HKDS2038 was ~~employed. The analyser was~~ installed inside a heated measurement container which was placed on the ~~boat deck~~ crew deck at about 6 m above the water surface. The ambient air was drawn into the container with a flow rate around ~~5~~ 8 slpm by a ~~flush~~ manifold pump through a ~~5 m long tube~~5 m long 1/4 inch stainless steel tube, heated to about 50 °C by self-regulating heating tape. The tube inlet was mounted ~~4~~ 4 m above the boat deck, protected from precipitation with a downward facing tin can. The ~~entire tube was maintained at about 50 C by a heating tape. The selected~~ selected time period from the research vessel was ~~measured~~ acquired during a CAO event between March 14 and 16, 2018. At the beginning of the event, the ~~humidity dropped from 6'000 to below 3'000 ppmv within 2 hours . Then the humidity stayed around 3'000~~ mixing ratio dropped from 6′000 to below 3′000 ppmv within 2 hours then stayed around 3′000 ppmv for about ~~24~~ 24 hours before it increased again to ~~8'000~~ 8′000 ppmv.

3 Isotope ~~composition–humidity~~ composition–mixing ratio dependency

In this section we present the isotope ~~composition–humidity dependence~~ composition–mixing ratio dependency from the characterisation result for instrument HIDS2254 ~~.~~ (Fig. 1). The characterisation is carried out using the method of discrete liquid injections (~~Sect. 2.4.2). The injections are done by an autosampler, using synthetic air as carrier gas in the vaporizer (~~experiment 1). ~~During the experiment, in total five standard waters are measured at humidity levels from ~500 to ~23'000 ppmv. At each humidity level, totally~~ At each mixing ratio, in total four injections in high precision mode are ~~applied, where~~ carried out, and the last three injections are averaged for further analysis. The ~~characterisation result is shown~~ uncertainty at each mixing ratio is calculated as the standard deviation of the three taken injections; this standard deviation (color error bars in Fig. 1~~, with the humidity on the horizontal axis and the isotope composition bias ($\Delta\delta$)on the vertical axis. Note again that all the presented isotope composition biases and humidities are raw measurements.~~) is substantially smaller than the standard deviation of one single injection (indicated as thick grey error bars in Fig. 1).

~~For the bias on~~ The mixing ratio dependency for δ^{18}O~~(i.e.~~, displayed as the deviation $\Delta\delta^{18}$O~~), the humidity dependency depicts a tilted and inversed "U" shape~~, exhibits a skewed, inverse U-shape (Fig. 1a~~, symbol)~~) for all of the water standards. As an example, standard GSM1 (dark blue ~~symbol~~symbols) starts with a ~~bias of -0.1~~ deviation of -0.1 ‰ for ~~humidities at 23'000 ppmv, which~~ a high mixing ratio of 23′000 ppmv, becomes positive after passing ~~20'000 ppmv~~20′000 ppmv, continues to increase until reaching a ~~positive maximum around 3'000~~ maximum around 3′000 ppmv. Then ~~the bias quickly drops with lower humidity~~$\Delta\delta^{18}$O quickly drops at lower mixing ratios, and becomes negative again around ~~500~~ 500 ppmv. As the

~~humidity~~ mixing ratio further decreases, the magnitude of the ~~bias~~ deviation increases substantially. Notably, the ~~humidity~~ mixing ratio dependencies of the other four standard waters (light blue, green, orange, and red symbols for MIX, VATS, DI and EVAP, respectively) also depict ~~a similar tilted and inversed "U" shape~~an inverse U-shape. However, the ~~bias maximum becomes smaller and shifts towards the direction of higher humidity~~ maxima become smaller and shift towards higher mixing ratios (bottom right in Fig. 1a) with more ~~heavy-enriched isotope compositions~~enriched isotope composition. This isotope-composition-related shift leads to ~~a substantial increase of the bias difference among the standard watersat the same humidity level~~an enlarged difference of $\Delta\delta^{18}$O between any the standard waters. For example, ~~the bias~~ $\Delta\delta^{18}$O for GSM1 (dark blue ~~symbol~~symbols) and EVAP (red ~~symbol~~symbols) differs by ~~$\sim$0.9~~ ~ 0.9 ‰ at ~~2'000~~ $2'000$ ppmv, and by ~~$\sim$2~~ 2.0 ‰ at ~~1'000~~ $1'000$ ppmv.

The isotope-composition-related shift is even ~~clearer~~ more pronounced for $\Delta\delta$D (Fig. 1b~~, symbol~~). For the standard waters with relatively ~~heavy-depleted~~ depleted isotope compositions (GSM1~~(dark blue symbol) and MIX(light bluesymbol)), the bias~~, dark blue and MIX, light blue), $\Delta\delta$D is positive and becomes larger as ~~the humidity decreases~~mixing ratios decrease. For the standard waters with relatively ~~heavy-enriched~~ enriched isotope compositions (VATS~~(green symbol), DI (orangesymbol) and EVAP(dark redsymbol)), the bias goes to more negative values as the humidity decreases~~, green; DI, orange; EVAP, dark red), $\Delta\delta$D becomes more negative with decreasing mixing ratios. This leads to ~~a~~ an increasing divergence of the ~~humidity dependency starting from $\sim$15'000 ppmv and spreading as the humidity decreases. The bias~~ mixing ratio dependency at $\sim 15'000$ ppmv and below. For example, $\Delta\delta$D for GSM1 (dark blue~~symbol~~) and EVAP (red~~symbol~~) differ by ~~$\sim$11~~ ~ 11 ‰ at ~~2'000~~ $2'000$ ppmv, and by ~~$\sim$21~~ ~ 21 ‰ at ~~1'000~~ $1'000$ ppmv.

The ~~isotope-composition-related shift in~~ isotope-composition dependency of $\Delta\delta^{18}$O and $\Delta\delta$D ~~results in a substantial shift for the humidity~~ have a substantial impact on the mixing ratio dependency of Δd-excess ~~. The humidity~~ for different water standards. The mixing ratio dependency of Δd-excess below ~~$\sim$15'000 ppmv also depicts an "U" shape. The minimum bias is located at between 4'000~~ $\sim 15'000$ ppmv now exhibits a U-shape, with the minimum located between $4'000$ (DI, orange) and ~~7'000~~ $7'000$ ppmv (GSM1, dark blue~~symbol~~). The ~~bias~~ deviation for GSM1 (dark blue~~symbol~~) and EVAP (red~~symbol~~) differs by ~~$\sim$3.8~~ ~ 3.8 ‰ at ~~2'000~~ $2'000$ ppmv, and by ~~$\sim$5.3~~ ~ 5.3 ‰ at ~~1'000~~ $1'000$ ppmv.

In summary, this characterisation shows that the ~~humidity dependence~~ mixing ratio dependency varies systematically according to the isotope composition of the measured standard water. It is most pronounced at low ~~humidity levels (below 10'000~~ mixing ratios (below $10'000$ ppmv) and ~~quickly becomes substantial as the humidity further decreases. For example, at a humidity of 1'000 ppmv, failing to account for the dependence on the isotope composition can cause a bias as large as $\sim$2, $\sim$21 and $\sim$5.3~~ increases at lower mixing ratios. The substantial deviations are clearly important for ~~δ^{18}O, δD and d-excess, respectively. This is of importance for~~ in situ water vapour ~~measurement~~ measurements in dry environments, in particular ~~where~~ when the water vapour has ~~largely varying isotope compositions~~large variations in isotope composition. As is demonstrated in Sect. 4, we find that this ~~isotope composition–humidity dependence persists irrespective of characterizing methods or dry gas supplies~~systematic isotope composition–mixing ratio dependency is irrespective of water vapour generation method and dry gas supply, and exists in ~~all three spectrometers investigated here.~~ similar form in all three CRDS spectrometers characterised here.

~~This measurement characteristic~~ The mixing ratio dependency of the HIDS2254 seems to vary systematically with isotope composition of the water standards, suggesting a potential spectroscopic origin (Sec. 7). This isotope composition–mixing ratio dependency will not be sufficiently removed by a ~~simple uniform correction of the humidity dependency only~~uniform correction based on a single water standard alone. However, the ~~bias~~ dependency can be corrected for if we can establish a ~~correct function of both the humidity~~ correction function that takes both the mixing ratio and the isotope composition ~~based on the characterisation result. A correction framework dedicated to this purpose is developed in the following section.~~ into account. First we investigate how robust and stable over time the described isotope dependency is, before proposing a correction framework based on our characterisation results.

4 Robustness and temporal stability of the isotope composition–mixing ratio dependency

We carefully analysed the robustness of the isotope composition–mixing ratio dependency with respect to the choice of the method for vapour generation, the dry gas supply, the measuring sequence, individual instruments and instrument type, and its stability over time using in total 15 experiments (Table 1). Here we provide a summary of the results from these different experiments, with the detailed results given in Appendix A.

The robustness test indicates that the isotope composition–mixing ratio dependency is consistent across the two tested vapour generation methods, i.e., discrete liquid injections and continuous vapour streaming (Appendix A1; Fig. Aa-c). Characterisations with synthetic air and N_2 are in agreement for δD, but deviate for δ^{18}O (Appendix A2, Fig. Ad-f). A particularly substantial disagreement is found for the experiment using Drierite. This is likely caused by the contribution from water vapour remaining in the matrix air after the drying unit. The measuring sequence from high to low mixing ratios, or reverse, shows great similarity in the results, indicating that the potential hysteresis effects are not substantial (Appendix A3, Fig. Ag-i). However, we do note a different result for δ^{18}O at the lowest mixing ratio during one of the repeated experiments using MIX water (not shown). We suspect that the high sensitivity of the isotope composition–mixing ratio dependency at this range of δ^{18}O values could lead to pronounced deviations. While this aspect deserves further attention, we consider it as second–order regarding to the existence and cause of an isotope composition–mixing ratio dependency in the investigated CRDS instruments. Tests of all three analysers with discrete autosampler injections and N_2 as matrix gas show a similar isotope composition–mixing ratio dependency in all three investigated analysers (Appendix A1; Fig. A2). The repeated characterisation of analysers HIDS2254 and HKDS2038 during an up to 2-year time period show that the isotope composition–mixing ratio dependency is an instrument characteristic that is to first order constant over time (Appendix A1, Fig. A3).

In summary, the isotope composition–mixing ratio dependency is at first order robust across a range of key parameters, and stable over time. However, it is also apparent that individual instruments have a different strength and shape of the instrument characteristic, requiring individual correction. In the next sections, we apply and evaluate a new scheme to correct for the isotope composition–mixing ratio dependency.

5 Correction framework

~~In this section, we~~ We now use the characterisation result from instrument HIDS2254 obtained above as an example on how to derive a correction procedure for the isotope ~~composition–humidity dependence.~~ composition–mixing ratio dependency, following 6 sequential steps. Due to the systematic behaviour observed in Fig. 1, we chose a simple, traceable fitting procedure to obtain the two-dimensional correction function that can potentially be related to a physical cause. For the sake of simplicity, ~~we have removed the isotope indicator in the following equations . In other words, the equations~~ the equations in the following are ~~equivalent for~~ formulated to be valid for both δ^{18}O and δD.

5.1 General formulation

1. ~~Measurements: We obtained raw measurements of five standard waters with a~~ We obtain the mixing ratio dependency for each water standard as raw (uncorrected, uncalibrated) measurements of the isotope compositions. The water standards thereby cover a wide range of isotope compositions~~from −33.07 to 5.03 and from −262.95 to 4.75 for δ^{18}O and δD, respectively. The measurements are carried out with discrete liquid injections via an autosampler; the mixing dry gas is synthetic air from a gas cylinder (experiment 1 in Table 1)~~, and different mixing ratios, in particular also at low mixing ratio.

2. ~~Data processing: We calculated the deviations~~ We express the mixing ratio dependency for each water standard as the deviation of the raw measurements to ~~a~~ the reference value at ~~20'000 ppmv (raw humidity).~~ $20'000$ ppmv (Eq. (3). The reference value is obtained by a linear interpolation between the closest measurements above and below ~~20'000 ppmv. The~~ $20'000$ ppmv. These deviations are denoted as $\Delta\delta^{18}$O, $\Delta\delta$D and Δd-excess as described in Sect. 2.1~~and are used to determine humidity dependency functions~~.

3. ~~Fitting procedure: (1) Firstly, the characterisation result for~~ A suitable fitting function is fitted to the mixing ratio dependency of each standard water~~is fitted with a function~~. Here we used fitting functions of the form ~~:~~

$$f_{\cancel{i}\delta}(x) = \cancel{\frac{a_i}{x}}\frac{a_\delta}{x} + b_{\cancel{i}\delta}x + c_{\cancel{i}\delta}, \tag{4}$$

   where x is ~~humidity, i indicates one~~ the mixing ratio, δ indicates the isotope composition of the standard waters, and ~~a_i, b_i and c_i~~ a_δ, b_δ and c_δ are fitting coefficients for each ~~standard water~~ water standard and isotope species.

   ~~(2) Then, we plot the obtained coefficients a, b and c for all the standard waters~~

4. We express the obtained fitting coefficients as a function of ~~the isotope composition of the~~ isotope composition as $a(\delta)$, $b(\delta)$ and $c(\delta)$ for all standard waters (Fig. 2, symbols). This reveals a ~~dependence of each fitting coefficient~~ dependency of the fitting coefficients on the isotope composition of the ~~measured water . We approximate this dependence with~~ water

standard. We now fit a suitable function to this dependency, here using a quadratic polynomial~~regression:~~ :

$$\underline{f_j(y) = m_j(y-n_j)^2 + k_j,} \begin{cases} a(\delta) = m_a(\delta - n_a)^2 + k_a, \\ b(\delta) = m_b(\delta - n_b)^2 + k_b, \\ c(\delta) = m_c(\delta - n_c)^2 + k_c, \end{cases} \tag{5}$$

where ~~y is~~ δ is the isotope composition, ~~j indicates coefficients a, b and c,~~ and ~~m_j, n_j and k_j are fitting coefficients of the quadratic polynomial function~~ m, n and k are the respective fitting coefficients of the quadratic polynomials.

5. The final isotope composition–mixing ratio correction function $g(x,\delta)$ is then obtained as a function of both the mixing ratio x, and the isotope composition of the measured water δ:

$$g(x,\delta) = \frac{a(\delta)}{x} + b(\delta)x + c(\delta). \tag{6}$$

6. Using the correction function above, given any measured raw mixing ratio and isotope composition within the range investigated here, we can now correct the measured isotope compositions to a reference mixing ratio at 20′000 ppmv. Thereby, the isotope composition at 20′000 ppmv (δ_{ref}) is the unknown; its analytical solution is found from solving the equation

$$\delta_{\text{meas}} - \delta_{\text{ref}} = \frac{a(\delta_{\text{ref}})}{h} + b(\delta_{\text{ref}}) \cdot h + c(\delta_{\text{ref}}), \tag{7}$$

where h is the measured raw mixing ratio and δ_{meas} is the measured isotope composition at that mixing ratio. The right hand side of the equation is the isotopic deviation determined from Eq. (6). The coefficients $a(\delta_{\text{ref}})$, $b(\delta_{\text{ref}})$ and $c(\delta_{\text{ref}})$ are determined from Eq. (5). Eq. (7) is a quadratic function; the procedure to obtain its analytical solution is given in Appendix C.

~~The obtained coefficients a, b and c in~~

5.2 Correction function for analyser HIDS2254

We now exemplify the general steps above for the analyser with serial number HIDS2254. The results from step 1 and 2 for HIDS2254 are presented in Sec. 3. Here we use a range from −33.07 to 5.03‰ for δ^{18}O and from −262.95 to 4.75‰ for δD, and mixing ratios between 500 and 25′000 ppmv (experiment 1 in Table 1).

The coefficients a_δ, b_δ and c_δ obtained in step 3 from Eq. (4) for the five standard waters measured on instrument HIDS2254 are given in Table 4. ~~Despite~~ While the magnitude differs between ~~a, b and c,~~ the coefficients, scaling analysis shows that each of the terms ($\frac{a}{x}$, bx and c) on the right hand side of Eq. (4) contributes similarly to the isotope ~~composition–humidity dependency~~ composition–mixing ratio dependency (not shown). The fitting results from step 4 are shown in Fig. 1 (solid color line). ~~It can be seen that with the~~ The choice of this type of function ~~,~~ captures the behaviour of ~~humidity~~ the isotope composition–mixing ratio dependency for both $\Delta\delta^{18}$O and $\Delta\delta$D of each standard water~~are faithfully captured. Note that~~ .

Hereby, the fit for Δd-excess is ~~obtained by calculation. Using~~ calculated from the fit of ~~δ^{18}O and δD for each standard water by $\delta_{\text{fit}} = \delta_{\text{ref}} + \Delta\delta_{\text{fit}}$, we first calculate the fit of d-excess for each standard water by the definition d-excess $= \delta$D $- 8 \cdot \delta^{18}$O. Then, we obtain the fit of Δd-excess by calculating the deviations to the d-excess at the reference humidity level.~~ $\Delta\delta$ by $\Delta d\text{-excess}_{\text{fit}} = \Delta\delta\text{D} - 8 \cdot \Delta\delta^{18}\text{O}$.

The ~~obtained~~ coefficients m, n and k obtained in step 4 in Eq. (5) are given in Table 5. The fitting results (solid line) with the fitting uncertainty (~~95~~ 95 % confidence interval; black dotted line) are shown in Fig. 2. Since we only fit five data points, the fitting uncertainty is ~~relatively~~ large, resulting in a relatively large standard deviation for the isotope composition ~~bias (~~deviations $\Delta\delta$~~)~~. This large standard deviation for $\Delta\delta$ can be reduced by using a ~~bootstrap~~ bootstraping approach (Efron, 1979) to estimate the fitting uncertainty in Eq. (5) ~~. More details on the bootstrap approach is found in~~ (Appendix B).

~~Correction function: The final correction function is obtained as a surface function of both the humidity, x, and the isotope composition of the measured water, y:~~

$$g(x,y) = \frac{a(y)}{x} + b(y)x + c(y),$$

~~where $a(y)$, $b(y)$ and $c(y)$ are coefficients determined by the isotope composition of measured water, y.~~

~~This~~ Following step 5, this results in a two-dimensional correction surface for each isotopologue as shown in Fig. 3 (black contours). ~~Note the denser contour and the increased contour intervals below 4'000~~ For illustration purposes, some contours are omitted below $4'000$ ppmv for both δ^{18}O and δD. ~~For the humidity dependency on~~ The isotope composition–mixing ratio dependency for both δ^{18}O and δD ~~, the magnitude of the bias increases~~ increase substantially at low ~~humidities~~mixing ratios. For δ^{18}O, the ~~bias~~ deviation changes from positive to negative as ~~humidity decreases below ~4'000~~ mixing ratio decreases below $\sim 4'000$ ppmv. For δD, the ~~bias starts to grow below 10'000 ppmv~~deviation increases below $10'000$ ppmv, and splits into both positive and negative ~~directions.~~

~~The surface function also reflects a clear isotope composition dependence. For example, at the humidity of 2'000 ppmv, the isotope compositionbias for a measured water with δ^{18}O of 5 is about -0.5 , while for a measured water with δ^{18}O of -35 , the bias is about 0.4 . This isotope composition dependence is even more substantial for δD where the humidity dependencies at low humidities diverge with respect to the isotope compositions of the measured waters. The isotope composition bias is negative for a measured water with δD > -140 and positive for a measured water with δD < -140 . In addition, the magnitude of the bias increases as δD of the measured water deviates from -140 . At the humidity of 2'000~~ contributions, depending on isotope composition. The uncertainty (one standard deviation) for the deviation $\Delta\delta$ is typically one order of magnitude smaller than the $\Delta\delta$ values at the corresponding position.

The surface function exhibits the same features as determined from the experimental results, underlining that the fitting procedure reflects the main characteristics of the isotope composition–mixing ratio dependency from the experimental data. At $20'000$ ppmv, ~~the isotope composition bias spans from ~ -8 for a measured water with δD of 50 to ~8 for a measured water with δD of -350 . At the same humidity level, the isotope composition bias for δD is about 10 times larger than that for δ^{18}O.~~

~~Bias correction:~~

~~Using the correction function above, given any measured raw humidity and isotope composition within the range investigated here, we can determine the bias and bring the measured isotope compositions to their values at 20'000 ppmv. Thereby, the isotope composition at 20'000 ppmv (δ_{ref}) is the unknown; its analytical solution is found from solving the equation:~~

$$\delta_{\text{meas}} - \delta_{\text{ref}} = \frac{a(\delta_{\text{ref}})}{h} + b(\delta_{\text{ref}}) \cdot h + c(\delta_{\text{ref}}),$$

~~where h is the measured raw humidity and δ_{meas} is the measured isotope composition at that humidity level. The right hand side of the equation is the bias determined from Eq. . The coefficients $a(\delta_{\text{ref}})$, $b(\delta_{\text{ref}})$ and $c(\delta_{\text{ref}})$ are determined from Eq. . Eq. is a quadratic function; the procedure to obtain its analytical solution is given in Appendix C.~~

~~Note that the bias at 20'000 ppmv is~~ the correction function is not exactly zero~~because~~ , as the fit which is based on all ~~the~~ measurements is not constrained to the point [~~20'000, 0~~20′000, 0] ~~. Also note that below 500 ppmvthe bias~~ ppmv. This deficiency could be adressed by a modified fitting procedure. Below 500 ppmv, the correction function has larger uncertainties due to the lack of measurements at this ~~humidity range.~~ mixing ratio range. Note that the fitting functions used here in Eq. (4) and Eq. (5) are not chosen on a particular physical consideration. While it is possible that physical processes underly the shape of the isotope-composition dependency, we recommend to consider how suitable the fitting functions used here are for each individual instrument that is characterized.

6 ~~Impact of the humidity dependence correction~~

6 Impact of the isotope composition–mixing ratio dependency correction

We now investigate the impact of the ~~humidity dependence correction on datasets from~~ isotope composition–mixing ratio dependency correction in situ measurements ~~onboard an aircraft~~ of the water vapour isotope composition with two CRDS analysers installed onboard a research aircraft (HIDS2254), and a research vessel ~~presented in Sect~~(HKDS2038, see Sec. 2.5).

6.1 ~~Correction impact~~ Impact on the aircraft measurements

~~The low humidities~~ Low water vapour mixing ratios and a relatively wide range of (~~heavy-depleted~~depleted) isotope compositions make ~~this profile measurement from~~ water vapour isotope measurements from a research aircraft particularly suitable for demonstrating the impact of ~~humidity dependence correction(~~the new isotope composition–mixing ratio dependency correction. Fig. ~~3~~4 shows a vertical profile of one-minute averaged water vapour isotope measurements above the Iceland Sea (Sec. 2.5). During the descent of the aircraft from ~~2'900~~ 2′900 m a.s.l to minimum safe altitude, the ~~measured humidity~~ water vapour mixing ratio gradually increases from about ~~800~~ 800 ppmv at the top to ~~2'300~~ 2′300 ppmv near the surface (Fig. 4d). The ~~isotope composition profile shows three main characteristics~~ stable isotope profiles (Fig. 4~~a, b, c)~~ a-c) show three main characteristics. Above about ~~1'800 m~~ 2′000 m a.s.l., δ^{18}O and δD are ~~quite heavy-depleted (around −42~~ depleted (~ -42 ‰ and ~~−320~~ -320 ‰ ~~respectively~~), with d-excess ~~being around 10~~ between 10 and 20 ‰. Between ~~1'800 and 1'500 m~~ 2′000 and 1′400 m a.s.l., there is a transition ~~stage~~ where δ^{18}O and δD increase to around ~~−30~~ -30 ‰ and ~~−270~~ -240 ‰ respectively, and d-excess ~~quickly drops to around −40~~ decreases to ~ -5 ‰. Below ~~1'500 m~~ $1'400$ m a.s.l., δ^{18}O, δD and d-excess gradually ~~increases until reaching around −22~~ increase until reaching about -22 ‰, ~~−170~~ -170 ‰ and ~~12~~ 8 ‰, respectively near the surface. The uncertainty (one standard deviation) of the profile is obtained using the uncertainty propagation law, including the uncertainty (one standard deviation) of the one-minute averaged dataset (here the dominating source of uncertainty), and the uncertainty of the correction scheme.

6.1.1 ~~Comparison of correction schemes~~

~~We have created four versions of corrected datasets by applying different humidity dependence correction schemes. The first and second version are corrected for only humidity dependence using the humidity dependency function of standard DI (Fig. 1, orange curve)~~First, we investigate the impact of the new correction scheme introduced here. This correction, abbreviated as *iso-hum-corr*, modifies the uncorrected dataset in the region above $2'000$ m a.s.l. by about -0.4 ‰ and ~~standard GSM1 (Fig. 1, dark blue curve), respectively (hereafter referred as *hum-corr-cal-DI* (~~-13.3 ‰ for δ^{18}O and δD, respectively, resulting in a change of about -10.4 ‰ for d-excess (Fig. 4, ~~orange curve)and *hum-corr-cal-GSM1*~~ red circles vs. black dots). The impact of applying the new correction scheme on the aircraft measurements can be understood by examining where the dataset align in the correction surface function (Fig. ~~4, blue curve). The third version is corrected for both the isotope composition and the humidity dependency using the correction surface in Sect. 5 (hereafter referred as *iso-hum-corr-cal*, black curve with asterisk symbols in Fig. 4). All these three versions are calibrated to VSMOW2-SLAP2 scale after applying the respective humidity dependence correctionscheme.~~ 3, red crosses). For both δ^{18}O and δD, the aircraft dataset which are characterised with low mixing ratio and depleted isotope compositions cluster in the left bottom corner of the surface function. This is the most sensitive area of the correction, causing thus the largest deviations in the surface function.

To assess the benefit of the new isotope composition–mixing ratio dependency correction, we take this new correction scheme as the reference scheme and compare its impact to three other correction schemes. The first scheme corrects only for mixing ratio dependency based on standard DI (*hum-corr-DI*, Fig. 4, orange crosses). The ~~calibration using the VSMOW2-SLAP2 scale for the aircraft dataset is computed using long term SDM measurements of standards~~ second correction follows the same procedure but is based on standard GSM1 ~~and DI before and after the flight survey (details described in a forthcoming publication).~~

~~The fourth version of the dataset is corrected using an alternative approach that has been applied~~ (*hum-corr-GSM1*, Fig. 4, blue squares), and the third correction follows an approach proposed by Bonne et al. (2014) for ~~their~~ in situ vapour measurements ~~on~~ in southern Greenland. Instead of correcting the ~~humidity dependence~~ mixing ratio dependency for the vapour measurements, ~~their~~ the Bonne et al. (2014) approach corrects the ~~humidity dependence for the measured~~ mixing ratio dependency for the calibration standards. Thus, assuming the ~~humidity~~ mixing ratio dependencies of the two employed standards remain stable during the measurement period, the measured isotope ~~ratios~~ compositions of these two standards are corrected using ~~humidity~~ mixing ratio dependency function to the ambient air ~~humidity level~~ mixing ratio of each single vapour measurement. Then, the linear regression computed from these two corrected standard measurements against their certified values is applied to calibrate the vapour measurement to VSMOW2-SLAP2 scale~~(~~. This scheme is hereafter referred as ~~*2-std-hum-corr-cal*~~*2-std-hum-corr* ~~, green curve in~~ (Fig. 4, green triangles).

The different correction schemes modify the ~~raw~~ uncorrected dataset differently. ~~For the~~ The δ^{18}O profile ~~, it does not make substantial difference for the measurements below 1'500 m~~ is only marginally affected by the correction below 1′400 m a.s.l. (Fig. 4a). For the measurements above ~~1'500 m , the version~~ 1′400 m a.s.l., differences become more pronounced, but are masked by large uncertainty as the aircraft was descending through a strong mixing ratio gradient. At elevations above 2′000 m a.s.l., all corrections show clear deviations, and we focus our comparison at this region. The ~~*hum-corr-cal-DI*~~*hum-corr-DI* stands out ~~from the rest by exhibiting a consistent positive offset of about 0.8~~ with a positive correction of about 0.8 ‰~~. The rest three versions depict similar negative offsets between −0.3 and −0.7~~ , while the other three schemes induce a negative correction of between −0.3 and −0.7 ‰. ~~For the~~ The δD profile ~~, a very similar patternexhibits~~ exhibits a similar pattern, but with more ~~visible offsets~~ apparent differences between the correction schemes (Fig. 4b). ~~The disagreement patterns in the corrected δ^{18}O and δD profiles lead to an even stronger offset~~ This results in an even more pronounced correction in the *d*-excess profile (Fig. 4c). ~~We can demonstrate the impacts of the different correction schemes by comparing the four versions of the corrected datasets at the same altitude. Since the impact is most substantial on the measurements above 1'500 m, we choose to use the measurements around 2'600 m as an example in the following.~~

~~First, we investigate the impact from applying the correction scheme introduced in this study, i.e., the version *iso-hum-corr-cal*. This version modifies the raw dataset by about −0.4 and −13.7 for δ^{18}O and δD, respectively, resulting in a change of about −10.6 for *d*-excess. Since this version accounts for both the isotope composition dependence and the humidity dependence, hereafter we regard this version as the reference.~~ The impact of applying the ~~reference correction schemes on the aircraft measurements can be understood by examining where the data points align in the correction surface function (Fig. 3, blue crosses). For both δ^{18}O and δD, the data points with low humidity and heavy-depleted isotope compositions cluster in the left bottom corner of the surface function. This is the most sensitive area of the correction, causing thus the largest biases in the surface function.~~

~~By comparing the other versions to the reference, we show the different impacts from other correction schemes. The impact of applying the correction scheme~~ correction scheme using single standard water (thus accounting for only ~~humidity dependence~~ mixing ratio dependency) relies on the choice of the used standard water. ~~In the case of the aircraft dataset here, using the humidity dependency function of standard DI (version~~ Using the correction ~~*hum-corr-cal-DI*~~*hum-corr-DI* ~~)~~ introduces the largest ~~bias (1.1~~ deviation (1.1 ‰, ~~18.8~~ 18.3 ‰ and ~~9.5~~ 9.5 ‰, for δ^{18}O, δD and *d*-excess, respectively)~~. On the contrary, using the humidity dependency function of standard GSM1 (version~~ , while using the correction ~~*hum-corr-cal-GSM1) produces results that are*~~ *hum-corr-GSM1* produces results much closer to ~~the version *iso-hum-corr-cal*~~ that of the reference scheme (with an offset of ~~0.1~~ 0.1 ‰ and ~~4.3~~ 4.2 ‰ for δ^{18}O and δD, respectively and ~~3.3~~ 3.4 ‰ for *d*-excess). ~~This is due to the fact that the~~ For this specific aircraft measurement (where the surface condition is already quite dry during cold air outbreak event) the isotope composition of standard GSM1 ~~closely resembles~~ happens to closely resemble the average isotope composition of the ~~aircraft dataset.~~ measurement. However, in the case of a previously unknown range of isotope compositions, or strongly varying conditions, a comprehensive characterisation of mixing ratio dependency with multiple standard waters can provide advantages and should be preferred. Unknown ranges are particularly likely for atmospheric measurements of vertical profiles in humid regions (e.g., tropics and subtropics), or over a wide area from moving platforms.

Finally, applying the alternative calibration approach used in Bonne et al. (2014) (~~*2-std-hum-corr-cal*~~*2-std-hum-corr*) results in ~~quite similar profiles to that from the reference version. The version *2-std-hum-corr-cal* is slightly more heavy-depleted~~only slightly more depleted isotope values than the reference, with an offset of about ~~−0.3~~ −0.3 ‰ and ~~−0.6~~ −0.5 ‰ for δ^{18}O and δD, respectively, resulting in a change of ~~1.8~~ 1.7 ‰ for *d*-excess. The small discrepancy between ~~these two versions are~~ the *2-std-hum-corr* and *iso-hum-corr* is mainly due to the following three factors. Firstly, depending on the number of used standard waters, the interpolation scheme for the ~~bias~~ isotopic deviations in between those of the used standard waters can be different. ~~The version *2-std-hum-corr-cal*~~*2-std-hum-corr* makes use of the ~~humidity~~ mixing ratio dependency functions of only two standard waters. ~~Therefore the bias~~ In this way the deviations can only be linearly interpolated between ~~both standards~~the two standard waters. In contrast, by measuring five standard waters, the reference ~~version~~ scheme is able to ~~reveal and account for the non-linearity~~ account for non-linearities during interpolation. Secondly, ~~the version *2-std-hum-corr-cal*~~*2-std-hum-corr* corrects the two ~~standards to the humidity level~~ standard waters to the mixing ratio of the measurement while the reference ~~version~~ scheme corrects the measurement to the ~~humidity level~~ mixing ratio of the two ~~standards~~ standard waters (i.e. the reference ~~humidity~~mixing ratio). Based on the ~~humidity~~ mixing ratio dependency feature of the two ~~standards~~standard waters, the choice of correcting the two ~~standards~~ standard waters will result in a ~~bigger~~ higher slope for VSMOW2-SLAP2 calibration line. Consequently, the measurements after calibration ~~is~~ are stretched to two ends, i.e., the measurements with isotope composition close to that of standard DI become more ~~heavy-enriched~~ enriched and those close to that of standard GSM1 become more ~~heavy-depleted~~depleted. Finally, the ~~humidity~~ mixing ratio dependency functions for GSM1 and DI ~~used in the version~~ in ~~*2-std-hum-corr-cal*~~*2-std-hum-corr* (using the ~~fit of the measurements~~ individual fit for GSM1 or DI respectively) are not exactly identical to those used in ~~version *iso-hum-corr-cal*~~ the reference scheme (from the surface function determined by the measurements of five standard waters). Despite the small discrepancy, the consistent results of ~~version *2-std-hum-corr-cal*~~*2-std-hum-corr* with ~~the reference version~~ that of the reference scheme indicate that a correction scheme using ~~humidity~~ mixing ratio dependency functions of only two standard waters covering the measured isotope composition range ~~could be sufficient.~~

6.2 ~~Correction impact on the ship-based measurements~~

~~The same four versions of corrected dataset have been created for the ship measurement. That dataset was calibrated to the VSMOW2-SLAP2 scale using the quasi-daily manual injection measurements of NEEM and GV standards onboard the research vessel~~can work sufficiently well in some situations. Note however, that the exact shape of the surface function of an individual analyser, and the space in the isotope composition–mixing ratio surface covered by the measurement data determine could lead to differing results for different analysers and measurement situations.

~~Applying~~

6.2 Impact on the ship-based measurements

Applying the four different correction schemes to the ship-based measurement data has a much weaker impact on the ~~vapour measurement onboard the research vessel~~ corrected series of vapour measurement (not shown). ~~The modification on the raw dataset after~~ After applying our isotope ~~composition–humidity dependence correction schemeis~~ composition–mixing ratio dependency correction scheme, the uncorrected dataset changes on the order of ~~0.06 and 0.15~~ 0.06 and 0.15 ‰ for δ^{18}O and δD, respectively, ~~yielding~~ leading to a change on the order of ~~−0.5~~ −0.5 ‰ for d-excess. ~~As can be identified from the location of the red dots in Fig. 3, these data points are located in an area with low sensitivity in the correction surface.~~ This is mainly because these ship measurements were carried out at the ocean surface with relatively higher ~~humidities (from 2’500 to 8’000~~ mixing ratios (from 2′500 to 8′000 ppmv), ~~but also less heavy-depleted isotope compositions , compared to the aircraft observations. The ocean surface evaporation dominates the isotope compositions which span between −23 to −12~~ and less depleted isotope compositions (−23 to −12 ‰ for δ^{18}O and ~~−160 to −100~~ −160 to −100 ‰ for δD~~. Essentially,~~), compared to the aircraft measurements. As can be identified in Fig. 3, the ~~measurements happen to cluster in a saddle region of the surface function, where the correction function is uniform and small.~~ ship data (blue dots) are located coincidentially in an area with low sensitivity in the correction surface. A linear interpolation between two standards may not capture such a saddle point correctly. This indicates that measurements are not under all conditions sensitive to the correction of the isotope ~~composition–humidity dependence. Under conditions where the isotope compositions of vapour vary within a small range or the ambient humidity is relatively high (as shown for aircraft dataset in Sect. 6.1), the bias caused by humidity dependence becomes smaller and a good choice of one or two standard waters representing or covering the measured isotope composition range could be sufficient to correct for the humidity dependence.~~ composition–mixing ratio dependency. Ultimately, however, certainty about a reliable correction will only be achieved by a complete characterisation of the isotope composition and mixing ratios covered by the measurements.

7 ~~Stability and robustness~~Discussion

~~In this section we present the results of stability and robustness tests of the isotope composition–humidity dependence. We address here the possible influence from the choice of the characterisation method, the variation among instruments, the potential instrument drift over time, the type of dry gas supply and the measuring sequence~~Our careful characterisation experiments show that the isotope composition–mixing ratio dependency affects measurements at low mixing ratios for all three investigated stable water isotope CRDS analysers. Here, we discuss possible causes of the isotope composition–mixing ratio dependency. In particular, we explore to what extent this dependency is an artefact from mixing with water remaining within the analyser, or an instrument behaviour resulting from spectroscopic effects.

7.1 ~~Vapour generation method~~Artefact from mixing

~~To investigate whether the isotope composition–humidity dependence is influenced by the choice of calibration method, we compare the characterisation result for instrument HIDS2254 using discrete liquid injections and the characterisation result using the SDM (experiment~~ If we assume the dependency is a result from mixing with remnant water, there would be mainly two candidates of the background moisture source: (1) the remaining water vapour in the dry gas supply; (2~~, 6) . The same standard waters (GSM1 and DI) and~~) the remaining water vapour from previous measurements in the analyser. By changing the dry gas supply ~~(synthetic air) are used in the two experiments. The measurement using the SDM usually has a higher uncertainty since the continuous vapour streaming does not provide entirely constant mixing conditions, and the vapour stream can become unstable due to clogging and bubbles in the capillary. The comparison is shown in Fig. **??**. For $\Delta\delta^{18}$O, the humidity dependency determined by discrete liquid injections corresponds well with those determined by the SDM within one standard deviation of the latter, despite a small offset of 0.2–0.5 for DI between 2'000 and 6'000~~ from the ambient air dried through Drierite to synthetic air or N_2 from cylinder which typically provides a dry gas with a mixing ratio below 10 ppmv, we can exclude the possible influence from the background moisture in the dry gas supply. In order to quantify the amount and the isotope compositions of the remaining water vapour from previous measurement, we have applied several successive, so called *empty injections* via the autosampler. Thereby, no liquid is injected, and only dry gas is flushed into the vaporizer. Results from these empty injections show that the remaining water vapour in the system typically has a mixing ratio of about 60–80 ppmv, with its isotope composition closely following those of the previous injections. If the mixing ratio dependency were a result of the mixing between the injected water and the remaining water vapour from previous measurement, by injecting the same standard water during a characterisation run, we would expect a mixing of two water vapour masses of the same isotope compositions at different mixing ratios. As a consequence, we would expect the mixed vapour to have the same isotope compositions, which is not the case. Finally, the shape of the isotope composition–mixing ratio dependency with a maximum between 2′000 and 6′000 ppmv (Fig. ~~**??**a) . For $\Delta\delta$D, the humidity dependencies for both GSM1 and DI determined by discrete liquid injections are located well within one standard deviation of those determined by the SDM (Fig. **??**b). The agreement between the two experiments for $\Delta\delta^{18}$O and $\Delta\delta$D leads to an overall agreement in the calculated Δd-excess~~ 1a) is not consistent with the expectation of a memory effect what would monotonously increase with decreasing mixing ratio. The slight hysteresis observed during the upward/downward calibration runs indicates that there may be contributions from remnant water, for example on walls or filter surfaces in the analyzer, that only exchange once a sufficiently humid airmass is introduced into the analyzer. Such contributions do however appear to be of second–order compared to the substantial changes of the mixing ratio dependency with isotope composition.

7.2 Spectroscopic effect

Now we explore the second hypothesis, namely that the isotope composition–mixing ratio dependency is an instrument behaviour resulting from spectroscopic effects. The manufacturer recommends a procedure for water vapour dependency calibration, using their SDM or similar device (Picarro, 2017), similar to what we have employed. While the first-order effect can be removed from a linear fit, there are second–order, non-linear components, that become more apparent the more the water concentration changes from the recommended range of operation (5′000 – 25′000 ppmv). In the following we discuss the potential reasons for the origin of the water vapour and isotope dependency from a spectroscopic standpoint based on the published literature (Steig et al., 2014; Rella et al., 2015; Johnson and Rella, 2017).

The two modules of CRDS analyser used in our experiments (i.e., Picarro L2140-i and L2140-i) target thee absorption lines of water vapour in the region 7199–7200 cm^{-1}, namely near 7199.960, 7200.135 and 7200.305 cm^{-1} for $H_2^{18}O$, H_2^{16} and $HD^{16}O$, respectively (Fig. ~~??c). A 1–3 offset between 2'000 to 6'000 ppmv results from the offset in $\Delta\delta^{18}O$ in the same humidity range.~~ 5). These absorption lines broaden or narrow, depending on the partial pressure of the gas mixture in the cavity, and can be affected by changes in their baseline due to other nearby strong absorption lines. A fitting algorithm then fits the measured absorption spectrum to an expected model spectrum and adjusts the model parameters in order to minimize the residual error. Broadening/narrowing of lines due to changing gas mixture, and baseline shifts are particular challenges to the fitting algorithm (Johnson and Rella, 2017), and cause residuals during the fitting procedure, which induce instrument error.

~~Comparison of the two vapour generation methods using N_2 as dry gas supply (experiment 3 and 8) also gives a similar isotope composition–humidity dependence for both methods (not shown), confirming that the isotope composition–humidity dependence does not depend substantially on either of the two tested methods to generate standard water vapour~~The L2130-i and earlier spectrometers use the absorption peak as a free parameter in the fitting algorithm. The peak shape and thus the peak amplitude can suffer from the above mentioned broadening/narrowing effect, introducing potential error under conditions of varying concentration or matrix gases. The fitting algorithms of the L2140-i spectrometers, in contrast, have a higher number of ring–downs due to a different strategy for obtaining laser resonance, using wavelength changes rather than cavity length modifications. This allows to fit the integrated absorption, rather than the peak amplitude, of each absorption line. Since the integrated absorption is a constant independent of pressure, the fitting is expected to be more accurate, with a low sensitivity to broadening/narrowing effects arising from changes of water concentrations and background gas compositions (Steig et al., 2014). One part of the retrieval algorithm is the removal of the baseline from the $H_2^{16}O$ spectrum. To this end, changes in the baseline from nearby strong absorption lines as a result from concentration changes or cross-interference from other gas species is a possible source of error for either fitting algorithm. Other possible source of error can be absorption loss nonlinearities due to small imperfections of the instrument such as the non-zero shut-off time of the laser and response time of the ring–down detector (Rella et al., 2015). Unless fitting algorithms take the actual line shapes into consideration directly, some residual effects are likely to persist.

The retrieval of H_2O concentration and the stable isotope compositions $\delta H_2^{18}O$ and $\delta HD^{16}O$ (identical to $\delta^{18}O$ and δD) is implemented similar to the procedure described for CH_4 and $\delta^{13}CH_4$ (Rella et al., 2015). Considering a linear dependency of absorption to concentration (which is not always true), where the mole fraction of $H_2^{18}O$ (c_{18}) is related to the absorption peak height α_{18} with a proportionality constant k_{18} and an error offset ϵ_{18}, we have:

$$c_{18} = k_{18}\alpha_{18} + \epsilon_{18}. \tag{8}$$

Note that the expressions above should apply to both the L2130-i and L2140-i spectrometers, with the only difference that the absorption peak height is replaced by the integrated absorption (Steig et al., 2014).

7.3 ~~Variations among CRDS analysers~~

~~To investigate the variations of the humidity dependency between the individual instruments~~Based on the molecular definition of a delta value with respect to Vienna Standard Mean Ocean Water (VSMOW), and an isotope ratio of the sample $^{18}R = \frac{[\mathrm{H_2^{18}O}]}{[\mathrm{H_2^{16}O}]}$ and of VSMOW $^{18}R_{\mathrm{VSMOW}} = 2005.20 \pm 0.45 \times 10^{-6}$, we have~~repeated the same characterisation on three analysers (experiment 3, 9 and 13) . The characterisation is carried out with four standard waters (GSM1, VATS, DI and EVAP), using liquid injections via an autosampler with N_2 as the mixing dry gas. The characterisation results for the three analysers are shown in Fig. A2.~~:

$$\delta\mathrm{H_2^{18}O}\ [\text{in ‰}] = 1000\left(\frac{R_{\mathrm{sample}}}{R_{\mathrm{VSMOW}}} - 1\right). \tag{9}$$

The retrieval can then be formulated as:

$$\delta\mathrm{H_2^{18}O} = 1000\left(\frac{k_{18}\alpha_{18} + \epsilon_{18}}{(k_{16}\alpha_{16} + \epsilon_{16})R_{\mathrm{VSMOW}}} - 1\right). \tag{10}$$

~~For $\Delta\delta^{18}$O, the positive bias for GSM1 below 4'000 ppmv on instrument HKDS2038 is about 0.2–1.8 stronger than those on the other two analysers (Fig. A2a , d, g, blue). The humidity dependency of VATS below 4'000 ppmv is nearly flat on instrumentHKDS2038 while exhibiting a substantially negative bias on the other two analysers. The humidity dependencies for the other two standard waters (DI and EVAP)are in good agreement among the three analysers. For $\Delta\delta$D, the humidity dependency of VATS below 2'000 ppmv is slightly positive on instrument HKDS2038 while being nearly flat on the other two analysers (Fig. A2b, e, h, green)~~For an ideal spectrometer, the calibration coefficients are constants (i.e., $k_{18} = \kappa_{18}$ and $k_{16} = \kappa_{16}$) and the calibration offsets are zero (i.e., $\epsilon_{18} = \epsilon_{16} = 0$). These assumptions lead to the expected retrieval for an spectrometer as:

$$\delta\mathrm{H_2^{18}O} = \frac{1000}{R_{\mathrm{VSMOW}}}\frac{\kappa_{18}\alpha_{18}}{\kappa_{16}\alpha_{16}} - 1000. \tag{11}$$

The actual spectrometer is not ideal, but in most situations has a highly linear and stable performance (Rella et al., 2015). Nevertheless, it can be calibrated based on the linear dependency of $\delta\mathrm{H_2^{18}O}$ to $\frac{\alpha_{18}}{\alpha_{16}}$, using a linear expression of the form:

$$\delta\mathrm{H_2^{18}O} = A\frac{\alpha_{18}}{\alpha_{16}} + B, \tag{12}$$

where calibration constants A and B can be determined based on the measurable quantities $\delta\mathrm{H_2^{18}O}$ and $\frac{\alpha_{18}}{\alpha_{16}}$ on a reference instrument in the factory. These determined calibration constants slightly deviate from the expected values in Eq. (11). They are then transferred from the reference instrument to each new instrument of the same type (Rella et al., 2015).

If Eq. (12) is used for calibration of the water analysers (not reported in the published literature), there are two potential sources of error. First, the dependencies on isotope ratio may not be entirely linear (even when assuming a linear relationship, the coefficient is not necessarily a constant and offset not necessarily to be zero), and remain as residuals. Second, the change of this relationship with differing mixing ratio may remain unexplored. Furthermore, manufacturing tolerances will induce deviations from the reference instrument on which such an initial calibration has been carried out, and instruments have therefore to be calibrated individually to obtain a suitable post-processing methods. The initial instrument calibration procedure may therefore be one potential origin for the isotope composition–mixing ratio dependency identified here.

Deviations from an ideal spectrometer stem from the potential spectrometer errors due to small imperfections of the instrument. One possible error is the absorption loss offset that could occur when the baseline loss is not reproduced well by the fitting algorithm. This absorption offset then leads to a mole fraction offset, ϵ_{18} in Eq. (8). The ~~humidity dependency for the other three standard waters (GSM1, DI and EVAP) agree well among the three analysers.The calculated *d*-excess (Fig. A2c, f, i) shows an increasing positive bias towards the low end of humidity for almost all standard waters measured on the~~ measured $\delta H_2^{18}O$ including the effecf of absorption offset can be formulated explicitly, following Rella et al. (2015) (their Appendix S1.1), as:

$$\delta H_2^{18}O = \frac{1000}{R_{\mathrm{VSMOW}}}\left(\frac{k_{18}\alpha_{18}}{k_{16}\alpha_{16}} + \frac{\alpha_0}{\alpha_{16}}\right) - 1000, \tag{13}$$

where α_0 is the net absorption loss parameter, that should to first order be independent of water concentration and isotope ratio. Comparing to Eq. (11) for an ideal spectrometer, the additional term $\frac{\alpha_0}{\alpha_{16}}$ in Eq. (13) creates an inverse relationship with water concentration, and should be responsible for deviations from the ideal spectrometer that are most evident at low mixing ratios.

Another possible spectrometer error is the so-called absorption loss non-linearity, which describes effects due to a shorter or longer ring–down time than expected in the optimal range of operations. These effects can be included as additional terms, again following Rella et al. (2015) (their Appendix S1.2), by including a non-linear dependency of α_{18} on α_{16} (i.e., $\alpha_{18} \Rightarrow \alpha_{18} + \beta\alpha_{16} + \gamma\alpha_{16}^2$):

$$\delta H_2^{18}O = \frac{1000}{R_{\mathrm{VSMOW}}}\left(\frac{k_{18}\alpha_{18}}{k_{16}\alpha_{16}} + \gamma\frac{k_{18}\alpha_{16}}{k_{16}} + \frac{\alpha_0}{\alpha_{16}}\right) + \left(\frac{1000}{R_{\mathrm{VSMOW}}}\frac{k_{18}}{k_{16}}\beta - 1000\right), \tag{14}$$

which can be simplified to the form:

$$\delta H_2^{18}O = A\frac{\alpha_{18}}{\alpha_{16}} + \Gamma c_{16} + \frac{c_0}{c_{16}} + B'. \tag{15}$$

The difference between Eq. (15) and Eq. (12) represents the deviation from an ideal spectrometer due to non-linearities from imperfections in the baseline removal and spectral cross-talk between $H_2^{18}O$ and $H_2^{16}O$, and can be denoted as:

$$\Delta\delta H_2^{18}O = \Gamma c_{16} + \frac{c_0}{c_{16}} + \mathrm{Const.}. \tag{16}$$

The dependency on water concentration (c_{16}) in Eq. (16) appears consistent with the mixing ratio dependency function (Eq. (C2)) identified in our systematic investigation of three analysers, ~~except for DI and GSM1 measured on instrument HKDS2038, whose humidity dependencies appear to be rather flat or even slightly negative.~~ supporting the hypothesis of a spectrometric origin for the mixing ratio dependency behaviour.

~~Despite of~~ A similar form of mixing ratio correction is applied to the ^{17}O measurements using L2140-i analyser in the study of Steig et al. (2014) (their Eq. (22)), where the integrated absorption area instead of peak amplitude is used to calculate the absorption loss and the cross-talk between $H_2^{18}O$ and $H_2^{16}O$ is modelled with a bilinear relationship. Steig et al. (2014) notes that the introduction of an integrated absorption detection leads to a substantially improved behaviour for the mixing ratio dependency over the peak amplitude detection for δ^{18}O, but not for δD, with the reason remaining unclear. It is also worth to note that their instrument has not been evaluated for the low mixing ratio range, which is in the ~~minor differences of the bias, it is clear that the~~ focus of this manuscript. It may be possible that part of the identified isotope composition dependency of the mixing ratio dependency stems from the so far lacking systematic analysis of the low mixing ratio range of the analyser for this effect.

8 Final remarks and recommendations

We have systematically investigated the mixing ratio dependency of water vapour isotope measurements for three commercially available infra–red cavity ring–down spectrometers. We found that the mixing ratio dependency varies with the isotope ~~composition–humidity dependency exists in all three analysers investigated here. The behaviour of dependency is to the first order in good agreement across the analysers. For the standard waters with relatively heavy-depleted isotope compositions, the measurements on all the three analysers exhibit a humidity dependency where the measured isotope composition becomes more heavy-enriched as the humidity decreases. For the standard waters with relatively heavy-enriched isotope compositions, the measurements exhibit a reversed humidity dependency~~composition of the measured vapour. We define this behaviour as isotope composition–mixing ratio dependency. The dependency is robustly identified across 3 similar analysers, regarding several first-order parameters, and found to be stable over time. Using the characterisation results of five standard waters on a Picarro L2130-i as an example, we propose a correction scheme for this isotope composition–mixing ratio dependency. Using such a correction scheme, we can correct the isotopic measurements for any measured mixing ratio and isotope composition within the range investigated here.

8.1 ~~Long term stability~~

~~To quantify the long term stability of the isotope composition–humidity dependency , we examine the temporal change of the fitting coefficients (a_i, b_i and c_i) in Eq. . The change over time is considered insignificant if it is within the 95 % confidence bounds for the fitted curve. Figure A3 shows the fitting coefficients for the humidity dependency characterised by liquid injections on instrument HIDS2254 in February 2017 (black line, experiment 1) and in May 2018 (red line, experiment 2). For the characterisation in May 2018, only four standard waters are measured. This results in a fit with a relatively large 95 % confidence interval. In this context, the change over time is considered insignificant if the coefficients (and their fitted curve) from the characterisation in May 2018 is within the 95 % confidence bounds for the fitted curve from the characterisation in February 2017.~~

~~For the humidity dependency on δ^{18}O, the change of coefficient a is insignificant. However, it is worth to note that the fitting coefficient a with respect to standard GSM1 (Fig. A3a , the first data point) changes slightly from negative to positive. This small change results in an opposite humidity dependency shape at low humidity level.~~ To demonstrate the impact of the mixing ratio dependency correction, we have compared the proposed correction scheme with other published correction schemes, using in situ measurements from dry environments. The ~~change of the humidity dependency for~~ impact is found to be most substantial on the measurements at the low mixing ratios. Applying a correction scheme accounting for only mixing ratio dependency relies on the choice of the used standard water. For an aircraft dataset, using the mixing ratio dependency function based on the standard DI produces a large deviation from our proposed scheme; using the mixing ratio dependency based on standard GSM1 ~~reflects partly on the sensitivity of~~ produces results similar to our proposed scheme, since it is closer to the average isotope composition of the aircraft dataset. Finally, we have investigated the impact of applying a correction scheme used by Bonne et al. (2014). This approach produces results in good agreement with that from our approach. The small discrepancy is due to the interpolation scheme (linear or non linear) of the isotopic deviation, the choice of correcting mixing ratio dependency of the standards or that of the vapour measurement and the small discrepancy in the ~~instrument on a certain range of~~ mixing ratio dependency functions of the two standards. The consistent results indicate that a correction scheme using mixing ratio dependency functions of only two standards covering the isotope composition could be sufficient if the correction surface can be sufficiently approximated by linear interpolation. Using ship measurements made at higher mixing ratio conditions, we find a weaker impact from the different correction schemes.

Given the non-monotonous characteristics of the isotope composition–mixing ratio dependency, we consider memory effects (i.e. mixing with water vapour from previous injections in the analyser) unlikely to be the dominanting factor. This renders a spectroscopic origin as the most likely cause, possibly resulting from imperfections of the fitting algorithm at low water concentrations, or non-linearities in the fitting procedures (Rella et al., 2015).

The correction for the isotope ~~composition and partly on the uncertainty arising from both low instrument precision and lack of measurements at low humidities. The change of coefficients b and c are substantial~~ composition–mixing ratio dependency is most relevant for in situ vapour isotope measurements where the ambient mixing ratio is low (below 4′000 ppmv) and the isotope composition of measured vapour spans a large range. At higher mixing ratios, the investigated CRDS analysers show negligible dependency on either the mixing ratio or the isotope composition. If the isotope composition of ambient vapour varies in a small range during the sampling period, a simpler correction scheme could be employed, using the mixing ratio dependency of two or even one suitable standard water with a similar isotope composition as that of ambient vapour.

Based on our conclusions above, we recommend to identify the isotope composition–mixing ratio dependency for all Picarro CRDS analysers used for in situ water vapour isotope measurements, in particular when low mixing ratio conditions are encountered.

If the measurements of multiple standard waters are not available, the approach used in Bonne et al. (2014) could be applied as an alternative correction approach. Their approach can produce similar results as that from the approach proposed here, but requires the characterisation of the mixing ratio dependency of two carefully selected calibration standards in a linear range of the correction surface. If the isotope composition of ambient vapour varies only within a small range during the sampling period, such as during measurements close to the ocean surface, it may be sufficient to correct for the mixing ratio dependency using one standard water that has a similar isotope composition as that of ambient vapour.

Our study is presently limited by the range of the standard waters used here (about $-33 \sim 5$ ‰ and $-263 \sim 5$ ‰ for ~~waters of relatively heavy-enriched~~ δ^{18}~~O (Fig. A3b, c). A less negative b and a less positive c reflects a weaker humidity dependency in May 2018. The humidity dependency on~~ O and δ~~D shows reasonable agreement for all three fitting coefficients (Fig. A3d, e, f), and points to the same basic shape of the humidity dependency on δD after a 15 month period.~~ D, respectively). Depending on the measurement environment, more depleted or enriched standards would be needed to derive a correction function over the entire measurement range of samples potentially encountered during atmospheric measurements.

The other limitation of the characterisations performed here is the substantial time demand. The characterisation method with liquid injections provides relatively high precision performance but requires an autosampler and takes about 1–2 weeks for four standard waters. The characterisation method with the SDM can be automated more easily, but requires manual intervention to apply more than two standards. A device that could provide any desired isotope composition and a given mixing ratio would be needed to fully automate the isotope composition–mixing ratio dependency of the instruments tested here.

~~A repeated characterisation with standard water DI via SDM in July 2016 (experiment 4), February 2018 (experiment 5) and June 2018 (experiment 6) indicates that the humidity dependency for standard water DI is still consistent after nearly two years (not shown). The humidity dependencies of the three~~ A reproducible and accepted characterisation method is of utmost importance for comparing measurements across disparate locations and in bottom–up networks, in particular in the polar regions, and appears as a prerequisite for detecting representative signals in the stable isotope record on a regional scale. In particular studies employing the d-excess as an indicator of moisture origin or other tracer applications are therefore likely to profit from a detailed characterisation of their analysers according to our characterisation procedure, either before, during or after field deployments.

Data availability. Data used in the generation of the figures is attached as a supplement to this article.

Appendix A: Robustness and temporal stability

Here we detail the experiments conducted to assess the robustness of the isotope composition–mixing ratio dependency with regard to the vapour generation method, the dry gas supply, the measurement sequence, the individual analyser and analyser type, and with respect to temporal stability.

A1 Vapour generation method

To investigate whether the isotope composition–mixing ratio dependency is influenced by the choice of vapour generation method, we compare the characterisation result from discrete liquid injections and the SDM for instrument HIDS2254 (experiment 2 and 6; Fig. Aa-c). The same standard waters (GSM1 and DI) and dry gas supply (synthetic air) are used in the two experiments. The measurement using the SDM usually has a higher uncertainty since the continuous vapour streaming does not provide entirely constant mixing conditions, and the vapour stream can become unstable due to clogging and bubbles in the capillary. Overall, the results from the two vapour generation methods exhibit consistent dependency behaviours. However, discrepancy exists. For $\Delta\delta^{18}$O, there is an offset of 0.2–0.5 ‰ for DI between 1′000 and 6′000 ppmv. Inconsistency appears for GSM1 measurement below 2′000 ppmv (Fig. Aa). For $\Delta\delta$D, the mixing ratio dependencies determined by the SDM method exhibit a slightly weaker dependency for both standard waters (~~GSM1, VATS and DI)determined by liquid injections via an autosampler (experiment 9~~ Fig. Ab).

It is interesting to mention that the result of the discrete liquid injections in Feb 2017 (experiment 1; Fig. 1) depicts a better agreement with that of the SDM in experiment 6 (comparison figure not shown). This indicates that the discrepancy in the results of the two vapour generation methods could be due to the small instrument drift as well as the high measurement uncertainty at lower mixing ratios.

Experiments using N_2 as dry gas supply (experiment 3 and ~~10) and the three standard waters (NEEM, GV and BERM)via manual injections on instrument HKDS2038 indicates a consistent isotope composition–humidity dependency after a running of one year and one month, respectively~~ 8) also gives a similar isotope composition–mixing ratio dependency between the two vapour generation methods (not shown)~~. Overall, the stability tests indicate~~ , confirming that the isotope ~~composition–humidity dependency of each analyser is to first order stable on a long term basis (1–2 years)~~composition–mixing ratio dependency does not depend substantially on either of the two tested methods.

A2 Influence of dry gas supply

Next, we investigate whether the type of the dry gas supply has an influence on the characterisation results. To this end, we test the characterisation method via the SDM on instrument HIDS2254 with a supply of synthetic air, a supply of N_2 and a supply of dried ambient air through Drierite (experiment 6–8). The synthetic air and N_2 are tested with two standard waters (GSM1 and DI), and the Drierite is tested with one standard water (GSM1).

For ~~humidity~~ mixing ratio dependency on δ^{18}O, the measurement with Drierite disagrees strongly from those with synthetic air and N_2 (Fig. ~~??a~~Ae). As ~~humidity~~ mixing ratio decreases below about ~~7'000~~ 7′000 ppmv, the measured GSM1 with Drierite exhibits a fast increasing positive ~~bias while those~~ deviation while that with synthetic air ~~and~~ or N_2 ~~exhibit~~ exhibits a rather flat dependency. The measurements with synthetic air and ~~with~~ N_2 show a largely similar shape. A small discrepancy exists below ~~15'000~~ 15′000 ppmv, where ~~both~~ the two standard waters measured with N_2 exhibit a small negative offset (~~∼0.5~~∼ 0.5 ‰). The ~~humidity~~ mixing ratio dependencies on δD from all three types of the dry gas supply are in good agreement, despite a small (~~<1.5~~< 1.5 ‰) offset between the measurement with synthetic air and that with N_2 (Fig. ~~??b~~Ae). The calculated *d*-excess follows the shape of δ^{18}O, with a different behaviour between the measurement with Drierite and those with synthetic air and N_2 below about ~~7'000~~ 7′000 ppmv (Fig. ~~??c~~Af). The *d*-excess of the experiment with N_2 exhibits a small positive offset (~~∼0.5~~∼ 0.5 ‰) compared to that of measurement with synthetic air. Overall, characterisation results with synthetic air and N_2 exhibit a ~~humidity~~ mixing ratio dependency in a good agreement for ~~both~~ the two investigated standard waters (GSM1 and DI). However, the characterisation result (for GSM1) with the Drierite differ significantly in δ^{18}O and thus ~~also~~ *d*-excess.

The characterisation method of liquid injections via an autosampler is also tested with synthetic air and N_2. Again, the results exhibit a similar isotope ~~composition–humidity~~ composition–mixing ratio dependency from the two types of dry gas supply, despite a small discrepancy for δ^{18}O ~~measured with N_2 in the dependency for~~ of GSM1 below ~~2'000~~ 2′000 ppmv and a ~~larger negative offset (0.5–1.3~~relatively larger offset (0.5–1.3 ‰) for ~~DI below 10'000~~ δ^{18}O of DI below 10′000 ppmv (not shown). A test of synthetic air from a gas cylinder and dried ambient air from Drierite in the study of Aemisegger et al. (2012) also shows that the ~~humidity~~ mixing ratio dependency for δ^{18}O is different while being more similar for δD. The observed discrepancy in the δ^{18}O ~~bias~~ deviation is possibly due to changes in the baseline of the spectrum around the ~~δ^{18}O (i.e.,~~ $^1H_2^{18}O$ and $^1H_2^{16}O$ ~~)~~ absorption peak, caused by slight differences in trace gas composition (Aemisegger et al., 2012; Rella et al., 2015).

A3 Influence from the measuring sequence

Finally, we investigate whether a measuring sequence with ascending or descending ~~humidity sequence influences humidity~~ mixing ratio sequence influences mixing ratio dependency characterisation. The ~~humidity~~ mixing ratio dependencies of GSM1, MIX and DI tap water characterised with ascending and descending ~~humidity~~ mixing ratio sequences are shown in Fig. ~~??. For~~ A(g-i). For both $\Delta\delta^{18}$O ~~(Fig. ??a), the humidity dependency from the two humidity sequences overall agree well for DI tap water (orange symbol and curve). The measurements for GSM1 with the descending humidity sequence (dark blue symbol and curve) exhibit a weaker humidity dependency below about 5'000 ppmv. However, the measurements for MIX below 2'000 ppmv (light blue symbol and curve) exhibit an interesting contrast. The measurement at the lowest humidity level (around 500 ppmv) has constrained the humidity dependency into opposite directions. The case for~~ and $\Delta\delta$D (Fig. ~~??b)is more uniform among the three tested waters. The~~ Ag, h), the results from the two measuring sequences are in good agreement for all three waters, indicating that the influence from measuring sequence is minor. Though, there is a slightly detectable weaker mixing ratio dependency for the descending mixing ratio sequence (e.g., ~~with a slightly but systematically weaker humidity dependency by the descending humidity sequence . The combination of the disagreement in $\Delta\delta^{18}$O and the weaker dependency in~~ $\Delta\delta$~~D results in various humidity dependencies for Δd-excess (Fig. ??c).For example, the results for DI tap water overall agree between the two sequences. However, the results for~~ D for GSM1 ~~exhibit contrary humidity dependencies.~~

~~In general, the measurements from descending humidity sequence exhibit slightly weaker humidity dependencies. One possible, but unlikely, explanation~~ and DI). One possible explanation for the slightly weaker dependency at descending sequence is the memory effect from ~~moisture remaining from previous injections~~previous injections, e.g., some remaining water molecules would stick to the inner wall of the system (even after flushing the system with ~~12 injections at 20'000 ppmv), which would~~ 12 injections at 20′000 ppmv) and still play a role during the characterisation measurements. If this is the case, ~~starting the measurements~~ the measurements from descending mixing ratio sequence (starting with injections of higher ~~humidity levels~~ mixing ratios at the beginning~~(i.e., descending humidity sequence~~) would help to ~~overwrite the memory from the previous samples.~~

~~The contrast $\Delta\delta^{18}$O measurement at about 500 ppm for MIX is not well understood, since it cannot be explained by a memory effect~~[1]~~, and errors in data handling and processing have been ruled out. The uncertainty in the dependency shape~~

[1] ~~This is because the instrument has been shut down for two weeks before running the measurement for MIX. The last measurement from two weeks ago was standard EVAP which is more heavy-enriched than MIX. If the disagreement between the results are caused by the memory from remaining EVAP sample in the system, the measurement should reflect that already in the ascending sequence (leading to positive $\Delta\delta$ values at low humidities) since the~~

~~of MIX is likely~~ replace the remaining molecules by molecular exchange and therefore is more likely to represent the true dependency behaviour. Nonetheless, the good agreement between the two measuring sequences indicates that the potential hysteresis effects if any are not substantial. The resulting mixing ratio dependencies for Δd-excess (Fig. Ai) overall exhibit an increasing positive deviation towards the low mixing ratios, except for one mixing ratio step of MIX and two mixing ratio steps of GSM1. This underlines the high sensitivity of d-excess measurements due to the increasing uncertainty of δ^{18}O and δD values at very low mixing ratios.

It is worth to note that we have repeated three experiments for MIX (only results from one of the experiments is shown here). For one of the three experiments (not shown), the measurements for MIX below 2′000 ppmv exhibit an interesting contrast in $\Delta\delta^{18}$O. The measurement at the lowest mixing ratio (around 500 ppmv) has constrained the mixing ratio dependency into slightly opposite directions. The contrast is not well understood. It is possible that this contrast stems from the fitting uncertainties due to the ~~uncertain dependency at this range of isotope compositions, where the dependency is between strongly heavy-depleted water (GSM1)and other relatively heavy-enriched waters~~lacking constraining points at the low end of mixing ratios. The contrast is not observed for the repeated experiment with added mixing ratio steps (Fig. Ag, green). It is also possible that for a standard whose isotopic composition is close to a turning point in the correction surface (Sect. 5), hysteresis effects with opposing sign may become visible within the range of uncertainty. This can be also found, for example, in the small shift of dependency shape in δD for VATS among the three analysers (Fig. A2b, e, h, green curve). Further tests with more in-between standards or a vapour generation approach that ~~do~~ does not suffer from memory is needed to address this uncertainty in the dependency shape.

Appendix B: ~~Discussion~~

A1 Variations among CRDS analysers

~~The isotope composition–humidity dependency appears as a robust feature of current-generation stable water isotope analysers of the Picarro brand. In a careful characterisation for low humidities, it is apparently independent of vapour generation method, instrument type and dry gas supply, to first order constant over several years, and independent of measuring sequence. Here we further discuss the possible causes of the isotope composition–humidity dependency . In particular, we explore whether the isotope composition–humidity dependency is an artefact from mixing with water remaining within the analyser, or an instrument behaviour resulting from spectroscopic or other design characteristics.~~

~~If we assume the dependency is a result from mixing with remnant water, there would be mainly two candidates of the background moisture source: (1)the remaining water vapour in the dry gas supply; (2) the remaining water vapour from previous measurement. By changing the dry gas supply from the ambient air dried through Drierite to synthetic air or~~ $\cancel{N_2}$ ~~from cylinder which typically provides a dry gas with a humidity below 10 ppmv, we can exclude the possible influence from the background moisture in the dry gas supply. In order to quantify the amount and the isotope compositions of the remaining water vapour~~

~~ascending sequence is measured before descending sequence. However, the measurements from ascending sequence exhibit a negative bias while those from the descending sequence exhibit a positive bias.~~

~~from previous measurement, we have applied several successive *empty injections* via the autosampler . Thereby, no liquid is injected, and only dry gas is flushed into the vaporizer, and mixed with any remnant moisture in the analyser system. Results from these empty injections show that the remaining water vapour in the system typically has a humidity of about 60–80 ppmv, with its isotope composition closely following those of the previous injections.If the humidity dependency were a result of the mixing between the injected water and the remaining water vapour from previous measurement, by injecting the same standard water during a characterisation run, we would expect a mixing of two water vapour masses of same isotope compositions at different humidities. As a consequence, we would expect the mixed vapour to have the same isotope compositions, which is not the case. Finally, the shape of the isotope composition–humidity dependency with a maximum between 2'000~~ To investigate the variations of the mixing ratio dependency between the individual instruments, we have repeated the same characterisation on three analysers (experiment 3, 9 and ~~6'000 ppmv (Fig~~14). ~~1a) is not consistent with the expectation of a memory effect what would monotonously increase with decreasing humidity.~~ The characterisation is carried out with four standard waters (GSM1, VATS, DI and EVAP), using liquid injections via an autosampler with N_2 as the mixing dry gas.

~~This leaves the second hypothesis to be explored further, namely that the isotope composition–humidity dependency is an instrument behaviour resulting from spectroscopic or other design characteristics. Spectroscopic effects can originate from low absorption at low water molecule concentrations in the cavity. Under such dry conditions, the fitting of absorption peak has a bigger uncertainty (Rella et al., 2015). While a full investigation of the actual physical reasons is beyond the scope of this manuscript, we note that the manufacturer recommends to either measure the standard water and the sample at the same concentrations, or to include at least two concentrations at the same (or similar) isotope composition in the calibration regime so that the non-linear concentration dependency can be quantified over time (Picarro, 2017).~~

~~Our study is currently limited by the limited range of the standard waters used here (−33∼5~~ The characterisation results for the three analysers are shown in Fig. A2. For $\Delta\delta^{18}$O, the positive deviation for GSM1 below $4'000$ ppmv on instrument HKDS2038 is about 0.2–1.8 ‰ ~~and −263∼5 for δ^{18}O and δD, respectively) . Depending on the measurement environment, more heavy-depleted (such as Antarctic inland snow) or heavy-enriched standards would be needed to derive a correction function over the entire measurement range of samples. A clear limitation of the characterisations performed here is~~ stronger than those on the other two analysers (Fig. A2a, d, g, blue). The mixing ratio dependency of VATS below $4'000$ ppmv is nearly flat on instrument HKDS2038 while exhibiting a substantial negative deviation on the other two analysers. The mixing ratio dependencies for the other two standard waters (DI and EVAP) are in good agreement among the three analysers. For $\Delta\delta$D, the ~~high time demand.The characterisation method with liquid injections provides relatively high precision performance but requires an autosampler and takes about 1–2 weeks for four standard waters . The characterisation method with a SDM can be automated more easily, but requires manual intervention to apply more than two standards. A device that could provide any desired isotope composition and a given humidity level would be needed to fully automate the isotope composition–humidity dependency of the instruments tested here.~~

Appendix B: ~~Final remarks and recommendations~~

~~We have systematically investigated the humidity dependency of water vapour isotope measurements for three commercially available infra-red cavity ring-down spectrometers. We found that the humidity dependency varies with the isotope composition of the measured vapour.We define this behaviour as isotope composition–humidity dependency. Using the characterisation results of five standard waters on a Picarro L2130-i as an example, we show how a bias correction scheme for this isotope composition–humidity dependency can be developed. Using the correction scheme, we can determine and correct the isotope composition bias for any measured humidity and isotope composition within the range investigated here and report all the measured isotope compositions at the same humidity level (e.g., 20'000 ppmv in this study)~~mixing ratio dependency of VATS below $2'000$ ppmv is slightly positive on instrument HKDS2038 while being nearly flat on the other two analysers (Fig. A2b, e, h, green). The mixing ratio dependency for the other three standard waters (GSM1, DI and EVAP) agree well among the three analysers. The calculated *d*-excess (Fig. A2c, f, i) shows an increasing positive deviation towards the low end of mixing ratio for almost all standard waters measured on the three analysers, except for DI and GSM1 measured on instrument HKDS2038, whose mixing ratio dependencies appear to be rather flat or even slightly negative.

~~To demonstrate the impact of the humidity dependency correction, we have compared the developed correction scheme with the correction schemes from the published literature, using in situ measurements from cold and dry environments. The impact is found to be most substantial on the measurements at the lowest humidity levels (below 1'600 ppmv). Applying a correction scheme accounting for only humidity dependency relies on the choice of the used standard water. For an aircraft dataset, using the humidity dependency function based on~~ Despite of the minor difference in the magnitude of the deviations, it is clear that the isotope composition–mixing ratio dependency exists in all three analysers investigated here. The behaviour of dependency is to the ~~standard DI produces a large deviation from the reference profile, while using the humidity dependency based on standard GSM1 produces profiles similar to the reference, since it is closer to the average isotope composition of the aircraft dataset. Finally, we have investigated the impact of applying a correction scheme used by Bonne et al. (2014). This approach produces results in good agreement with that from our approach. The small discrepancy is due to the scheme of bias interpolation (linear or non linear), the choice of correcting humidity dependency of the standards or that of the vapour measurement and the small discrepancy in the humidity dependency functions of the two standards. The consistent results indicate that a correction scheme using humidity dependencyfunctions of only two standards covering the isotope composition could be sufficient if the correction surface can be sufficiently approximated by linear interpolation. Using ship measurements made at higher humidity conditions, we find a weaker impact from the different correction schemes.~~ first order in good agreement across the analysers. For the standard waters with relatively depleted isotope compositions, the measurements on all the three analysers exhibit a mixing ratio dependency where the isotopic value increases as the mixing ratio decreases. For the standard waters with relatively enriched isotope compositions, the measurements exhibit a reversed mixing ratio dependency.

A1 Long-term stability

~~We have further evaluated the stability and robustness~~ To quantify the long term stability of the isotope ~~composition–humidity dependencyregarding the vapour generation methods,~~ composition–mixing ratio dependency, we examine the temporal change of the fitting coefficients (a_δ, b_δ and c_δ) in Eq. (4). Figure A3 shows the fitting coefficients for the mixing ratio dependency characterised by liquid injections on instrument HIDS2254 in February 2017 (black line, experiment 1) and in May 2018 (red line, experiment 2). For the characterisation in May 2018, only four standard waters are measured; this results in a fit with a relatively large 95 % confidence interval. In this context, the change over time is considered insignificant if the coefficients (and their fitted curve) from the characterisation in May 2018 is within the 95 % confidence bounds for the fitted curve from the characterisation in February 2017.

For the mixing ratio dependency on δ^{18}O, the ~~variation among the instruments, the possible long term drift, the type of dry gas supplies and the measuring sequence.The robustness test indicates that the~~ change of coefficient a is insignificant. However, it is worth to note that the fitting coefficient a with respect to standard GSM1 (Fig. A3a, the first data point) changes slightly from negative to positive. This small change results in an opposite mixing ratio dependency shape at low mixing ratio. The change of the mixing ratio dependency for GSM1 reflects partly on the sensitivity of the instrument on a certain range of isotope ~~composition–humidity dependency is consistent disregarding the two vapour generation methods, i.e., discrete liquid injections~~ composition and partly on the uncertainty arising from both low instrument precision and lack of measurements at low mixing ratios. The change of coefficients b and ~~continuous vapour streaming. It is clear that this isotope composition–humidity dependency exists in a similar fashion in all three investigated analysers. Repeated characterisations during a 1–2 year time period show that the isotope composition–humidity dependency is an instrument characteristic that is to the first order constant. Characterisations with synthetic air and~~ ~~N_2~~ ~~are similar, while results using Drierite differ substantially in~~ c are substantial for standard waters of relatively higher δ^{18}~~O, likely due to the mixing effect from the remaining moisture after the dry unit. The measuring sequence from high to low or revers shows slightly differing results, pointing to potentially unresolved issues in the vapour generation method. We suspect this is most likely due to the high sensitivity of the humidity dependency at this range of~~ ~~δ^{18}O values.~~ O (Fig. A3b, c). A less negative b and a less positive c reflects a weaker mixing ratio dependency in May 2018. For the mixing ratio dependency on δD, reasonable agreement exhibits for all three fitting coefficients (Fig. A3d, e, f); this points to the same basic shape of the mixing ratio dependency on δD after a 15 month period.

~~In the end, we have discussed the possible origin of the robust isotope composition–humidity dependency. We have excluded the possible mixing effect from the remaining moisture in the dry gas supply and that from previous injections. Even though a full investigation of the physical reason is beyond the scope of this manuscript, we propose that the isotope composition–humidity dependency is to first order a constant instrument characteristic.It probably has aspectroscopic origin, resulting from a larger uncertainty in the fitting of absorption peak at low water molecular concentrations (Rella et al., 2015).~~

~~The correction for the isotope composition–humidity dependency is most relevant for in situ vapour isotope measurements where the ambient humidity is low (below~~ A repeated characterisation with standard water DI determined via the SDM in July 2016, February 2018 and June 2018 (experiment 4~~'000 ppmv) and the isotope composition of measured vapour spans a large range. At higher humidities, Picarro analysers show negligible dependency on either the humidity or the isotope composition. If the isotope composition of ambient vapour varies in a small range during the sampling period, a simpler correction scheme could be employed, using the humidity dependency of two or even one suitable standard water with a similar isotope composition as that of ambient vapour.~~

~~Based on our conclusions above, we recommend the following procedures for the correction of~~ , 5 and 6) indicates that the mixing ratio dependency for standard water DI is still consistent after nearly two years (not shown). The mixing ratio dependencies of the three standard waters (GSM1, VATS and DI) determined by liquid injections via an autosampler (experiment 9 and 10) and the other three standard waters (NEEM, GV and BERM) via manual injections on instrument HKDS2038 (experiment 12 and 13) indicate a consistent isotope composition–mixing ratio dependency after a running of one year and one month, respectively (not shown). Overall, the stability tests indicate that the isotope ~~composition–humidity dependency for in situ vapour isotope measurements using Picarro infra-red laser spectrometers. The procedures are particularly relevant for those measurements under cold and dry conditions (with a humidify below 4’000 ppmv) and subject to a relatively large variation in the isotope compositions, such as during aircraft experiments.~~

~~(1) A correction scheme with a surface function should be established for each individual instrument according to the characterisation results from the multiple standard waters following the procedures in this paper.~~

~~(2) Even though the isotope composition–humidity dependency appears at first order similar across the three analysers, the detailed shape can vary from instrument to instrument. We recommend to characterise each individual instrument to obtain a specific correction function.~~

~~(3) Five or more standard waters that span the full range of ambient vapour isotope compositions should be used to determine the isotope composition–humidity dependency surface.~~

~~(4) While the isotope composition–humidity dependency was found to be overall stable within a period of one year for the instruments investigated here, we recommended to repeat the characterisation at least every 6–12 months to capture the possible change in humidity dependency behaviour.~~

~~(5) If the measurements of multiple standard waters are not available, the approach used in Bonne et al. (2014) could be applied as an alternative correction approach. Their approach can produce similar results as that from the approach proposed here, but requires the characterisation of the humidity dependency of two carefully selected calibration standards in a linear range of the correction surface. If the isotope composition of ambient vapour varies only within a small range during the sampling period, such as during measurements close to the ocean surface, it may be sufficient to correct for the humidity dependency using one standard water that has a similar isotope composition as that of ambient vapour.~~

composition–mixing ratio dependency of each analyser is to first order stable on a long term basis (1–2 years).

~~A reproducible and accepted characterisation method is of utmost importance for comparing measurements across disparate locations and in bottom-up networks, in particular in the polar regions, and appears as a prerequisite for detecting representative signals in the stable isotope record on a regional scale. In particular studies employing the d-excess as an indicator of moisture origin or other tracer applications are therefore likely to profit from a detailed characterisation of their analysers according to our characterisation procedure, either before, during or after field deployments.~~

Appendix B: Fitting uncertainty estimated using a ~~bootstrap~~ bootstrapping approach

Since we only have ~~5~~ 5 available data points to fit in ~~Eq.~~ (5), the resulted 95 % confidence interval of the fit is relatively broad (black dotted line, Fig. 2). This broad confidence interval results in a relatively large standard deviation for the ~~isotope composition bias~~ isotopic deviation ($\Delta\delta$). For example, the resulted standard deviation for $\Delta\delta$ at ~~2’000~~ $2'000$ ppmv is about ~~0.20, 2.69 and 3.13~~ 0.20, 2.69 and 3.13 ‰ for δ^{18}O, δD and *d*-excess, respectively. To reduce this large standard deviation for $\Delta\delta$, we use a ~~bootstrap~~ bootstrapping approach (Efron, 1979) to estimate the fitting uncertainty in Eq. (5).

The ~~bootstrap~~ bootstrapping approach can be explained by considering for example the coefficient a. Firstly, for each individual observation of a, we generate ~~1’000~~ $1'000$ random values under a normal distribution with the mean and standard deviation being those of each available observation. We obtain now five sets of ~~1’000~~ $1'000$ random values since we have five a from five standard waters. Then, we sample one value from each set of the ~~1’000~~ $1'000$ random values and fit those sampled five values using Eq. (5). Finally, we repeat this process ~~1’000~~ $1'000$ times, thus obtain ~~1’000~~ $1'000$ fits. The standard deviation of the ~~1’000~~ $1'000$ fits is the standard deviation that is adopted here (blue dotted line, Fig. 2).

In this way, the standard deviations estimated for the coefficients ~~s~~a, b and c are lowered to about ~~15, 0.4×10^{-6} and 8×10^{-3}~~ 15, 0.4×10^{-6} and 8×10^{-3} for δ^{18}O and ~~100, 3×10^{-6} and 0.1~~ 100, 3×10^{-6} and 0.1 for δD, respectively. This in turn substantially reduces the resulted standard deviation for $\Delta\delta$. For example, the standard deviation for $\Delta\delta$ at ~~2’000~~ $2'000$ ppmv is reduced by a factor of ~~20~~20, being about ~~0.01, 0.11 and 0.14~~ 0.01, 0.11 and 0.14 ‰ for δ^{18}O, δD and *d*-excess, respectively.

Appendix C: Analytical solution for δ_{ref}

In the following we derive the analytical solution for δ_{ref} in Eq. (7) at a reference ~~humidity q_{ref} =20’000~~ mixing ratio $q_{\mathrm{ref}} = 20'000$ ppmv. The derivation applies for both δ^{18}O and δD.

The coefficients a(δ_{ref}), b(δ_{ref}) and c(δ_{ref}) are given according to Eq. (5):

$$\begin{cases} a(\delta_{\mathrm{ref}}) = m_a(\delta_{\mathrm{ref}} - n_a)^2 + k_a, \\ b(\delta_{\mathrm{ref}}) = m_b(\delta_{\mathrm{ref}} - n_b)^2 + k_b, \\ c(\delta_{\mathrm{ref}}) = m_c(\delta_{\mathrm{ref}} - n_c)^2 + k_c, \end{cases} \tag{C1}$$

Substitute Eq. (C1) into Eq. (7) and rearrange the terms, we get:

$$A\delta_{\mathrm{ref}}^2 + B\delta_{\mathrm{ref}} + C = 0, \text{ where } \begin{cases} A = \dfrac{m_a}{h} + m_b h + m_c, \\ B = 1 - \dfrac{2m_a n_a}{h} - 2m_b n_b h - 2m_c n_c, \\ C = \dfrac{m_a n_a^2}{h} + m_b n_b^2 h + m_c n_c^2 + \dfrac{k_a}{h} + k_b h + k_c - \delta_{\mathrm{meas}}, \end{cases} \tag{C2}$$

Eq. (C2) is a quadratic equation with its only physical solution being:

$$\delta_{\mathrm{ref}} = \frac{-B + \sqrt{B^2 - 4AC}}{2A}. \tag{C3}$$

The coefficients m, n and k are already obtained from the fits in Eq. (5). When given a measured ~~humidity~~mixing ratio, h, and the corresponding isotope composition, δ_{meas}, we can obtain the isotope composition at $\cancel{q_{\text{ref}} = 20'000}$ $q_{\text{ref}} = 20'000$ ppmv, δ_{ref}, according to the solution Eq. (C3).

Competing interests. The authors declare that no competing interests are present in this study.

Acknowledgements. We thank Iris Thurnherr, Franziska Aemisegger and Pascal Graf from the Institute for Atmospheric and Climate Sciences, ETH Zurich, Hans Christian Steen-Larsen and Sonja Wahl from the Geophysical Institute, University of Bergen, Jean-Lionel Lacour and Tomas Foldes, for valuable discussions. Thanks for Árný Erla Sveinbjörnsdóttir from the Isotope Laboratory of University of Iceland for providing the UI standard waters. Jarle Berntsen from the Department of Mathematics at University of Bergen is acknowledged for helping to identify a suitable fitting function. We are grateful to the scientists and other personnel who made the measurements during the Iceland-Greenland Seas campaign in 2018 possible. This publication received funding from the Research Council of Norway through Projects SNOWPACE (Contract no. 262710) and FARLAB (Contract no. 245907).

References

Aemisegger, F., Sturm, P., Graf, P., Sodemann, H., Pfahl, S., Knohl, A., and Wernli, H.: Measuring variations of δ^{18}O and δ^{2}H in atmospheric water vapour using two commercial laser-based spectrometers: an instrument characterisation study, Atmos, Meas. Tech, 5, 1491–1511, 2012.

Bailey, A., Noone, D., Berkelhammer, M., Steen-Larsen, H. C., and Sato, P.: The stability and calibration of water vapor isotope ratio measurements during long-term deployments, Atmospheric Measurement Techniques, 8, 4521–4538, https://doi.org/10.5194/amt-8-4521-2015, 2015.

Bastrikov, V., Steen-Larsen, H. C., Masson-Delmotte, V., Gribanov, K., Cattani, O., Jouzel, J., and Zakharov, V.: Continuous measurements of atmospheric water vapour isotopes in western Siberia (Kourovka), Atmospheric Measurement Techniques, 7, 1763–1776, https://doi.org/10.5194/amt-7-1763-2014, 2014.

Bonne, J.-L., Masson-Delmotte, V., Cattani, O., Delmotte, M., Risi, C., Sodemann, H., and Steen-Larsen, H.: The isotopic composition of water vapour and precipitation in Ivittuut, southern Greenland, Atmospheric Chemistry and Physics, 14, 4419–4439, 2014.

Bonne, J.-L., Behrens, M., Meyer, H., Kipfstuhl, S., Rabe, B., Schönicke, L., Steen-Larsen, H. C., and Werner, M.: Resolving the controls of water vapour isotopes in the Atlantic sector, Nature communications, 10, 1632, 2019.

Crosson, E. R.: A cavity ring-down analyzer for measuring atmospheric levels of methane, carbon dioxide, and water vapor, Applied Physics B-Lasers And Optics, 92, 403–408, 2008.

Dansgaard, W.: The abundance of O18 in atmospheric water and water vapour, Tellus, 5, 461–469, 1953.

Dansgaard, W.: The O18-abundance in fresh water, Geochimica et Cosmochimica Acta, 6, 241–260, http://www.sciencedirect.com/science/article/B6V66-488Y5HP-1V6/2/e7ca8aaef7549373eab07d45b525387c, 1954.

Dansgaard, W.: Stable isotopes in precipitation, Tellus, 16, 436–468, 1964.

Efron, B.: Bootstrap Methods: Another Look at the Jackknife, Annals of Statistics, 7, 1–26, 1979.

Gat, J. R.: Oxygen and hydrogen isotopes in the hydrologic cycle, Annual Review of Earth and Planetary Sciences, 24, 225–262, 1996.

Goldenstein, C. S., Miller, V. A., Spearrin, R. M., and Strand, C. L.: SpectraPlot.com: Integrated spectroscopic modeling of atomic and molecular gases, Journal of Quantitative Spectroscopy and Radiative Transfer, 200, 249 – 257, https://doi.org/https://doi.org/10.1016/j.jqsrt.2017.06.007, http://www.sciencedirect.com/science/article/pii/S0022407317302996, 2017.

Gupta, P., Noone, D., Galewsky, J., Sweeney, C., and Vaughn, B. H.: Demonstration of high-precision continuous measurements of water vapor isotopologues in laboratory and remote field deployments using wavelength-scanned cavity ring-down spectroscopy (WS-CRDS) technology, Rapid Communications In Mass Spectrometry, 23, 2534–2542, 2009.

IAEA: Reference Sheet for VSMOW2 and SLAP2 international measurement standards, 2009.

Johnson, J. E. and Rella, C. W.: Effects of variation in background mixing ratios of N2, O2, and Ar on the measurement of δ 18O–H2O and δ 2H–H2O values by cavity ring-down spectroscopy, 2017.

Kerstel, E.: Isotope ratio infrared spectrometry, in: Handbook of stable isotope analytical techniques, pp. 759–787, Elsevier, 2004.

Kerstel, E. and Gianfrani, L.: Advances in laser-based isotope ratio measurements: selected applications, Applied Physics B-Lasers And Optics, 92, 439–449, 2008.

Kurita, N., Newman, B. D., Araguas-Araguas, L. J., and Aggarwal, P.: Evaluation of continuous water vapor delta D and delta O-18 measurements by off-axis integrated cavity output spectroscopy, Atmospheric Measurement Techniques, 5, 2069–2080, https://doi.org/10.5194/amt-5-2069-2012, 2012.

Lis, G., Wassenaar, L., and Hendry, M.: High-precision laser spectroscopy D/H and 18O/16O measurements of microliter natural water samples, Analytical chemistry, 80, 287–293, 2008.

Mook, W. G., Gat, J. R., Meijer, H. A., Rozanski, K., Froehlich, K., et al.: Environmental isotopes in the hydrological cycle: principles and applications, in: Technical Documents in Hydrology, UNESCO, 2001.

Picarro, I.: Calibration guide for Picarro analyzers, 2017.

Rella, C. W., Hoffnagle, J., He, Y., and Tajima, S.: Local- and regional-scale measurements of CH_4, $\delta^{13}CH_4$, and C_2H_6 in the Uintah Basin using a mobile stable isotope analyzer, Atmospheric Measurement Techniques, 8, 4539–4559, https://doi.org/10.5194/amt-8-4539-2015, https://www.atmos-meas-tech.net/8/4539/2015/, 2015.

Renfrew, I., Pickart, R., Våge, K., Moore, G., Bracegirdle, T., Elvidge, A., Jeansson, E., Lachlan-Cope, T., McRaven, L., Papritz, L., et al.: The Iceland Greenland Seas Project, Bulletin of the American Meteorological Society, 2019.

Schmidt, M., Maseyk, K., Lett, C., Biron, P., Richard, P., Bariac, T., and Seibt, U.: Concentration effects on laser-based $\delta^{18}O$ and $\delta^{2}H$ measurements and implications for the calibration of vapour measurements with liquid standards, Rapid Communications in Mass Spectrometry, 24, 3553–3561, 2010.

Sodemann, H., Aemisegger, F., Pfahl, S., Bitter, M., Corsmeier, U., Feuerle, T., Graf, P., Hankers, R., Hsiao, G., Schulz, H., et al.: The stable isotopic composition of water vapour above Corsica during the HyMeX SOP1 campaign: insight into vertical mixing processes from lower-tropospheric survey flights, Atmospheric Chemistry and Physics, 17, 6125–6151, 2017.

Steen-Larsen, H. C., Johnsen, S. J., Masson-Delmotte, V., Stenni, B., Risi, C., Sodemann, H., Balslev-Clausen, D., Blunier, T., Dahl-Jensen, D., Ellehoj, M. D., Falourd, S., Grindsted, A., Gkinis, V., Jouzel, J., Popp, T., Sheldon, S., Simonsen, S. B., Sjolte, J., Steffensen, J. P., Sperlich, P., Sveinbjornsdottir, A. E., Vinther, B. M., and White, J. W. C.: Continuous monitoring of summer surface water vapor isotopic composition above the Greenland Ice Sheet, Atmospheric Chemistry and Physics, 13, 4815–4828, https://doi.org/10.5194/acp-13-4815-2013, 2013.

Steen-Larsen, H. C., Sveinbjörnsdottir, A. E., Peters, A. J., Masson-Delmotte, V., Guishard, M. P., Hsiao, G., Jouzel, J., Noone, D., Warren, J. K., and White, J. W. C.: Climatic controls on water vapor deuterium excess in the marine boundary layer of the North Atlantic based on 500 days of in situ, continuous measurements, Atmospheric Chemistry and Physics, 14, 7741–7756, https://doi.org/10.5194/acp-14-7741-2014, 2014.

Steig, E., Gkinis, V., Schauer, A., Schoenemann, S., Samek, K., Hoffnagle, J., Dennis, K., and Tan, S.: Calibrated high-precision 17O-excess measurements using cavity ring-down spectroscopy with laser-current-tuned cavity resonance, Meas. Tech, 7, 2421–2435, 2014.

Sturm, P. and Knohl, A.: Water vapor $\delta^{2}H$ and $\delta^{18}O$ measurements using off-axis integrated cavity output spectroscopy, Atmospheric Measurement Techniques, 3, 67–77, 2010.

Wen, X. F., Lee, X., Sun, X. M., Wang, J. L., Tang, Y. K., Li, S. G., and Yu, G. R.: Intercomparison of four commercial analyzers for water vapor isotope measurement, Journal of Atmospheric and Oceanic Technology, 29, 235–247, https://doi.org/10.1175/JTECH-D-10-05037.1, 2012.

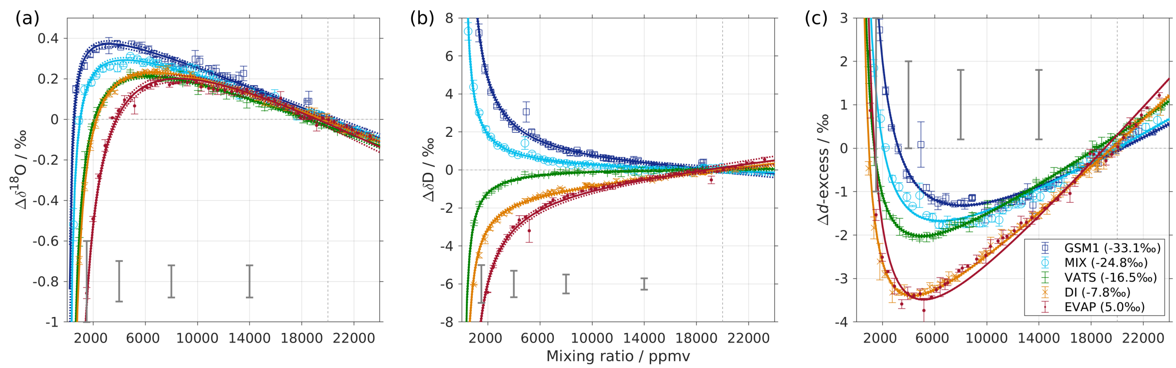

Figure 1. ~~Humidity~~ Mixing ratio dependency of uncalibrated measurements for (**a**): δ^{18}O, (**b**): δD and (**c**): *d*-excess ~~. Humidity dependency is expressed as the deviation Δ of the measured isotope composition at each humidity with respect to the reference humidity of 20'000 ppmv~~ for five standard waters (GSM1, MIX, VATS, DI and EVAP) on instrument HIDS2254 (Picarro L2130-i) with discrete liquid injections via an autosampler (experiment 1). Mixing ratio dependency is expressed as the deviation Δ of the measured isotope composition at each mixing ratio with respect to the reference mixing ratio of $20'000$ ppmv. Symbol and error bar represents the mean and the standard deviation of the mean for the last three of total four injections at each mixing ratio. Solid lines are fits with the function $f(x) = \frac{a}{x} + bx + c$. Dashed lines are the 95 % confidence interval for the corresponding fit. Measurements and fits for *d*-excess are calculated from ~~d-excess $= \delta$D $- 8 \cdot \delta^{18}$O~~ Δd-excess $= \Delta\delta$D $- 8 \cdot \Delta\delta^{18}$O. The typical one standard deviation of a single injection at the corresponding mixing ratio is indicated by grey error bars. Two outliers (at about ~~4'300~~ $4'300$ and ~~8'900~~ $8'900$ ppmv) are removed from GSM1 measurements and one outlier (at about ~~9'000~~ $9'000$ ppmv) is removed from VATS measurements.

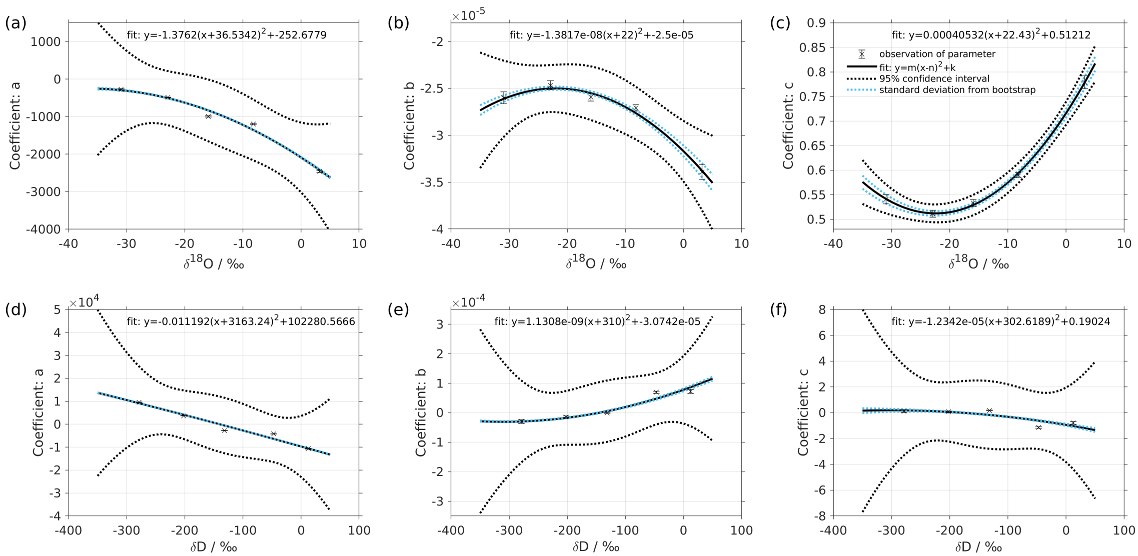

Figure 2. Dependency of fitting coefficients a, b and c on δ^{18}O **(a)–(c)** and on δD **(d)–(f)**. The coefficients a, b and c are from the fits for the five standard waters in Fig. 1. Solid line is the quadratic fit with $f_j(y) = m_j(y-n_j)^2 + k_j$. Black dotted line shows the ~~95~~ 95 % confidence interval. Blue dotted line shows the standard deviation estimated from a ~~bootstrap~~ bootstrapping method.

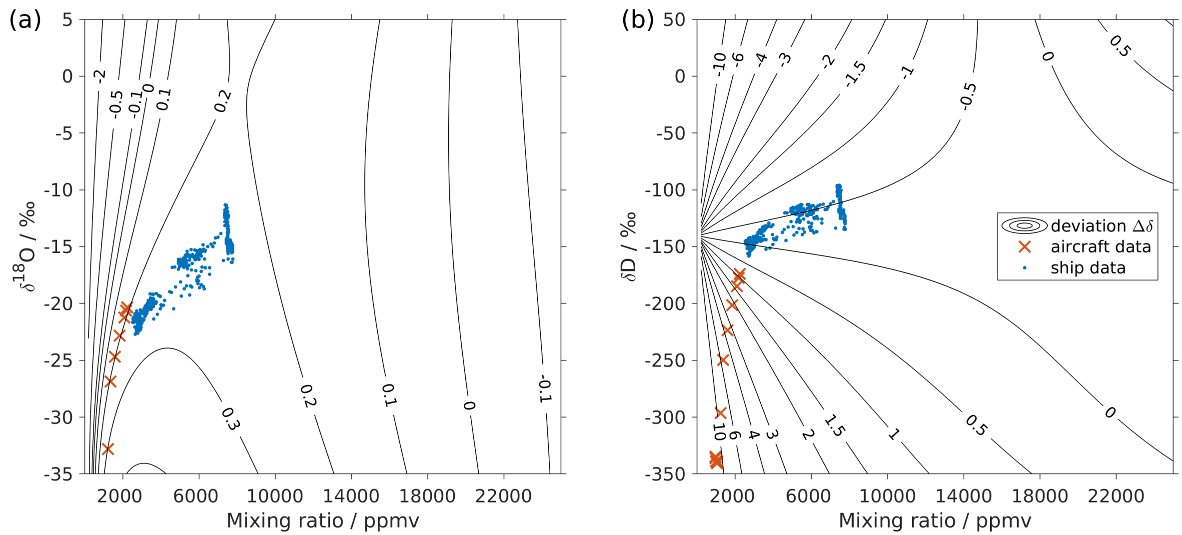

Figure 3. Surface function of the ~~bias~~ isotopic deviations for **(a)** δ^{18}O and **(b)** δD, based on the isotope ~~composition–humidity~~ composition–mixing ratio dependency of instrument HIDS2254 (Picarro L2130-i). The *x*-axis is the raw ~~humidity~~ mixing ratio and *y*-axis shows the raw isotope composition at ~~20’000~~ 20′000 ppmv. Contours with numbers indicate the ~~isotope composition bias~~isotopic deviation, $\Delta\delta$. Symbols show the isotope measurements ~~during cold and dry conditions~~ over the Iceland Sea: one min averaged measurements ~~in every 10 seconds~~ from an aircraft in the lower troposphere (~~blue~~ red crosses) and ~~in every 10~~ measurements at 10 minutes resolution from a research vessel ~~on the ocean surface~~ (~~red~~ blue dots). The measurements from the aircraft were done with instrument HIDS2254 (Picarro L2130-i) and those on the research vessel were done with instrument HKDS2038 (Picarro L2140-i).

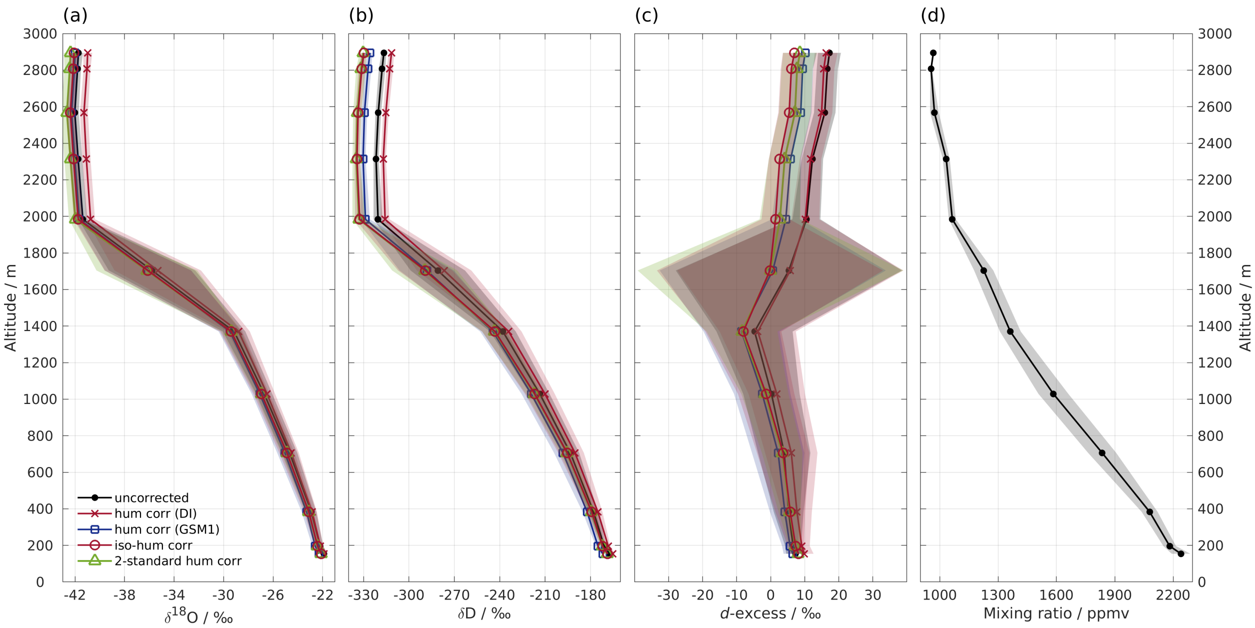

Figure 4. Vertical profiles of **(a)** δ^{18}O, **(b)** δD, **(c)** *d*-excess and **(d)** ~~humidity~~ mixing ratio measured by instrument HIDS2254 on an aircraft above the Iceland Sea on Mar 04, 2018. Shown are one min averaged profiles of the ~~raw~~ uncorrected dataset (black ~~curve~~ line with dot) and four datasets using different isotope ~~composition–humidity~~ composition–mixing ratio dependency correction schemes: using the ~~humidity~~ mixing ratio dependency of standard DI (orange curve with cross), standard GSM1 (blue curve with square), the isotope ~~composition–humidity~~ composition–mixing ratio dependency surface function (~~black~~ red curve with ~~asterisk~~circle), and using two ~~humidity-dependency-corrected~~ mixing ratio-dependency-corrected standards (green curve with ~~dot~~triangle). All the ~~shown~~ datasets are calibrated to VSMOW2-SLAP2 scale. Shading shows the total uncertainty (one standard deviation) for the corresponding profiles. Note that the profile of δD has been adjusted 30 s forward to account for the longer response time of molecular $HD^{16}O$. The large uncertainty between 1′400 and 2′000 m for *d*-excess is partly due to the rapid evolution of δ^{18}O and δD profiles and partly due to the dephasing between δ^{18}O and δD profiles caused by different response time.

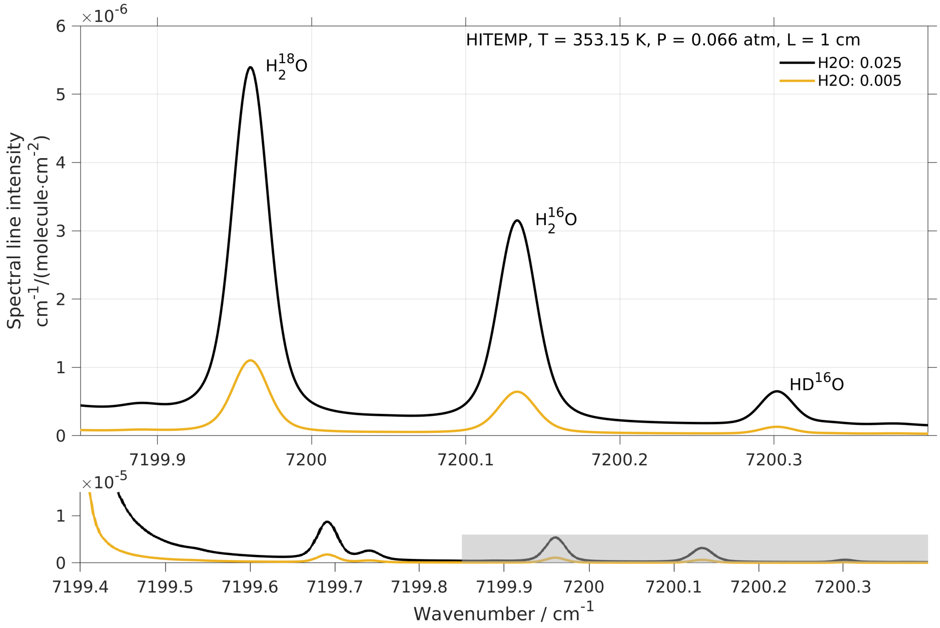

Figure 5. ~~Humidity~~ Absorption spectrum of $H_2^{18}O$, H_2^{16} and $HD^{16}O$ in the frequency range targeted by the laser of Picarro L2130-i and L2140-i. Simulations with two water concentrations were performed using spectraplot.com with HITRAN/HITEMP database (Goldenstein et al., 2017). Simulation parameters are set according to the cavity conditions of the Picarro analyser: $T = 80\ ^{\circ}\mathrm{C}$, $P = 50$ Torr and $L = 1$ cm.

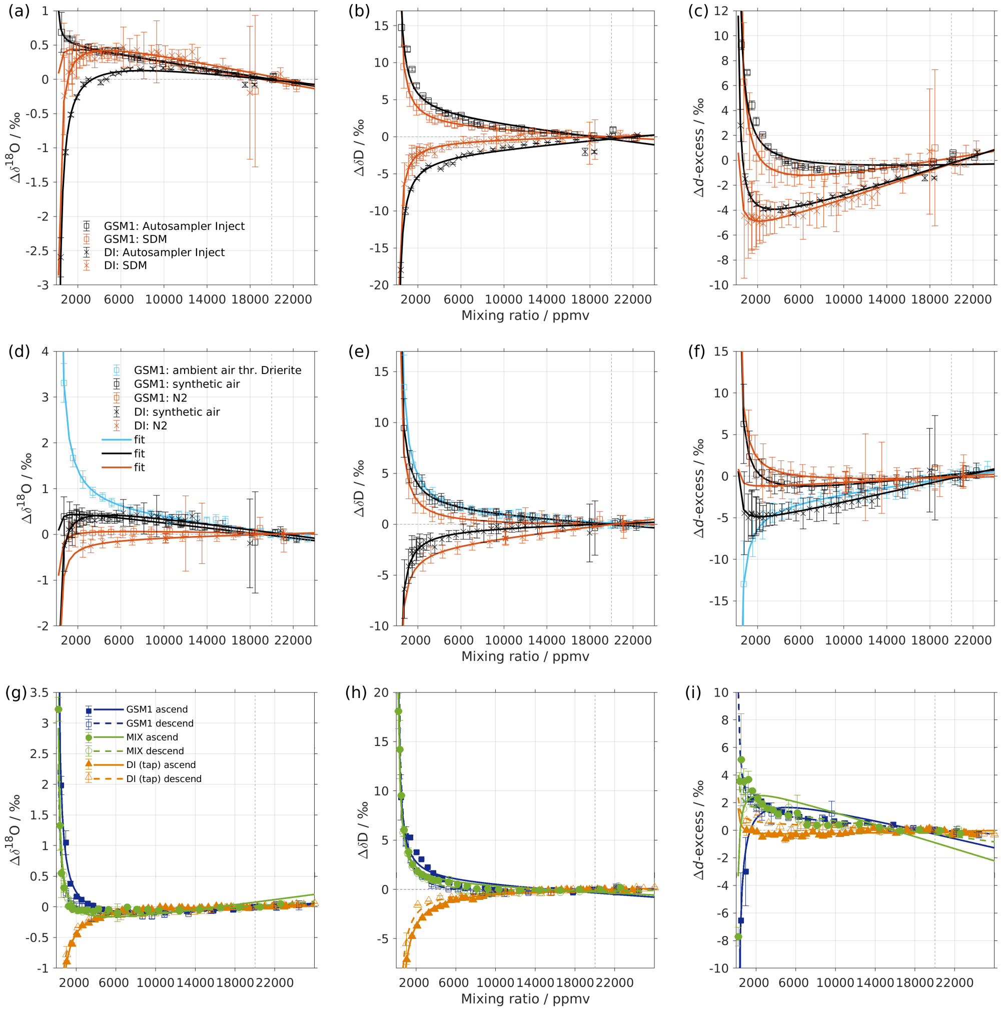

~~Humidity dependency of uncalibrated measurements for instruments **(a)–(c)** HIDS2254; **(d)–(f)** HKDS2038 and **(g)–(i)** HKDS2039. The measurements are carried out with discrete injections using an autosampler with N_2 being the carrier gas (experiment 3, 9 and 13). Only the data below 10'000 ppmv are shown. Symbols and solid lines are the same as in Fig.1.~~

(d-f) Same as ~~Fig. 2~~**(a-c)**, but ~~a comparison between results in Feb 2017 (black symbols, experiment 1) and May 2018 (red symbols, experiment 2). A larger 95 % confidence interval for the fit of May 2018 (red dotted line) is due to the fewer available data points (only four standards measured).~~

~~Same as Fig **??**, but~~ comparing between different carrier gases. The measurements are carried out on instrument HIDS2254 (Picarro L2130-i) with continuous vapour streaming via SDM (experiment 6–8). Two standard waters (GSM1 and DI) are tested with synthetic air (black symbol) and N_2 (orange symbol). The standard water GSM1 is also tested with ambient air that is dried through Drierite (blue symbol).

~~Humidity~~ **(g-i)** Mixing ratio dependency of GSM1 (dark blue symbol), MIX (light blue symbol) and ~~DI tap~~ TAP water (orange symbol)~~for **(a)** δ^{18}O, **(b)** δD and **(c)** *d*-excess,~~ with ascending (closed symbol) and descending (open symbol) ~~humidity~~ mixing ratio sequences. Solid curves represent the fits for ascending ~~humidity~~ mixing ratio sequences and dashed curves the fits for descending ~~humidity~~ mixing ratio sequences. All the measurements are uncalibrated and carried out with discrete injections using an autosampler with N_2 being the carrier gas. The measurements for ~~MIX~~ TAP and ~~DI tap water~~ MIX are carried out on instrument HKDS2038 (Picarro L2140-i) (experiment 9 and 11). The measurements for GSM1 are carried out on instrument HKDS2039 (Picarro L2140-i) and one outlier around ~~500~~ 500 ppmv has been excluded (experiment 15).

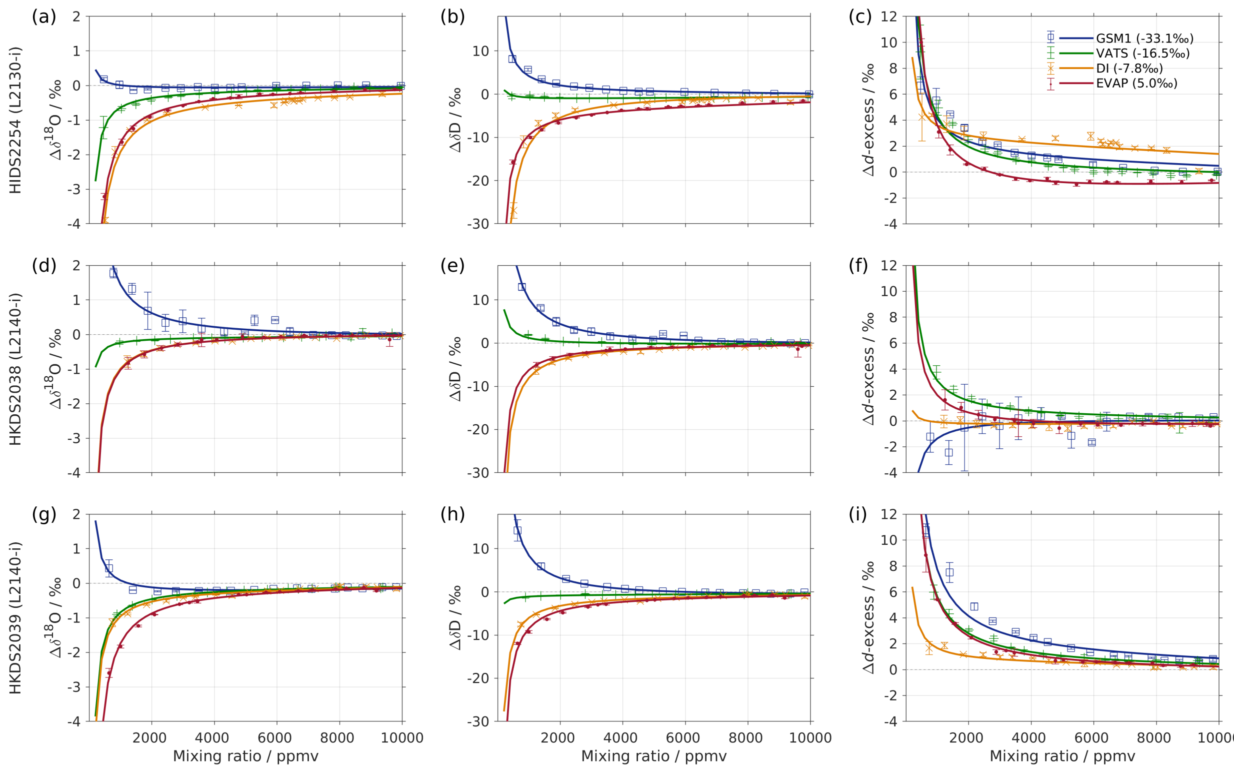

Figure A2. Mixing ratio dependency of uncalibrated measurements for instruments **(a)–(c)** HIDS2254; **(d)–(f)** HKDS2038 and **(g)–(i)** HKDS2039. The measurements are carried out with discrete injections using an autosampler with N_2 as carrier gas (experiment 3, 9 and 14). Only the data below $10'000$ ppmv are shown. Symbols and solid lines indicate measurements and fits respectively as in Fig.1.

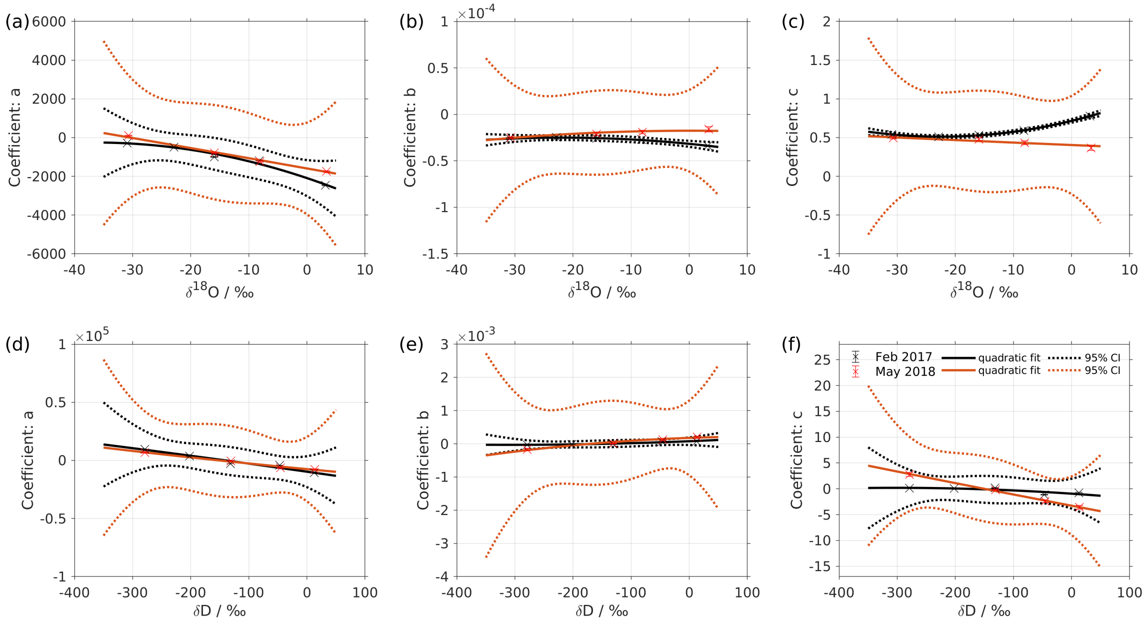

Figure A3. Same as Fig. 2, but a comparison between results in Feb 2017 (black symbols, experiment 1) and May 2018 (red symbols, experiment 2). A larger 95 % confidence interval for the fit of May 2018 (red dotted line) is due to the fewer available data points (only four standards measured).

Table 1. ~~Isotope compositions~~ Overview of all 14 characterisation experiments regarding the instrument, the vapour generation method, the type of dry gas supply, the measured standard waters~~used in this study. The values are reported on~~ , the ~~VSMOW2-SLAP2 scale. *FARLAB standards* are the laboratory standards in use at FARLAB~~mixing ratio steps, ~~University of Bergen~~ the mixing ratio span and ~~*UI standards* are~~ the ~~laboratory standards in use at the Isotope Laboratory of University of Iceland~~experiment time. ~~All the waters~~ For characterisations with injections, typically four injections are ~~laboratory working standards except MIX and DI (tap)~~carried out at each mixing ratio. ~~MIX~~ For characterisation with continuous vapour streaming via SDM, normally 20–40 min of measurement is ~~obtained from an even~~ carried out at each mixing ~~of GSM1 and VATS~~ratio. ~~DI (tap) is deionized tap water in Bergen, Norway.~~ The ~~isotope compositions~~ values of ~~these two waters~~ the water concentrations are ~~calibrated in experiment 9 using~~ the uncalibrated values measured ~~working standards. σ for *FARLAB standards* represents~~ on the ~~standard deviation of means from six liquid injections~~corresponding analyser. Instrument HIDS2254 is model type L2130-i, while ~~σ for *UI standards* a long term standard deviation~~instruments HKDS2038 and HKDS2039 are of model type L2140-i.

~~δ^{18}O σ δD σ *d*-excess σ GSM1 -33.07 ± 0.02 -262.95 ± 0.04 1.63 ± 0.17 MIX -24.78 ± 0.02 -193.90 ± 0.08 4.30 ± 0.20 VATS -16.47 ± 0.02 -127.88 ± 0.09 3.89 ± 0.18 DI -7.78 ± 0.01 -50.38 ± 0.02 11.83 ± 0.10 DI (tap) -7.98 ± 0.01 -52.89 ± 0.05 10.97 ± 0.13 EVAP 5.03 ± 0.02 4.75 ± 0.11 -35.47 ± 0.16 NEEM -33.52 ± 0.05 -257.11 ± 0.6 11.05 ± 0.72 GV -8.54 ± 0.05 -57.72 ± 0.6 10.60 ± 0.72 BERM 0.52 ± 0.05 6.26 ± 0.6 2.10 ± 0.72~~

~~Overview of all 14 characterisation experiments regarding the instrument, the vapour generation method, the type of dry gas supply, the measured standard waters, the humidity steps, the humidity span and the experiment time. For characterisations with injections, typically four injections are carried out at each humidity level. For characterisation with continuous vapour streaming via SDM, normally 20-40 min of measurement is carried out at each humidity level. The values of the water concentrations are the uncalibrated values measured on the corresponding analyser. Instrument HIDS2254 is model type L2130-i, while instruments HKDS2038 and HKDS2039 are of model type L2140-i.~~

No.	Instrument	Method	Dry gas	Standard water	Steps	Span [ppmv]	Time
1	HIDS2254	autosampler	synthetic air	GSM1, MIX, VATS, DI, EVAP	47–49	∼500–23000	Feb 2017
2		autosampler	synthetic air	GSM1, VATS, DI, EVAP	27–30	∼1000–23000	May 2018
3		autosampler	N_2	GSM1, VATS, DI, EVAP	25–29	∼500–23000	May 2018
4		SDM	synthetic air	DI	24	∼700–23000	Jul 2016
5		SDM	synthetic air	DI	11	∼1300–20000	Feb 2018
6		SDM	synthetic air	GSM1, DI	23,27	∼700–23000	Jun 2018
7		SDM	N_2	GSM1, DI	13,16	∼1200–23000	Jun 2018
8		SDM	air thr. Drierite	GSM1	27	∼700–23000	Dec 2016
9	HKDS2038	autosampler	N_2	GSM1, MIX, VATS, ~~DI (tap)~~TAP, EVAP	42–44	∼800–27000	Jan 2017
10		autosampler	N_2	GSM1, VATS, DI	36,29,19	∼600–30000	Feb 2018
11		autosampler	N_2	MIX	19	∼300–23000	Dec 2019
12		manual injection	synthetic air	NEEM, GV, BERM	8	∼2400–24000	Feb 2018
~~12~~ 13		manual injection	synthetic air	NEEM, GV, BERM	8	∼2600–22000	Mar 2018
~~13~~ 14	HKDS2039	autosampler	N_2	GSM1, MIX, VATS, DI, EVAP	45–47	∼500–27000	Jan 2017
~~14~~ 15		autosampler	N_2	GSM1	20	∼500–24000	Jul 2019

Table 2. ~~Summary~~ Isotope compositions of ~~experiment design, ordered by~~ the ~~aims including the dependence~~ standard waters used in this study. The values are reported on ~~vapour generating method,~~ the ~~dependence on~~ VSMOW2-SLAP2 scale. *FARLAB standards* are the ~~tested instrument~~laboratory standards in use at FARLAB, ~~the long term stability~~ University of Bergen and *UI standards* are the ~~dependence behaviour,~~ laboratory standards in use at the ~~influence~~ Isotope Laboratory of University of Iceland. All the waters are laboratory working standards except MIX and TAP. MIX is obtained from ~~dry gas supply~~ an even mixing of GSM1 and VATS. TAP is deionized tap water in Bergen, Norway. The isotope compositions of these two waters are calibrated in experiment 9 using the ~~influence from~~ measured working standards. σ for *FARLAB standards* represents the ~~measuring sequence~~standard deviation of the mean for the six liquid injections, while σ for *UI standards* a long term standard deviation.

	δ^{18}O [‰]	σ [‰]	δD [‰]	σ [‰]	*d*-excess [‰]	σ [‰]
FARLAB standards						
GSM1	-33.07	± 0.02	-262.95	± 0.04	1.63	± 0.17
MIX	-24.78	± 0.02	-193.90	± 0.08	4.30	± 0.20
VATS	-16.47	± 0.02	-127.88	± 0.09	3.89	± 0.18
DI	-7.78	± 0.01	-50.38	± 0.02	11.83	± 0.10
TAP	-7.98	± 0.01	-52.89	± 0.05	10.97	± 0.13
EVAP	5.03	± 0.02	4.75	± 0.11	-35.47	± 0.16
UI standards						
NEEM	-33.52	± 0.05	-257.11	± 0.6	11.05	± 0.72
GV	-8.54	± 0.05	-57.72	± 0.6	10.60	± 0.72
BERM	0.52	± 0.05	6.26	± 0.6	2.10	± 0.72

Table 3. Summary of experiment design, ordered by the aims including the dependency on vapour generating method, the dependency on the tested instrument, the long term stability of the dependency behaviour, the influence from dry gas supply and the influence from the measuring sequence.

Experiments
2, 6
3, 7
6, 7, 8
2, 3
9, 11, 15
3, 9, ~~13~~ 14
1, 2
4, 5, 6
9, 10
~~11,~~ 12, 13
~~6, 7, 8 influence from dry gas supply synthetic air vs N_2 vs Drierite HIDS2254, SDM 8 2, 3 influence from dry gas supply synthetic air vs N_2 HIDS225~~

Table 4. Fitting coefficients for the ~~humidity~~ mixing ratio dependency behaviour of the five standard waters measured on HIDS2254. Coefficients a, b, c are with respect to fitting function $\cancel{f_i(x) = \frac{a_i}{x} + b_i \cdot x + c_i}$ $f_\delta(x) = \frac{a_\delta}{x} + b_\delta \cdot x + c_\delta$. The reported uncertainty is one standard deviation. The fitting lines are shown in Fig. 1.

	Standard	a	b	c
$\delta^{18}O$	GSM1	-274.95 $\pm$ 16.62	-2.60$\times10^{-5}$ $\pm$ 6.23$\times10^{-7}$	0.54 $\pm$ 0.01
	MIX	-488.93 $\pm$ 9.36	-2.47$\times10^{-5}$ $\pm$ 4.73$\times10^{-7}$	0.51 $\pm$ 0.01
	VATS	-996.35 $\pm$ 14.46	-2.59$\times10^{-5}$ $\pm$ 4.19$\times10^{-7}$	0.53 $\pm$ 0.01
	DI	-1195.79 $\pm$ 6.53	-2.71$\times10^{-5}$ $\pm$ 3.28$\times10^{-7}$	0.59 $\pm$ 0.01
	EVAP	-2465.30 $\pm$ 20.33	-3.39$\times10^{-5}$ $\pm$ 7.95$\times10^{-7}$	0.78 $\pm$ 0.01
δD	GSM1	9511.99 $\pm$ 163.45	-2.96$\times10^{-5}$ $\pm$ 6.13$\times10^{-6}$	0.12 $\pm$ 0.10
	MIX	3663.09 $\pm$ 85.40	-1.47$\times10^{-5}$ $\pm$ 4.32$\times10^{-6}$	0.07 $\pm$ 0.07
	VATS	-2778.43 $\pm$ 64.83	-6.71$\times10^{-7}$ $\pm$ 1.88$\times10^{-6}$	0.17 $\pm$ 0.03
	DI	-4219.07 $\pm$ 73.51	6.93$\times10^{-5}$ $\pm$ 3.69$\times10^{-6}$	-1.15 $\pm$ 0.06
	EVAP	-10648.36 $\pm$ 168.65	7.23$\times10^{-5}$ $\pm$ 6.59$\times10^{-6}$	-0.79 $\pm$ 0.11

Table 5. Fitting coefficients for the isotope composition dependency of the ~~humidity~~ mixing ratio dependency coefficients a, b and c in Table 4. Coefficients m, n and k are with respect to fitting function $f_j(y) = m_j(y - n_j)^2 + k_j$. The reported uncertainty is one standard deviation. The fitting lines are shown in Fig. 2.

	Coefficient	m	n	k
δ^{18}O	a	-1.38 $\pm$ 1.27	-36.54 $\pm$ 21.61	-252.80 $\pm$ 585.65
	b	-1.38$\times10^{-8}$ $\pm$ 4.41$\times10^{-9}$	-22.00 $\pm$ 3.14	-2.50$\times10^{-5}$ $\pm$ 7.20$\times10^{-7}$
	c	3.92$\times10^{-4}$ $\pm$ 1.30$\times10^{-4}$	-22.57 $\pm$ 3.42	0.52 $\pm$ 0.02
δD	a	-0.01 $\pm$ 0.25	-3228.00 $\pm$ 69350.00	1.04$\times10^{5}$ $\pm$ 2.35$\times10^{6}$
	b	1.19$\times10^{-9}$ $\pm$ 2.16$\times10^{-9}$	-300.00 $\pm$ 312.85	-3.00$\times10^{-5}$ $\pm$ 5.18$\times10^{-5}$
	c	-8.93e-06 $\pm$ 5.53$\times10^{-5}$	-364.70 $\pm$ 1460	0.23 $\pm$ 2.67